Polarization Control in VCSELs for Compact LiDAR and AR/VR Applications

Kevin Pikul, Leah Espenhahn, and John Dallesasse

Holonyak Micro and Nanotechnology Laboratory
Department of Electrical and Computer Engineering
University of Illinois at Urbana-Champaign

Introductions: II-VI Supported Students

Kevin Pikul

B.S. (2018), M.S. (2021), Ph.D. (current)
VCSEL Fabrication and Characterization
(Anti-Phase Coatings)

Leah Espenhahn

B.S. (2020), Ph.D. (current)
VCSEL Fabrication and Characterization
(Integration)

Research Group Capabilities

Heterogeneous Integration Methods

- Methods for epitaxial transfer of III-V materials onto silicon have been developed in the Dallesasse Research Group
- Transfer method results in top epitaxial layer facing “up” after transfer, facilitating device fabrication after transfer
- Precise positioning of III-V material in a wafer-scale process
- Thickness of transferred material can be precisely controlled

Photonic Devices

- Design and fabrication of mid-IR emitters for sensing systems (quantum cascade)
- VCSEL mode control for LIDAR/3D Imaging/Data Center

Nitride Photonics

- Preliminary work on photonic integration using arsenide/phosphide gain material heterogeneously integrated with III-N material for photon control
- Device designs have been examined for MZMs, tuning elements for tunable lasers, electrically-controlled polarization rotators
- Low static power dissipation – field-controlled devices
- Mn in III-N materials – photon control of spin state, possible quantum information application

Modeling Capabilities

- Band structure calculations for III-N materials, photonic device modeling (waveguides, coupling structures, DBRs, Schrodinger-Poisson solvers), strained quantum dots

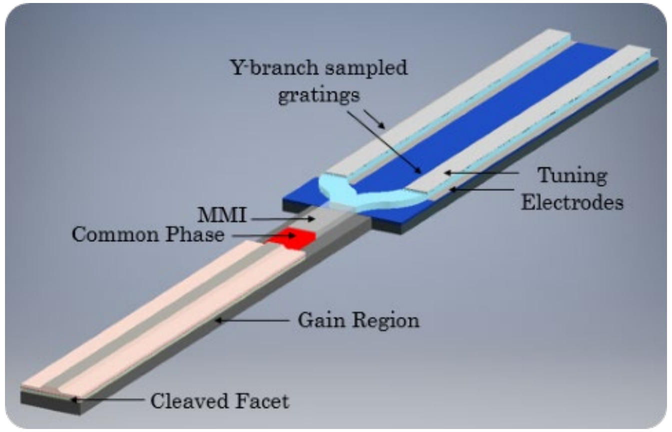

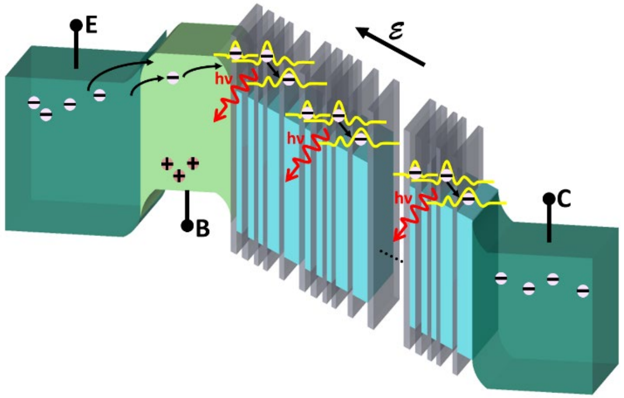

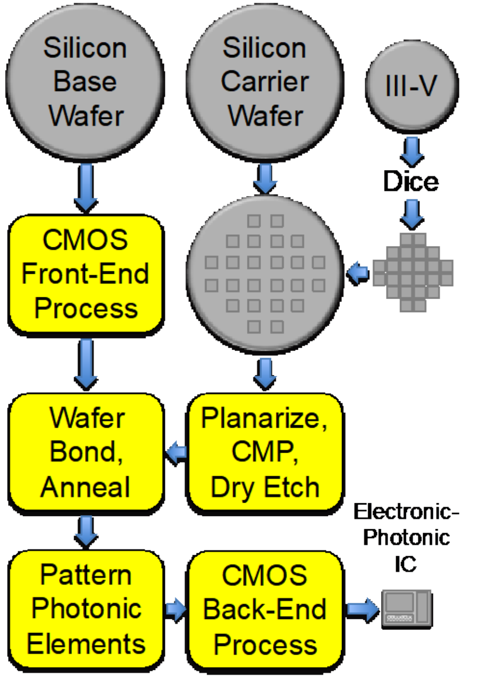

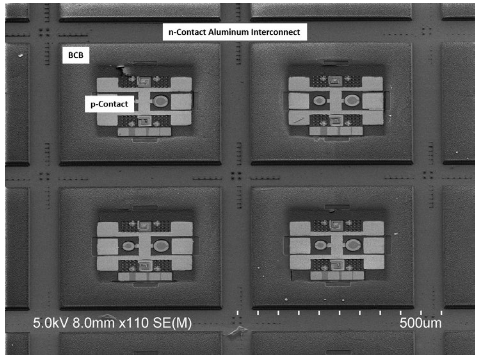

Research Areas [1]

Heterogeneous Integration

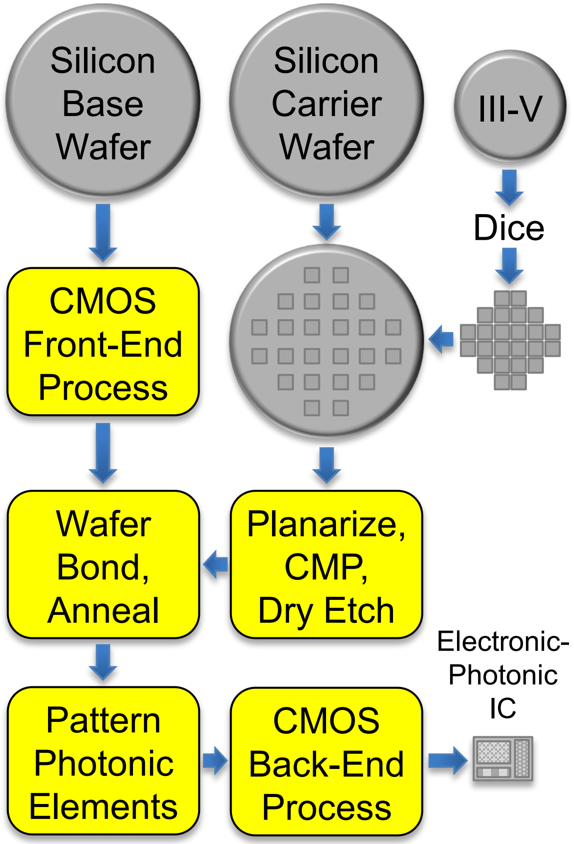

VCSEL Mode Control

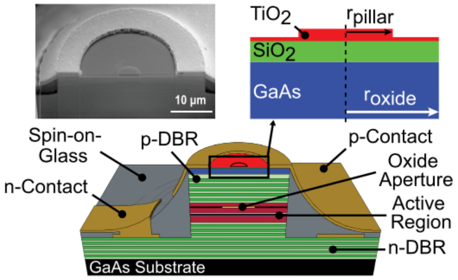

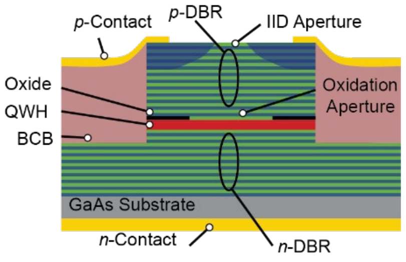

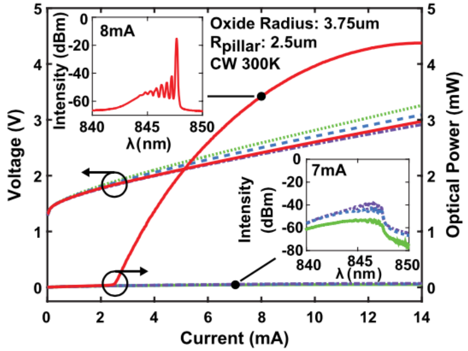

Transistor Laser Integration

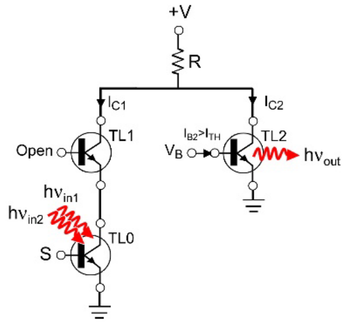

TL: Enabling Electronic-Photonic Circuit Element

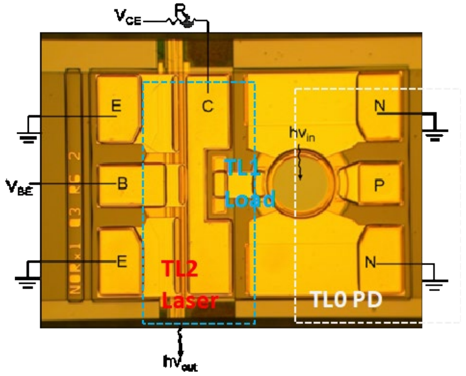

Research Areas [2]

Transistor-Injected QCL

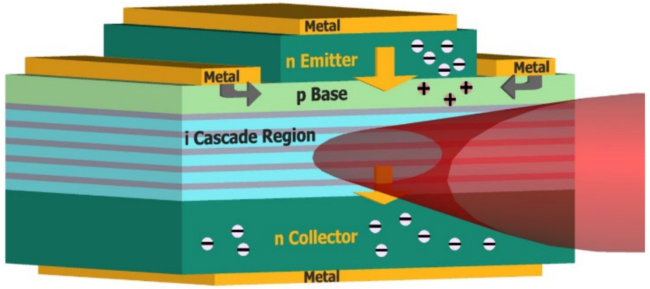

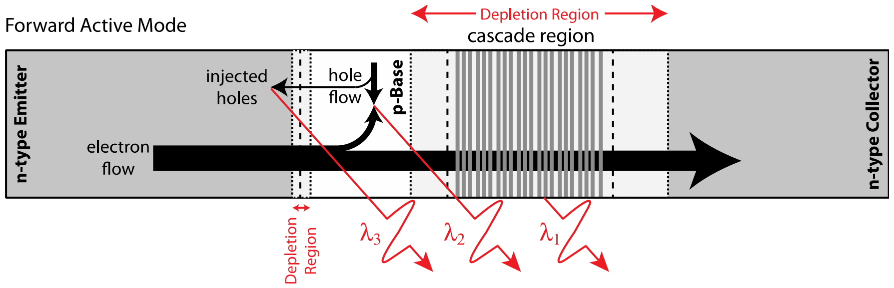

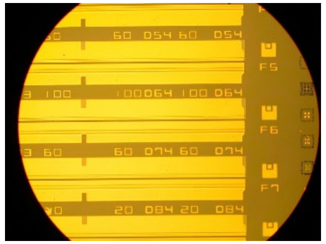

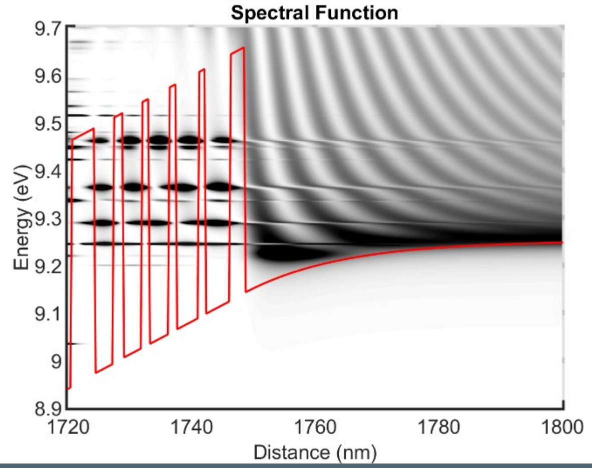

4

III-N Photonics

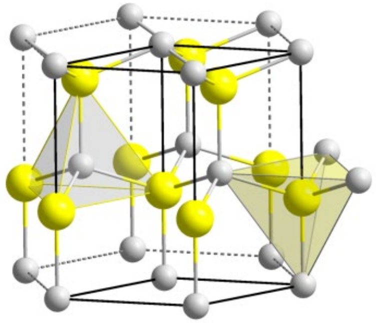

III-N MZMs & PICs

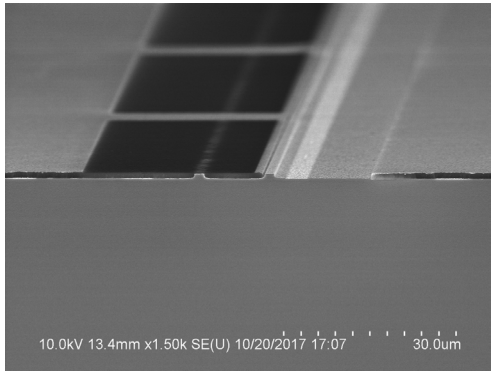

- Tunable Lasers, MZMs, Coherent Rx
- V-Controlled Polarization Rotators
- Quantum Computing

Presentation Outline

Single-Polarization VCSEL Motivation

- Optical Polarization Control for VCSELs

Polarization-Controlled IID VCSELs

- High-Power Single-Mode IID VCSELs
- Disorder-Defined Apertures for Single-Polarization
- Polarization-Resolved LIV and OPSR Analysis

Anti-Phase Coating VCSELs

- Anti-Phase Coating Theory and Simulation
- High-Power Single-Mode VCSEL Operation
- Single-Mode, Single-Polarization VCSELs

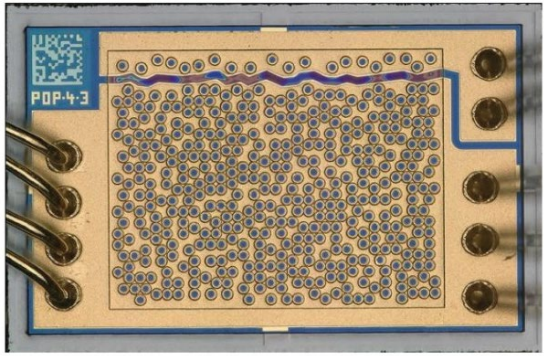

2D VCSEL Array [1]

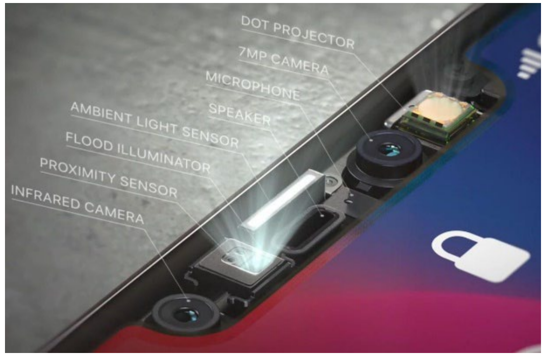

VCSEL-based FaceID [2]

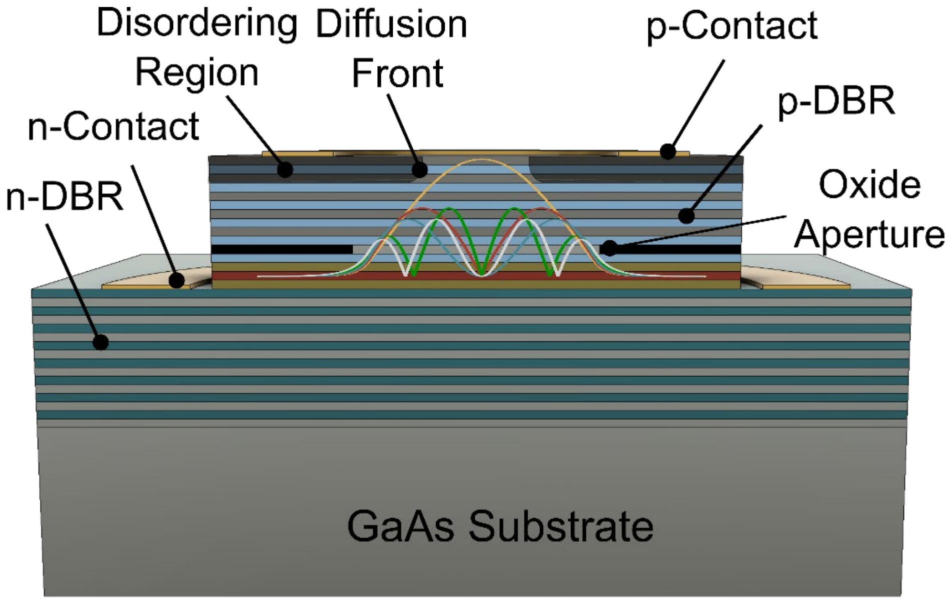

Cross-Section of Disorder-Defined VCSEL

Block-Gift Grant Tasks and Milestones

Program Tasks in Year 1 Single-Polarization Operation in VCSELs	Program Tasks in Year 2 Optical Transverse-Mode and Polarization Controlled VCSEL	Program Tasks in Year 3 Single-Mode and Single-Polarization 2-D VCSEL Arrays
✓ 1.1: Optical modeling of polarization modes in VCSEL structures	o 2.1: Optical modeling of a single-mode, single-polarization VCSEL structure	o 3.1: Optical modeling of single mode, single polarization 2-D VCSEL arrays
✓ 1.2: Design of optical polarization coating utilizing mode-control technologies	✓ 2.2: Design of optical polarization coating modified for transverse-mode control	✓ 3.2: Calculation of near-/far-field patterns of single mode, single polarization VCSELs
✓ 1.3: Single device layout and mask design of polarization controlled VCSEL	✓ 2.3: Mask design and layout of single-mode, single-polarization VCSEL design	✓ 3.3: Mask design and layout of single mode, single polarization 2D VCSEL array
✓ 1.4: Process development and fabrication of polarization controlled VCSEL design	✓ 2.4: Process flow and fabrication of optical mode and polarization controlled VCSELs	o 3.4: Process flow and fabrication of single mode, single polarization 2D VCSEL arrays
✓ 1.5: Benchmark of VCSEL design for single-polarization performance through polarization-resolved light-current-voltage (PR-L-I-V) measurements	✓ 2.5: Benchmark of VCSEL design for single mode, single polarization performance	o 3.5: Benchmark of VCSEL beam quality for various 2D array layout designs
		o 3.6: Experimental analysis of near-/far-field emission patterns of 2-D VCSEL arrays

Current and Emerging VCSEL Applications

3-D Facial Recognition Systems [2]

Augmented and Virtual Reality (AR/VR) Headsets [4,5]

Optical Transceivers in Datacenters [6]

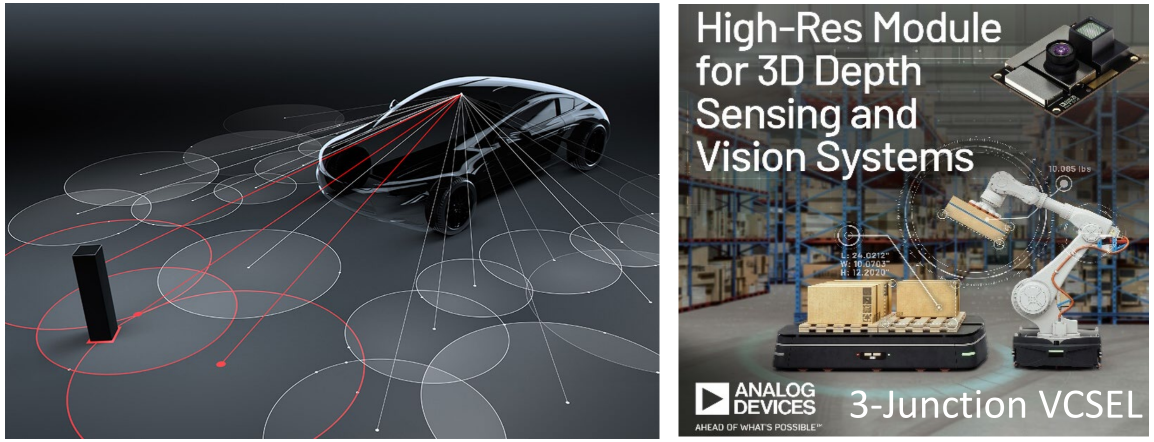

ToF LiDAR for Autonomous Driving and Robotics [7,8]

Optical Depth Sensing Techniques

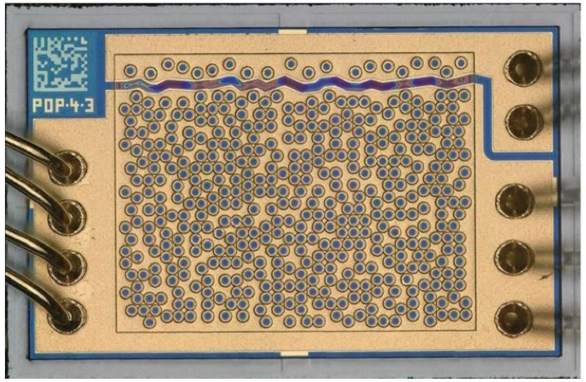

2D VCSEL Array [1]

VCSEL-based FaceID [9]

Structured Light

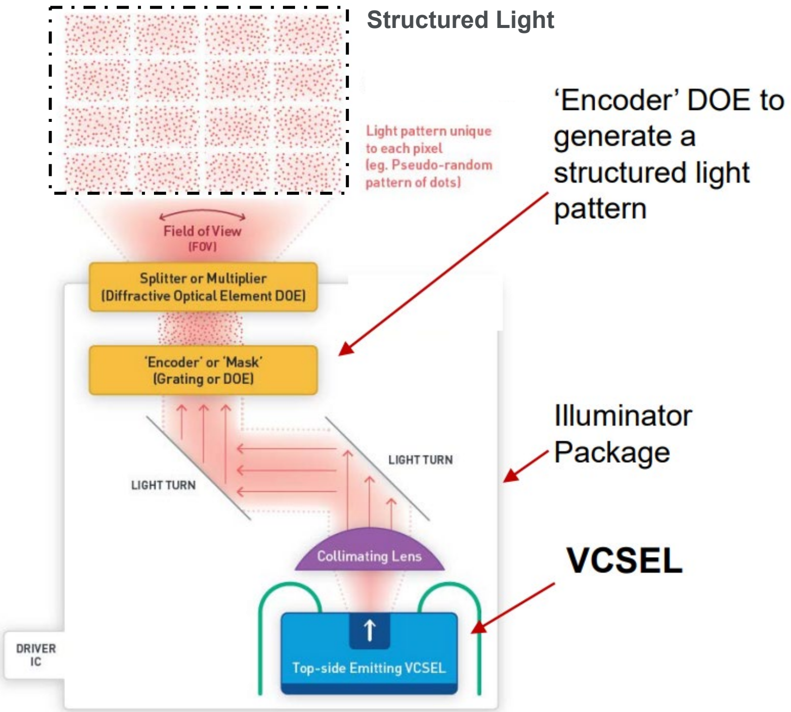

VCSEL Module for Structured Light [10]

STRUCTURED LIGHT

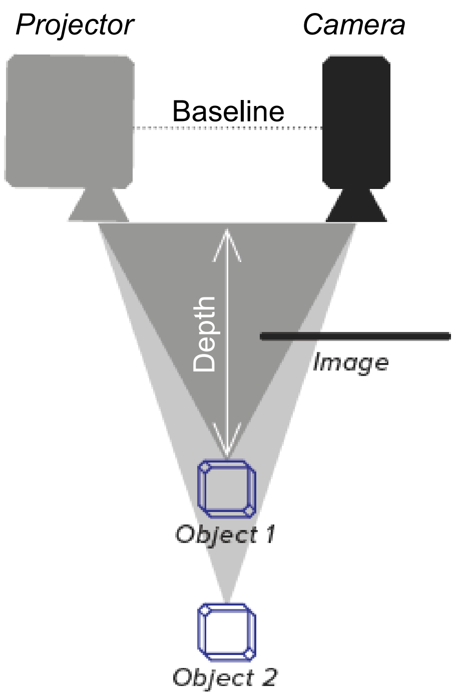

Principles of Structured Light [11]

- Structured light utilizes VCSEL arrays as the premier illumination source for sensing
- Benefit from spatial profile, brightness and spectral characteristics of the VCSEL light

Presentation Outline

Single-Polarization VCSEL Motivation

- Optical Polarization Control for VCSELs

Polarization-Controlled IID VCSELs

- High-Power Single-Mode IID VCSELs
- Disorder-Defined Apertures for Single-Polarization
- Polarization-Resolved LIV and OPSR Analysis

Anti-Phase Coating VCSELs

- Anti-Phase Coating Theory and Simulation
- High-Power Single-Mode VCSEL Operation
- Single-Mode, Single-Polarization VCSELs

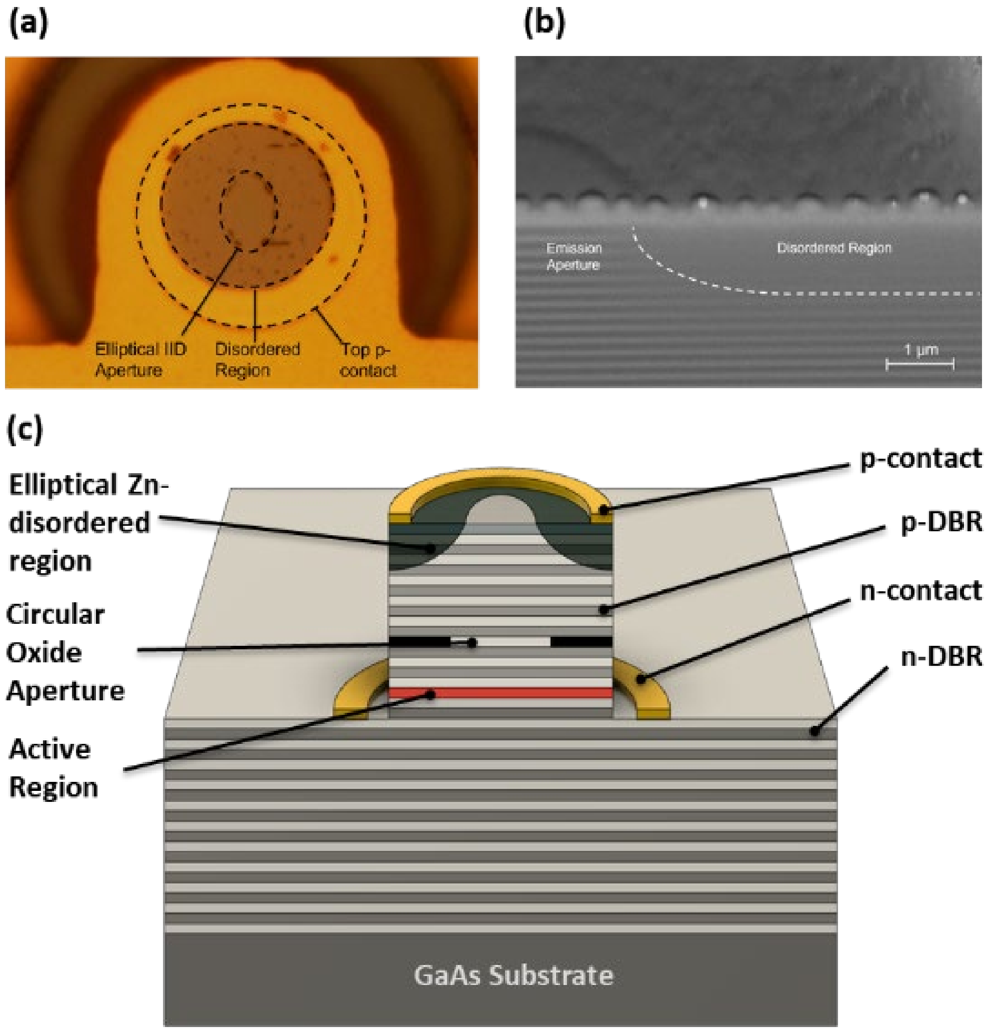

Impurity-Induced Disordering

Significance of Impurity-Induced Disordering

- Laidig and Holonyak et al. [14] recognized diffused Zn intermixes and disorders discrete AlAs-GaAs superlattices
- Zinc diffusion results in smooth, homogenous, bulk $Al_xGa_{1-x}As$ of the original superlattice pairs
- Enables spatially modified index of refraction, bandgap, optical reflectivity, and conductivity of $Al_xGa_{1-x}As$

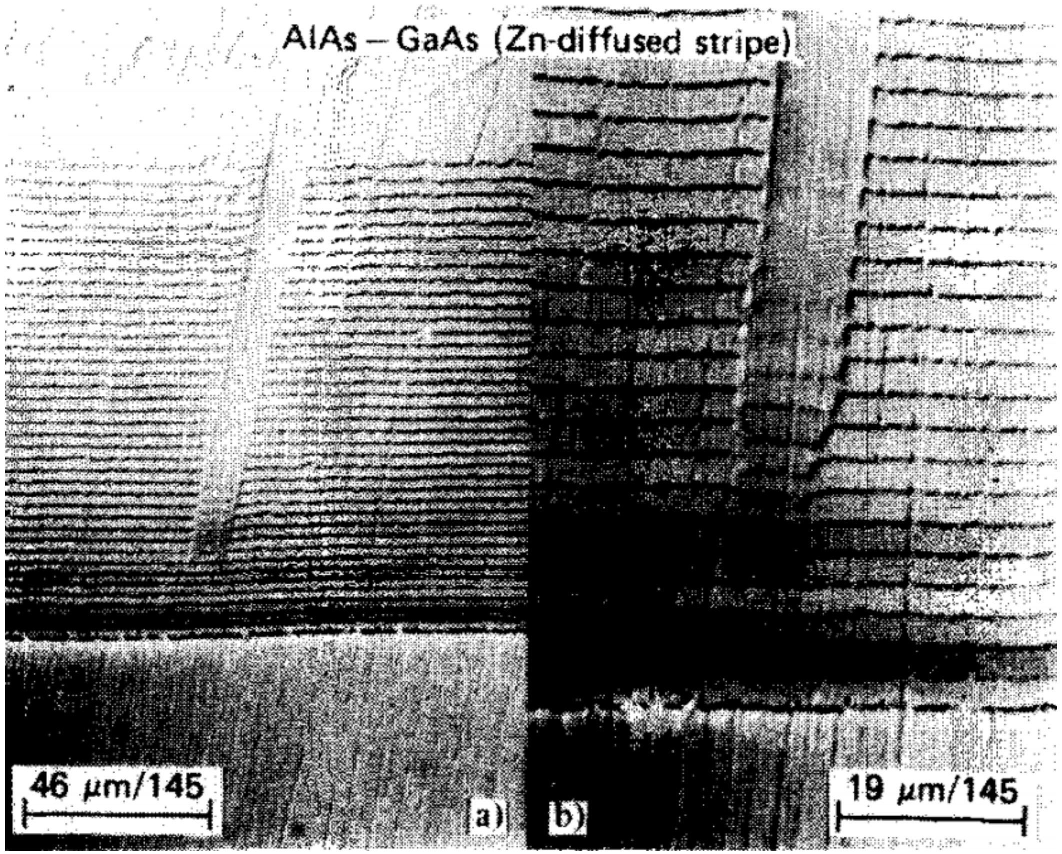

Angle-lapped Micrograph of a Disordered AlAs-GaAs Superlattice via Zn-Diffusion

Laidig, W. D., et al. "Disorder of an AlAs-GaAs superlattice by impurity diffusion." Applied Physics Letters 38.10 (1981): 776-778.

Disorder-Defined Apertures for Single-Mode

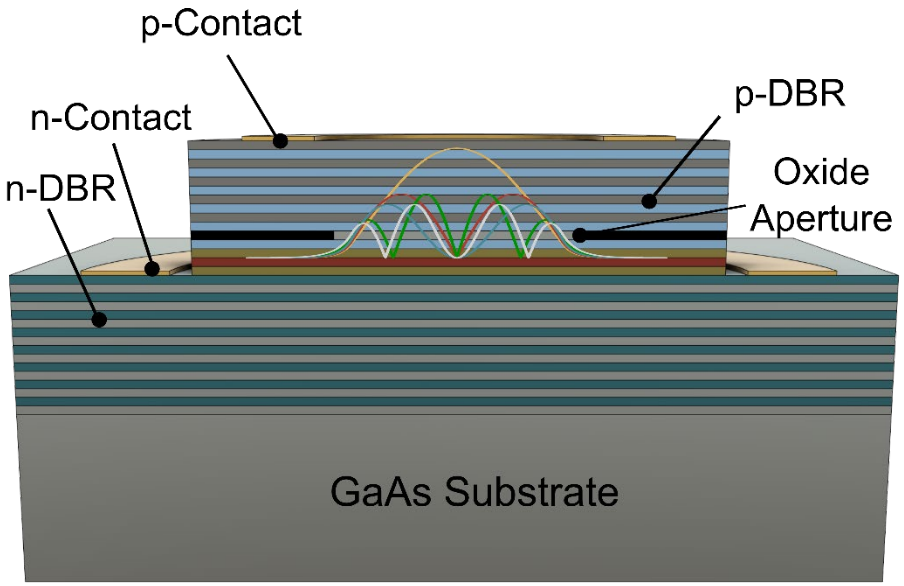

Cross-sectional view of
a Traditional VCSEL

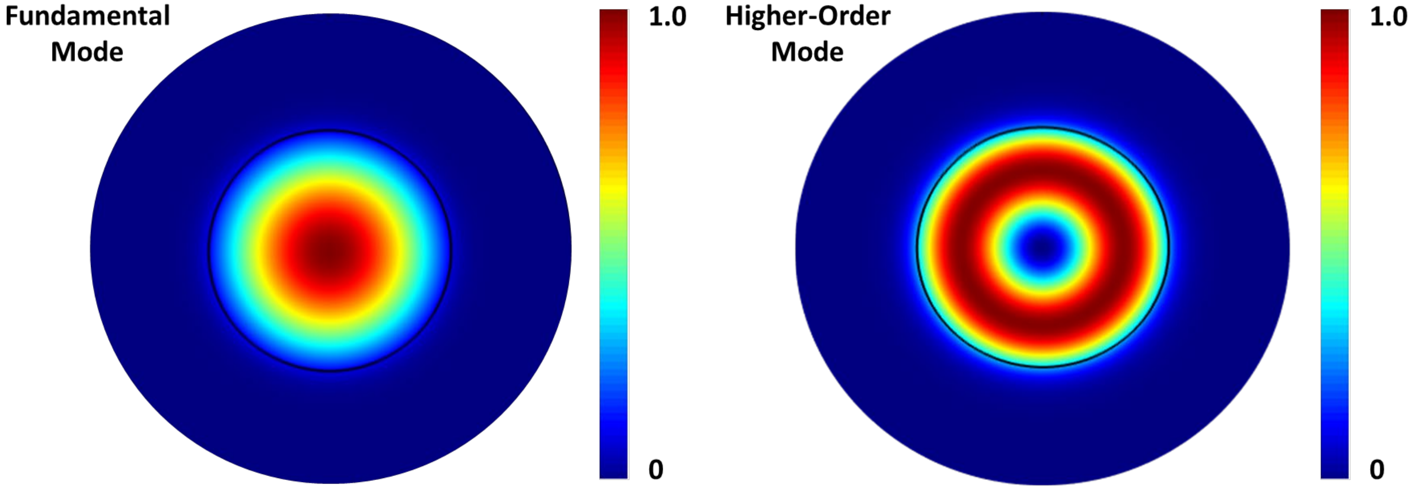

Top-Side View of Optical Transverse Modes in
a Traditional VCSEL

- Design disordering region in the shape of an aperture that leaves the center unaffected
- Disorder-defined aperture designed to induce higher threshold modal gain selectively to higher-order modes

Disorder-Defined Apertures for Single-Mode

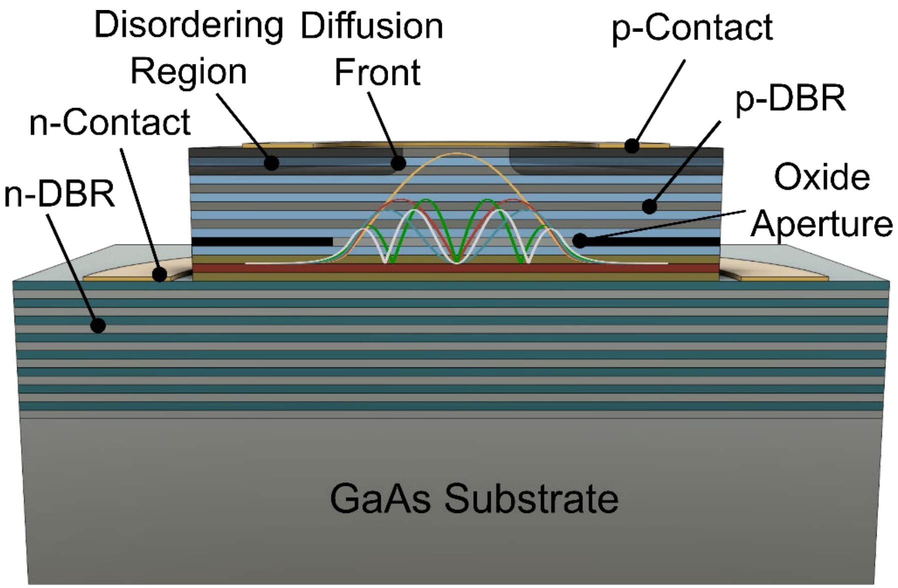

Cross-sectional view of
a Disorder-Defined VCSEL

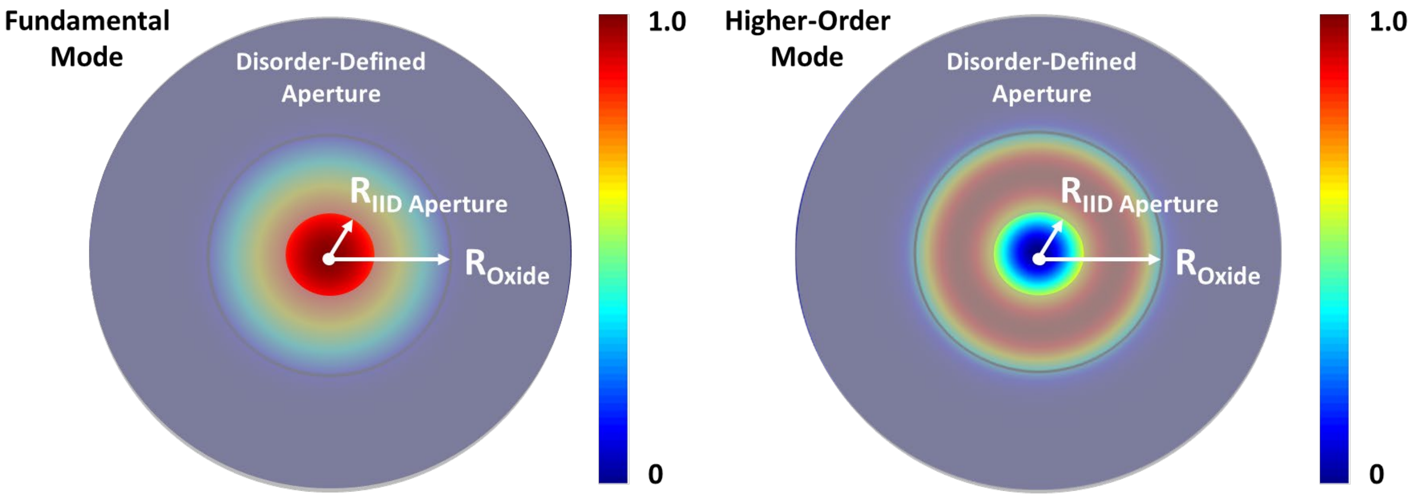

Top-Side View of Optical Transverse Modes in
a Disorder-Defined VCSEL

- Design disordering region in the shape of an aperture that leaves the center unaffected
- Disorder-defined aperture designed to induce higher threshold modal gain selectively to higher-order modes

Impact of Diffusion Mask Strain

Varying Diffusion Mask Strain

- Compressively-, unstrained, and tensilely-strained SiN_x diffusion masks are utilized for fabricating single-mode IID VCSELs
- Diffusion mask strain impacts single-mode performance
- Devices fabricated using high-power designed epitaxy and standard-oxide confined VCSEL process with 0.5 µm larger IID aperture

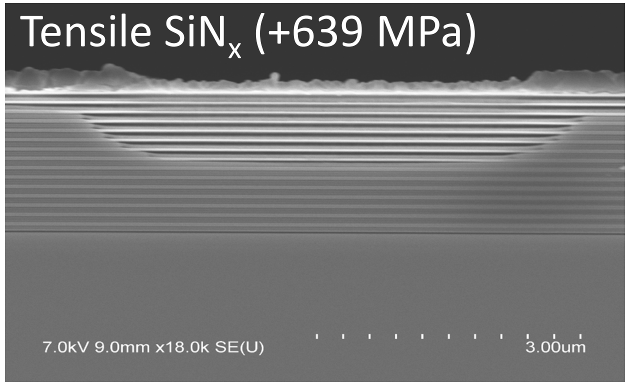

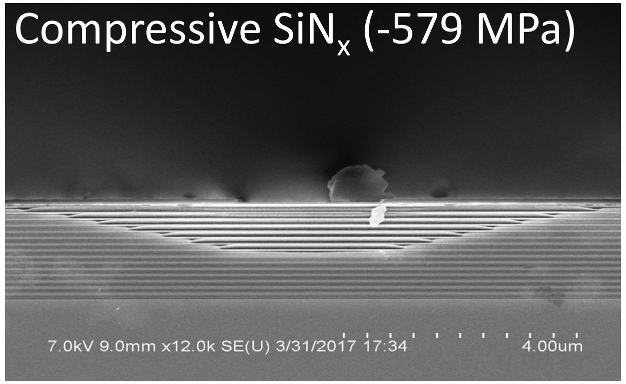

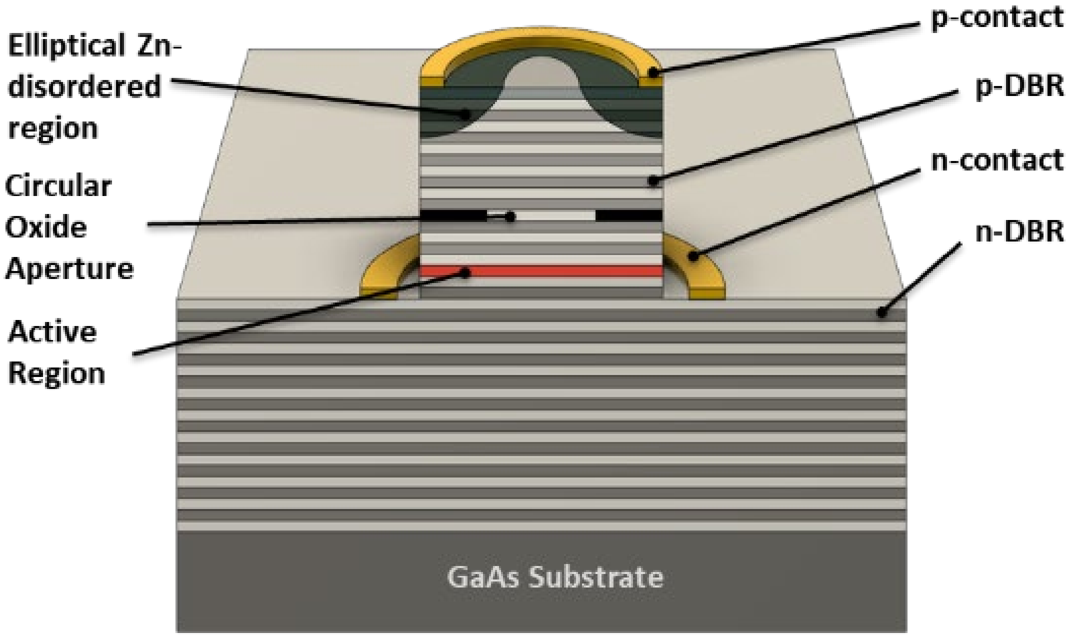

High-Power VCSEL Characterization

Electro-optic and Spectral Performance

- VCSELs tested under continuous-wave (CW), room-temperature operation
- Spectra collected confirms single-fundamental-mode lasing (SMSR > 30 dB)

Oxide-Aperture Diameter	Disordering Aperture	Max SM Power	Diff. Resistance
9 µm	3.0 µm	8.52 mW	92 Ω
10 µm	3.6 µm	9.57 mW	82 Ω
11 µm	4.0 µm	10.20 mW	79 Ω
12 µm	4.1 µm	10.57 mW	64 Ω
13 µm	4.7 µm	10.95 mW	58 Ω

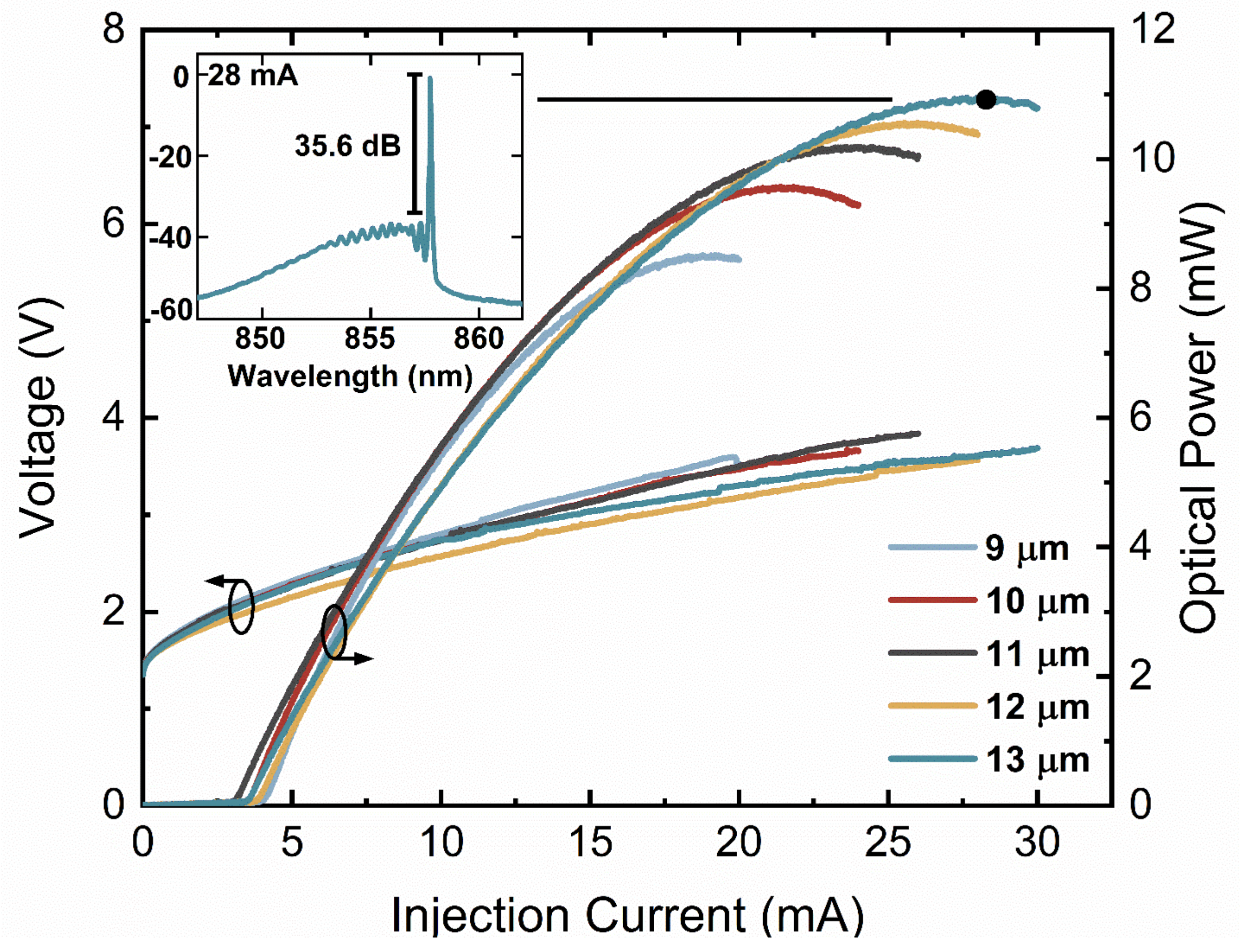

Light-current-voltage characteristics and with optical spectra inset of 13 µm IID VCSEL [13]

[13] Su, Patrick, et al. "High-power single-mode vertical-cavity surface-emitting lasers using strain-controlled disorder-defined apertures." Applied Physics Letters 119.24 (2021): 241101.

Benchmarking High-Power Single-Mode VCSELs

Record-Setting Single-Mode Output Power

- Literature review of high-power single-mode VCSELs using any method
- Surface relief, high contrast gratings, ARROW design, holey-structures, anti-phase filters, and other Zn-diffusion/IID VCSEL work shown
- Strain-controlled disorder-defined apertures achieves world-record single-mode output powers

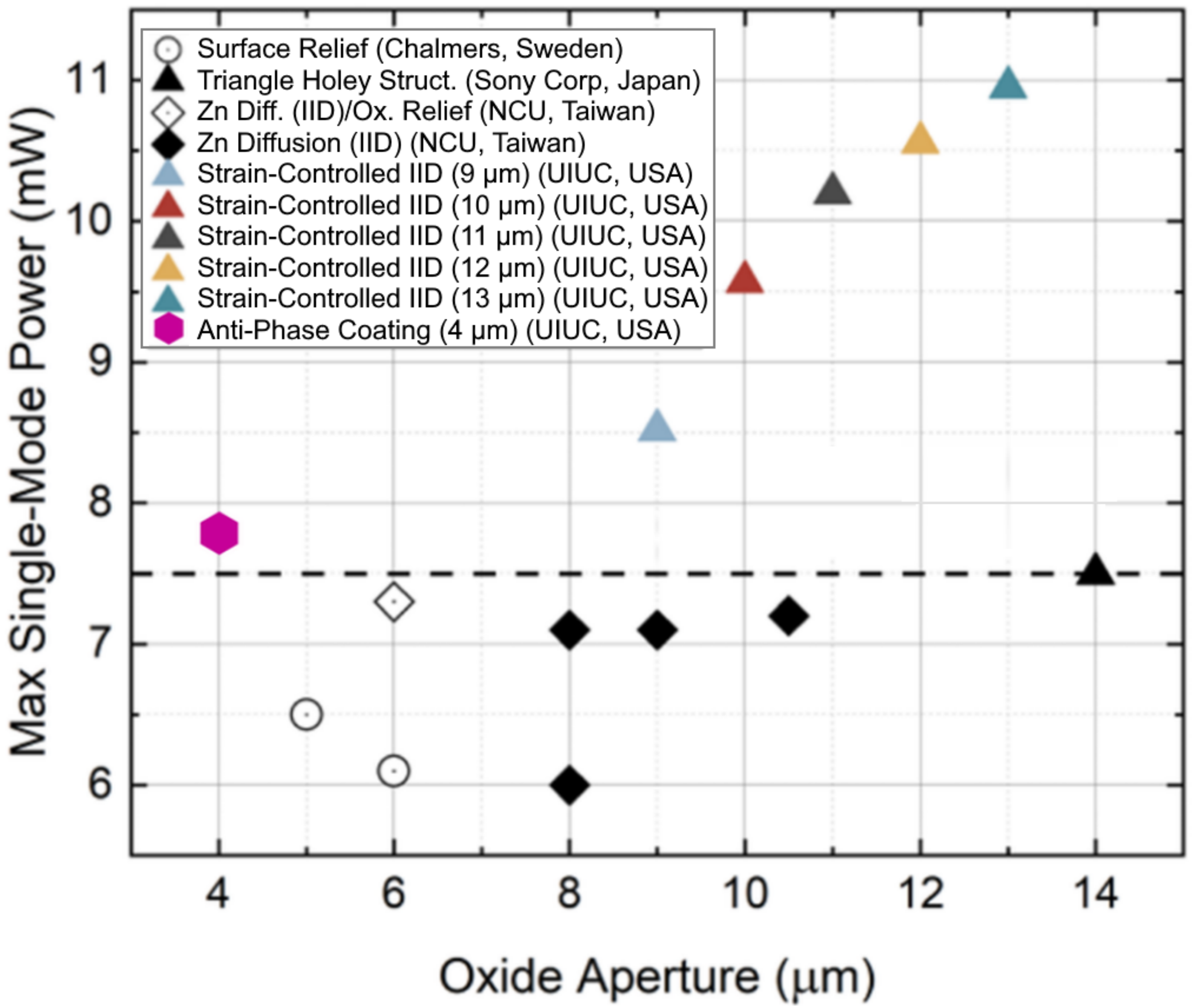

Single-Polarization VCSELs using Elliptical Apertures

Polarization Control in VCSELs

- VCSELs inherently emit in an unstable polarization state [12], aligned to either the [110] and [1$\bar{1}$0] crystal axes
- Any fluctuation in temperature, injection current, and package strain leads to “polarization-switching”
- Singe-polarization emission reduces RIN [22] and improves fidelity in depth sensors [23]
- Asymmetric disorder-defined/anti-phase coating apertures are designed to suppress certain polarization states

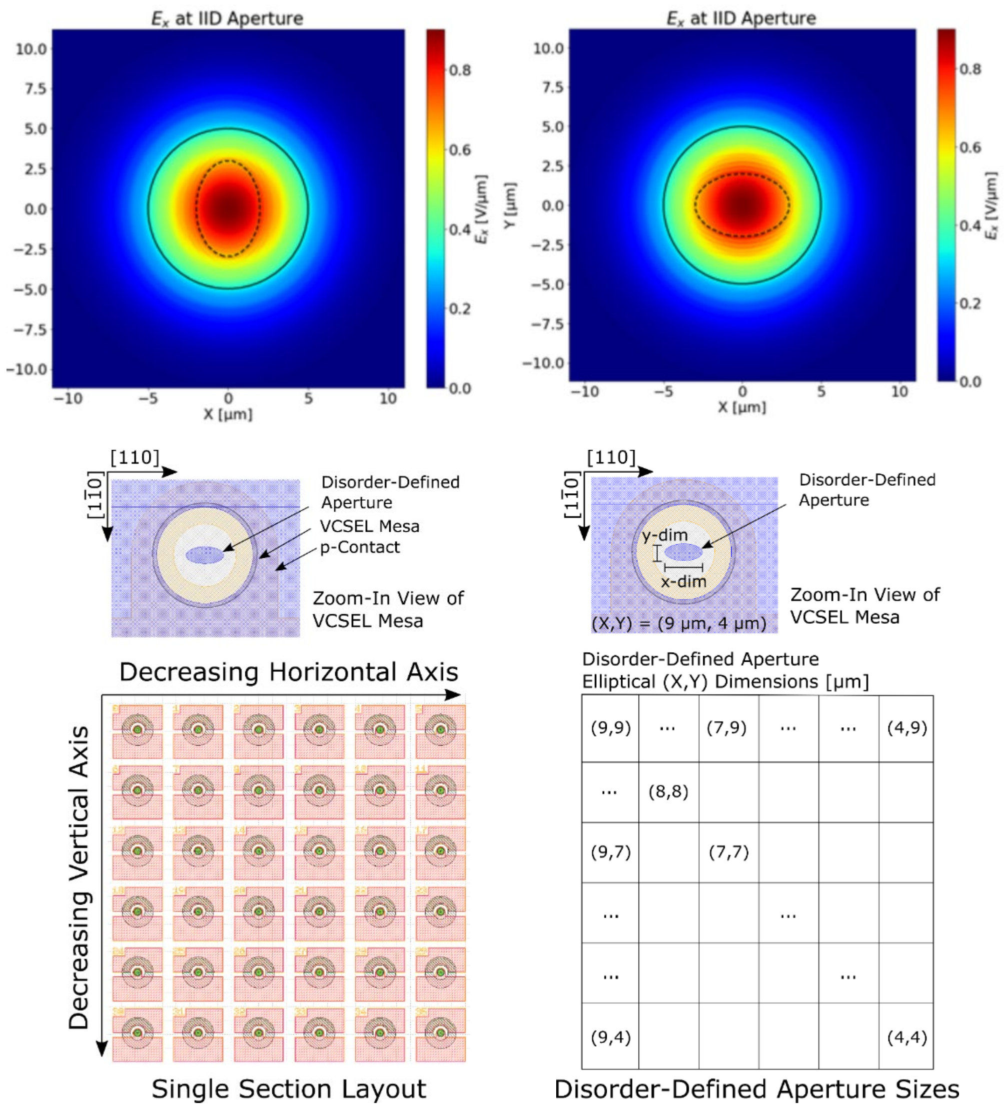

PR-LIV of 10 µm Non-Disordered VCSELs

Baseline PR-LIV Measurements

- Non-disordered 10 µm VCSELs are characterized for their PR-LIV characteristics
- Major and minor axis measurements are swept separately
- Major and minor axis L-I show fluctuations in polarization emission
- Total major + minor axis L-I returns smooth VCSEL L-I characteristic

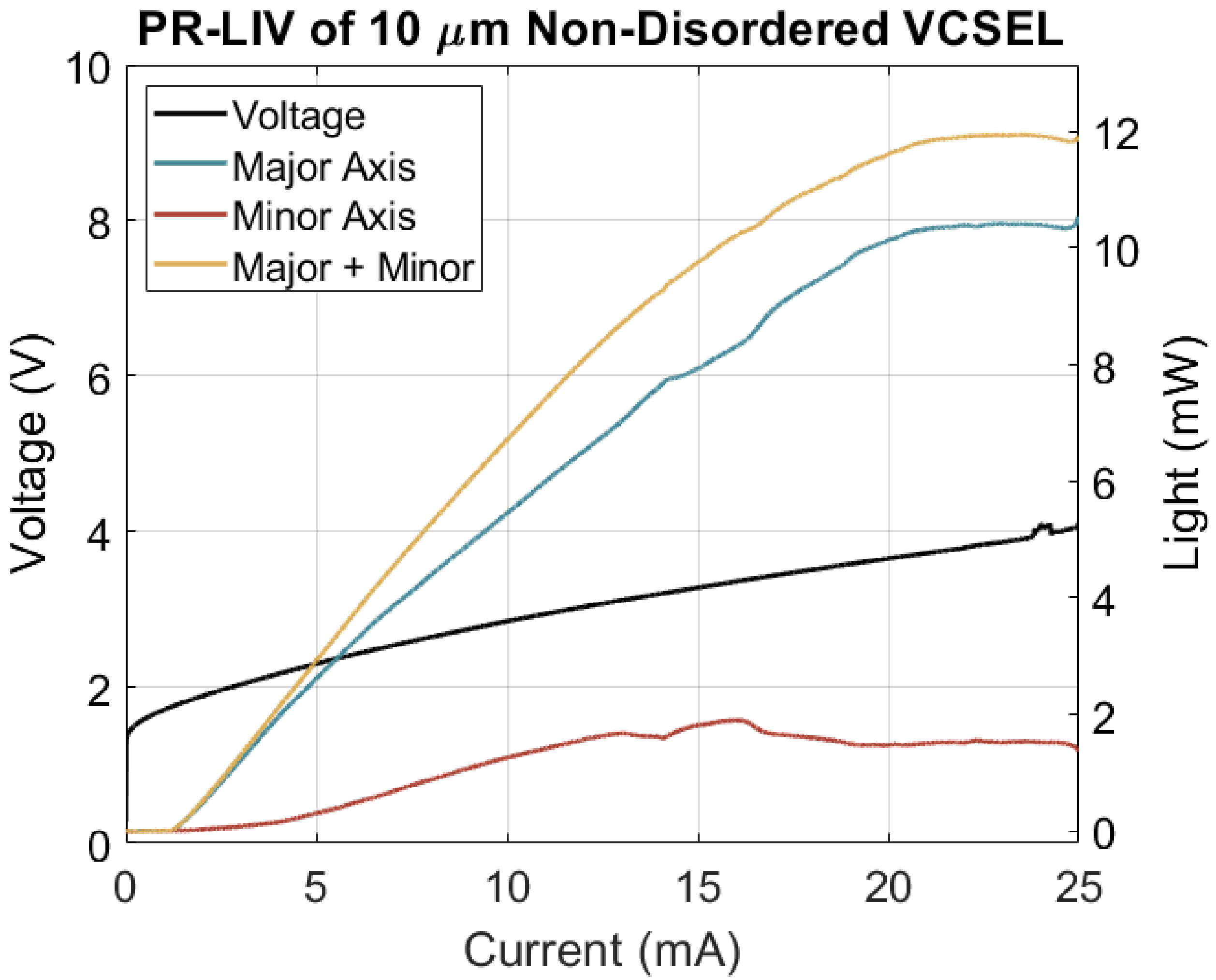

OPSR of 10 μm Non-Disordered (ND) VCSELs

Baseline OPSR Measurements

$$\text{OPSR} = 10\log_{10}\left(\frac{P_{maj.}}{P_{min.}}\right)$$

- OPSR is calculated using PR-LIV characteristic measured for three separate ND VCSEL devices
- OPSR target mark is 20 dB from major axis to minor axis using total power as opposed to spectral peak-to-peak
- OPSR of ND VCSELs show rather unstable, low-degree of polarization emission
- Minor degree of polarization attributed to strained MQW and 2° off-cut GaAs substrate

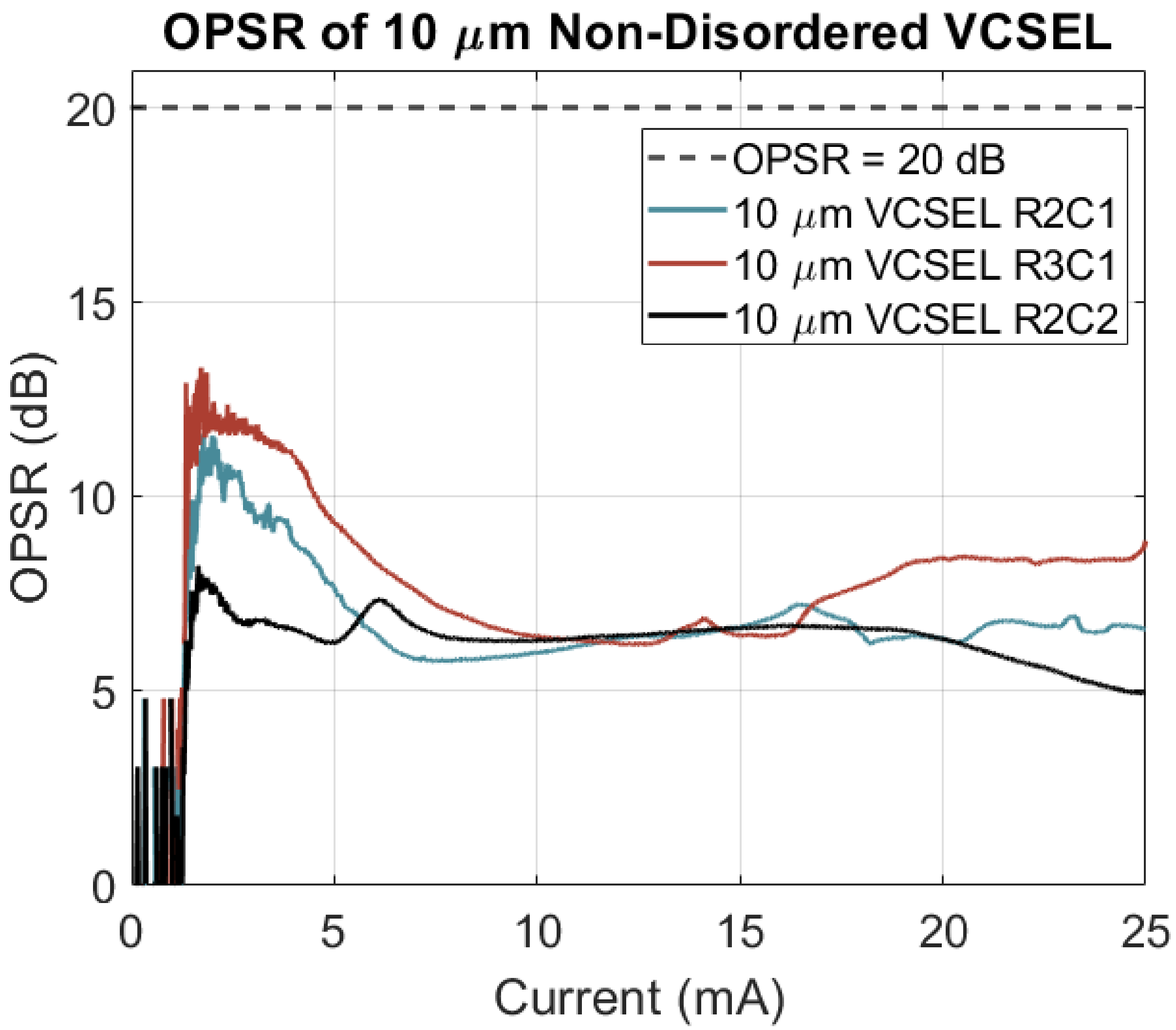

PR-LIV of Circularly-Disordered 10 μm VCSELs

Circularly-Shaped Disorder-Defined VCSELs

- Symmetrically shaped disorder-defined VCSELs are characterized for PR-LIV and OPSR
- For a (9,9) μm IID apertures, improvement in single-polarization emission is shown
- Delayed stimulated emission from minor axis until 7 mA and falls off at 14 mA
- Major and minor axis are separate sweeps, shows consistency of polarization switching effect

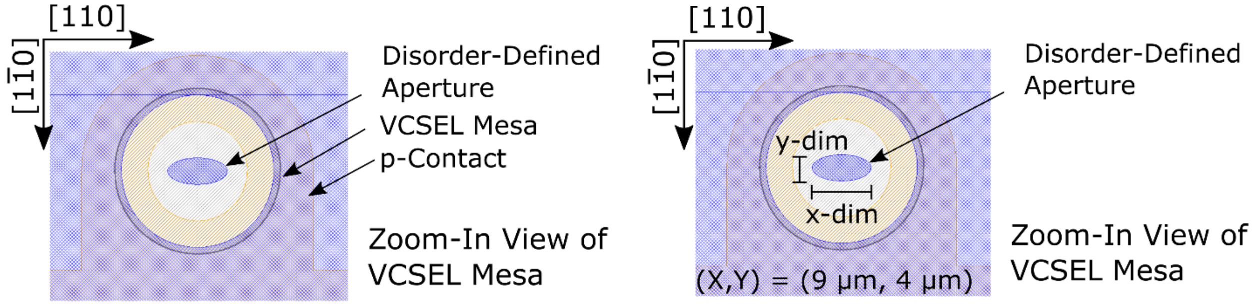

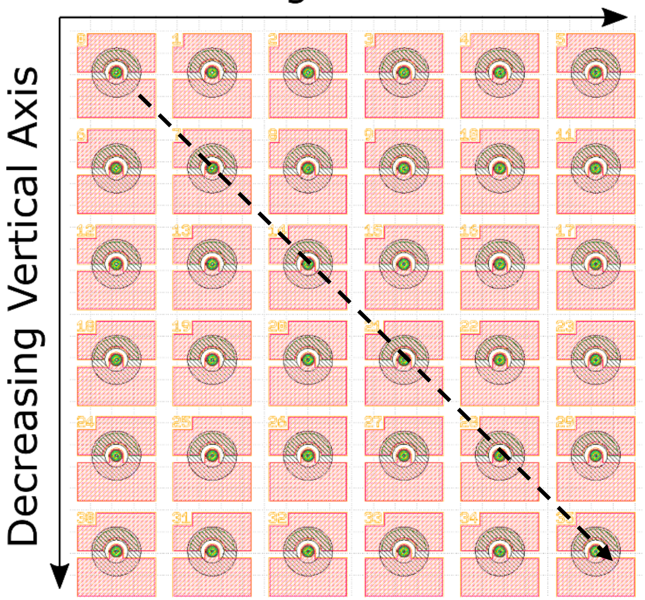

Single Section Layout

Disorder-Defined Aperture Elliptical (X,Y) Dimensions [μm]

(9,9)	...	(7,9)	...	...	(4,9)
...	(8,8)				
(9,7)		(7,7)			
...			...		
...				...	
(9,4)					(4,4)

Disorder-Defined Aperture Sizes

PR-LIV of Circularly-Disordered 10 µm VCSELs

Circularly-Shaped Disorder-Defined VCSELs

- Symmetrically shaped disorder-defined VCSELs are characterized for PR-LIV and OPSR
- For a (9,9) µm IID apertures, improvement in single-polarization emission is shown
- Delayed stimulated emission from minor axis until 7 mA and falls off at 14 mA
- Major and minor axis are separate sweeps, shows consistency of polarization switching effect

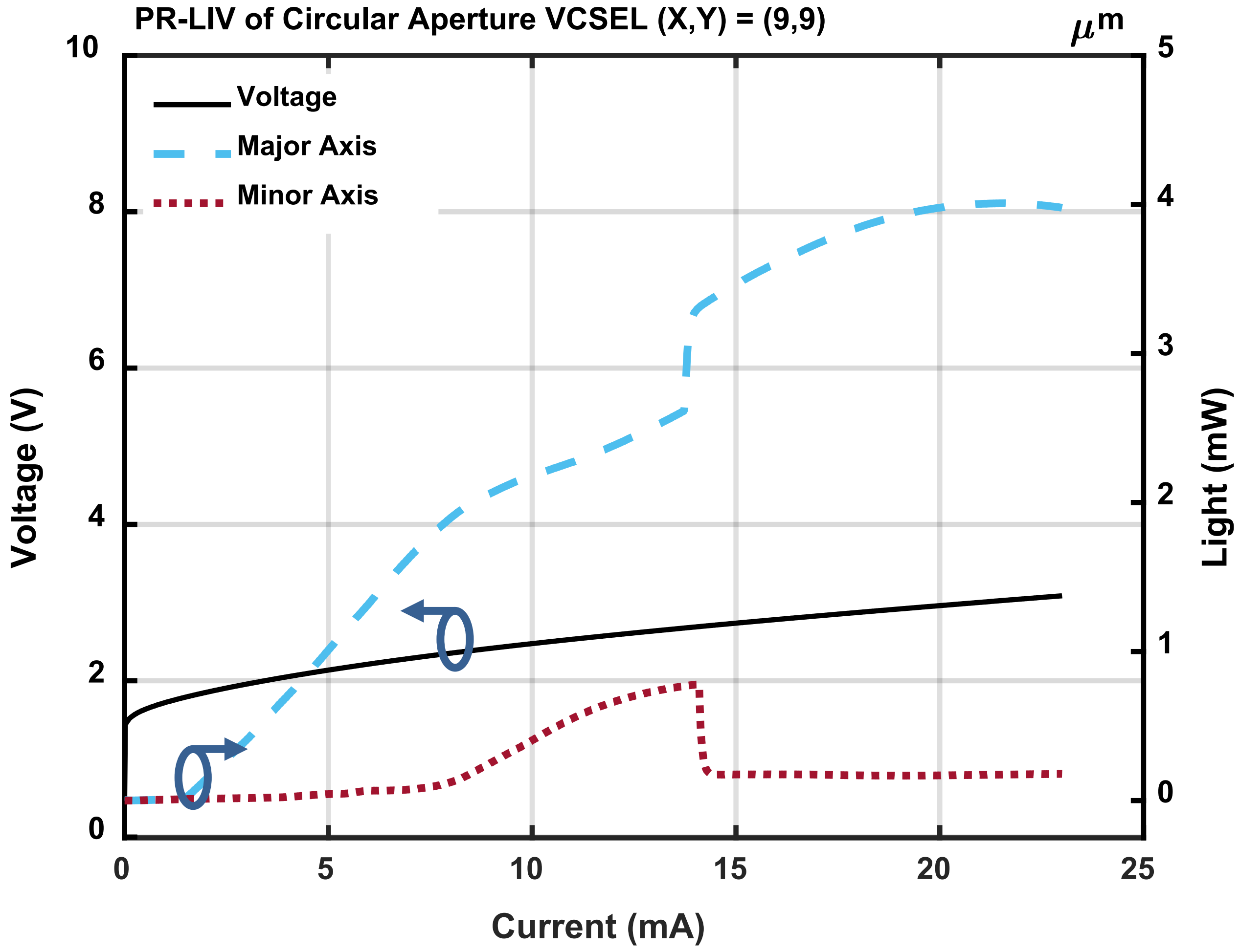

OPSR of Circularly-Disordered 10 µm VCSELs

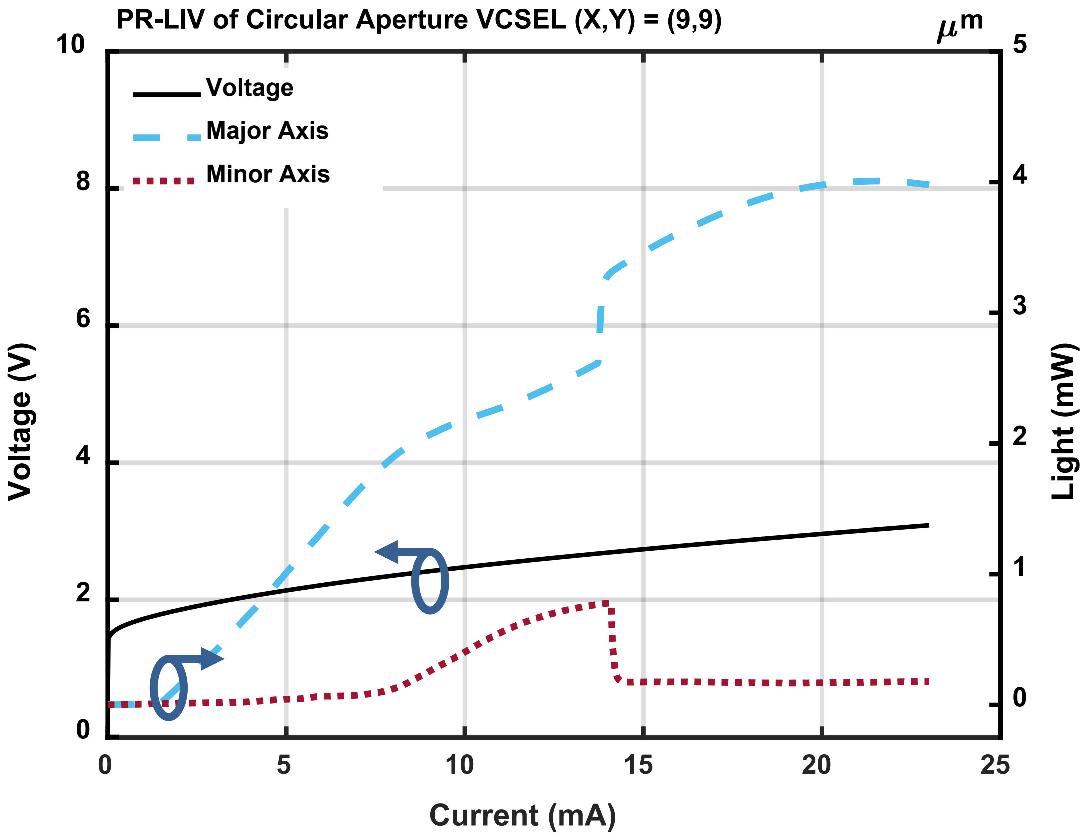

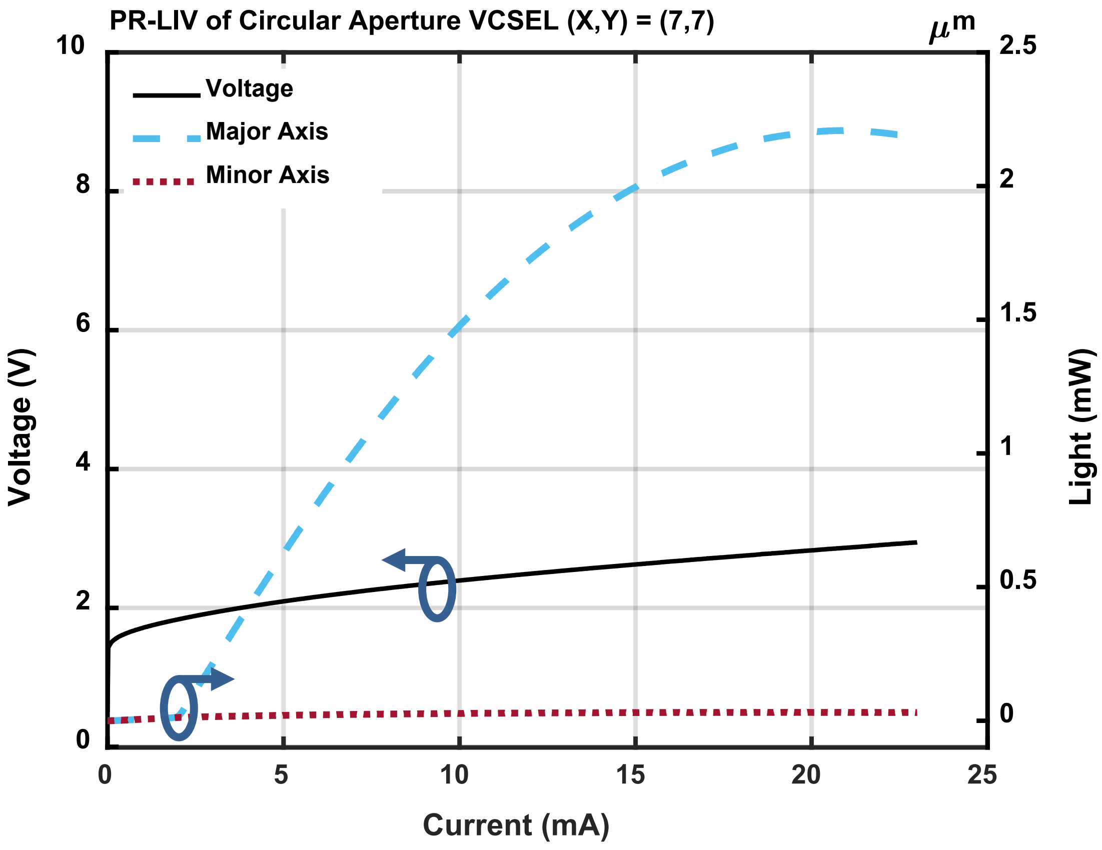

- OPSR of (7,7) µm circularly-shaped improvement over (9,9) µm circularly-shaped with lower output power

OPSR of Circularly-Disordered 10 µm VCSELs

Circularly-Shaped Disorder-Defined VCSELs

- For large (9 µm) circularly-disordered VCSELs, the degree of polarization improves (~13 dB)
- For smaller (7 µm) circularly-disordered VCSELs, single polarization achieved (~18 dB)
- Smallest (5 µm) circularly-disordered VCSELs degrades major axis, hence, lower OPSR (~15 dB)

$$\text{OPSR} = 10\log_{10}\left(\frac{P_{maj.}}{P_{min.}}\right)$$

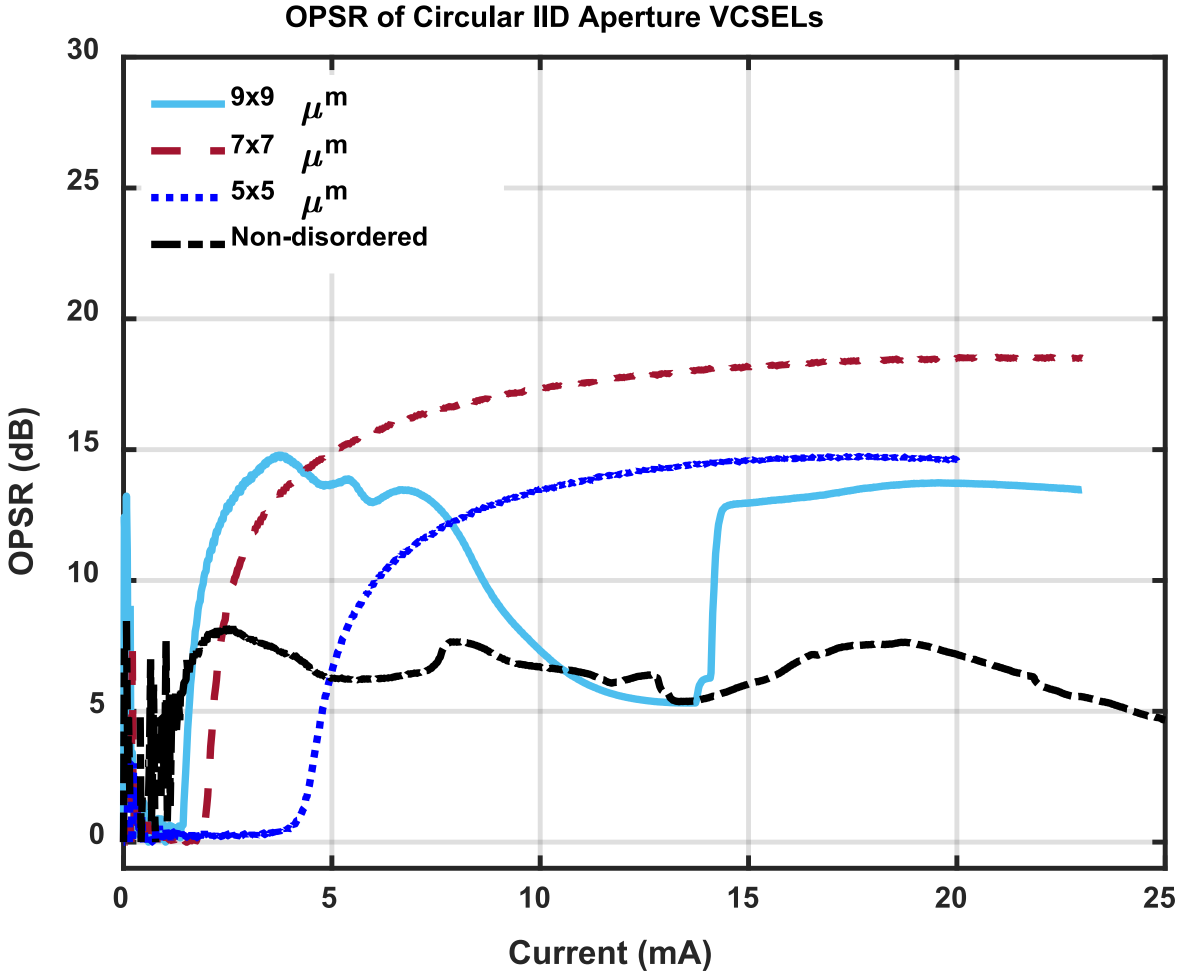

PR-LIV of Elliptically-Shaped 10 µm VCSELs

Elliptically-Shaped Disordered VCSELs

- PR-LIV of circular (9,9) µm IID VCSEL shows moderate polarizations switching
- PR-LIV of elliptical (9,8) µm IID VCSEL shows strong single-polarization emission
- PR-LIV of elliptical (9,6) µm IID VCSEL shows single-polarization emission with less output power

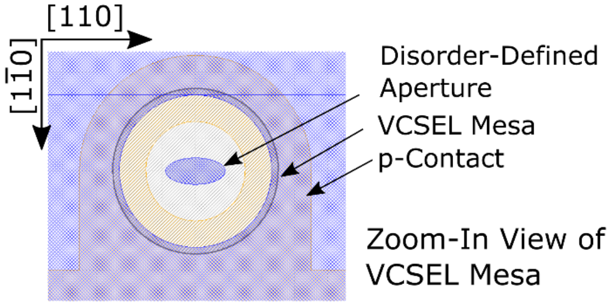

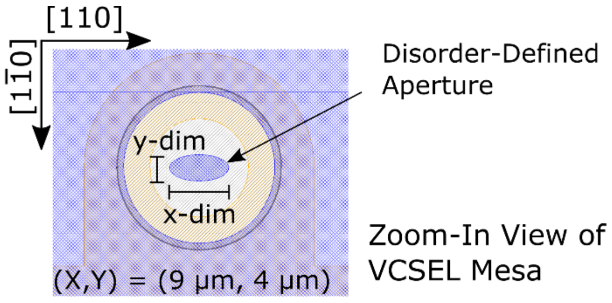

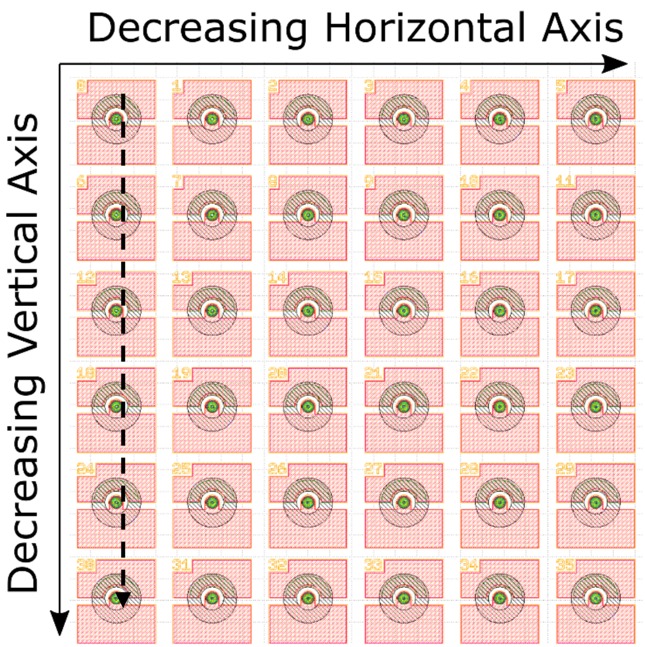

Single Section Layout

Disorder-Defined Aperture Elliptical (X,Y) Dimensions [µm]

(9,9)	…	(7,9)	…	…	(4,9)
…	(8,8)				
(9,7)		(7,7)			
…			…		
…				…	
(9,4)					(4,4)

Disorder-Defined Aperture Sizes

PR-LIV of Elliptically-Shaped 10 µm VCSELs

Elliptically-Shaped Disordered VCSELs

- PR-LIV of circular (9,9) µm IID VCSEL shows moderate polarizations switching
- PR-LIV of elliptical (9,8) µm IID VCSEL shows strong single-polarization emission
- PR-Spectra of elliptical (9,8) µm IID VCSEL confirms single-polarization emission with spectral OPSR >19 dB
- PR-LIV of elliptical (9,6) µm IID VCSEL shows single-polarization emission with less output power

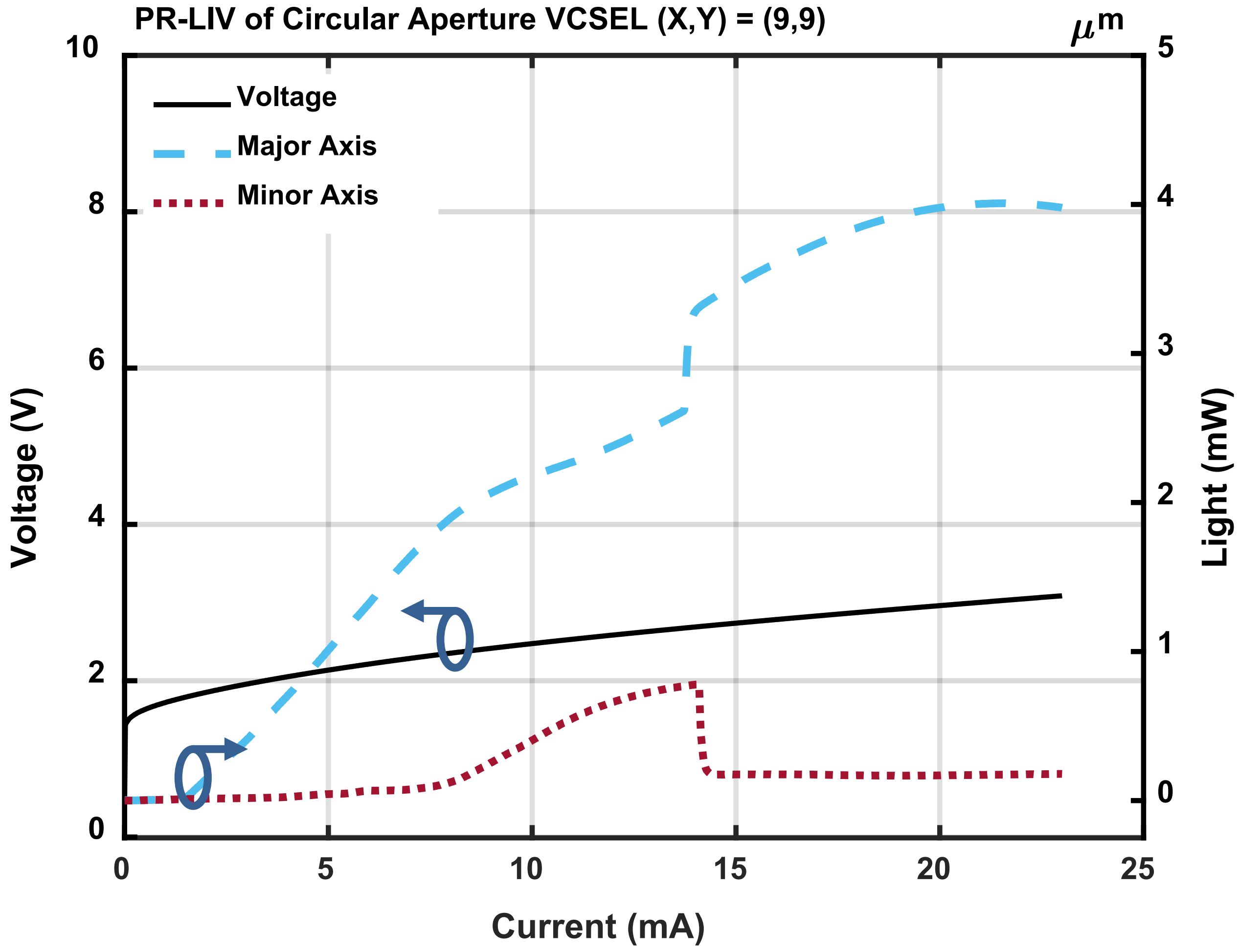

PR-LIV of Elliptically-Shaped 10 µm VCSELs

<u>Elliptically-Shaped Disordered VCSELs</u>

- PR-LIV of circular (9,9) µm IID VCSEL shows moderate polarizations switching
- PR-LIV of elliptical (9,8) µm IID VCSEL shows strong single-polarization emission
- PR-Spectra of elliptical (9,8) µm IID VCSEL confirms single-polarization emission with spectral OPSR >19 dB
- PR-LIV of elliptical (9,6) µm IID VCSEL shows single-polarization emission with less output power

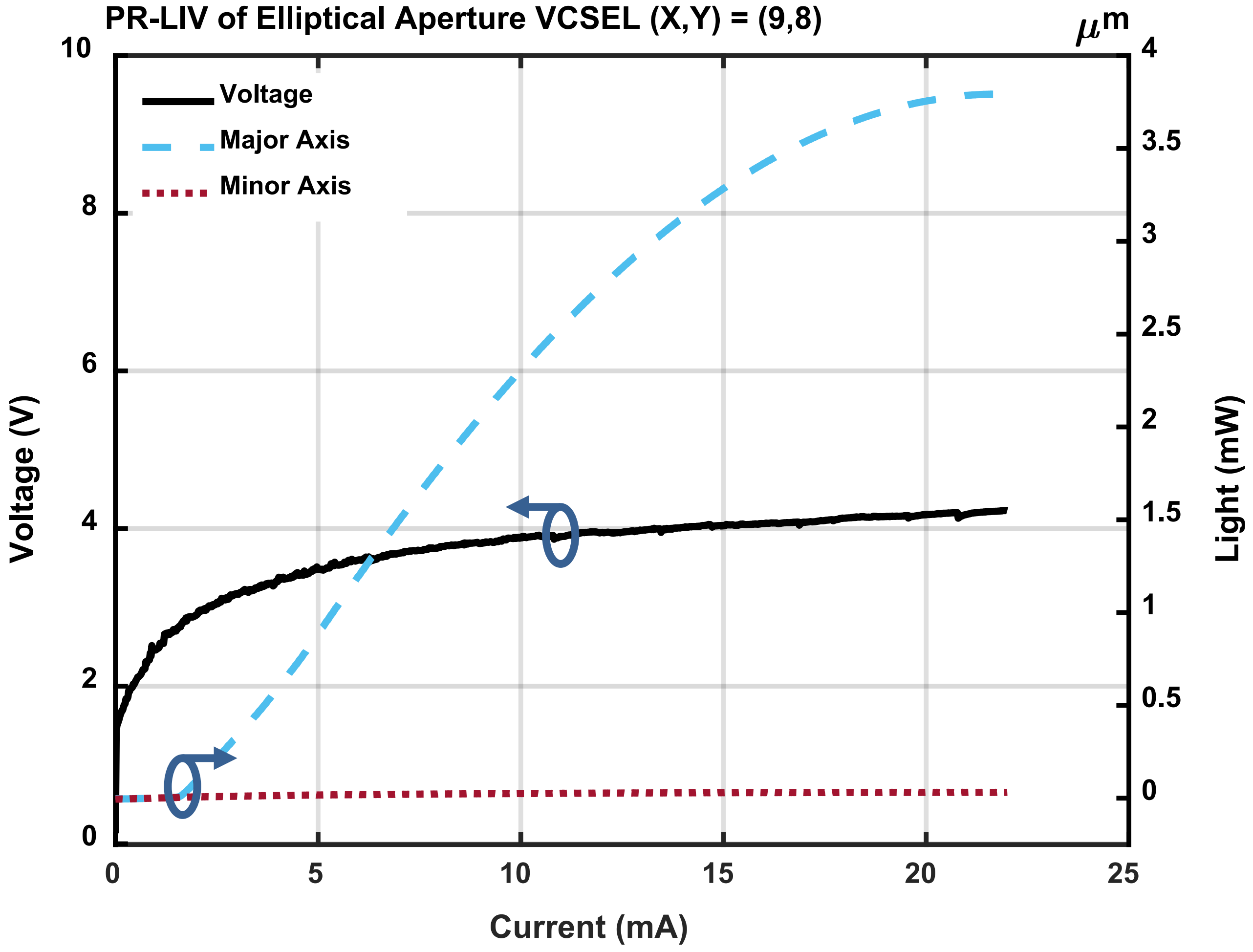

PR-LIV of Elliptically-Shaped 10 µm VCSELs

Elliptically-Shaped Disordered VCSELs

- PR-LIV of circular (9,9) µm IID VCSEL shows moderate polarizations switching
- PR-LIV of elliptical (9,8) µm IID VCSEL shows strong single-polarization emission
- PR-Spectra of elliptical (9,8) µm IID VCSEL confirms single-polarization emission with spectral $OPSR_s$ >19 dB
- PR-LIV of elliptical (9,6) µm IID VCSEL shows single-polarization emission with less output power

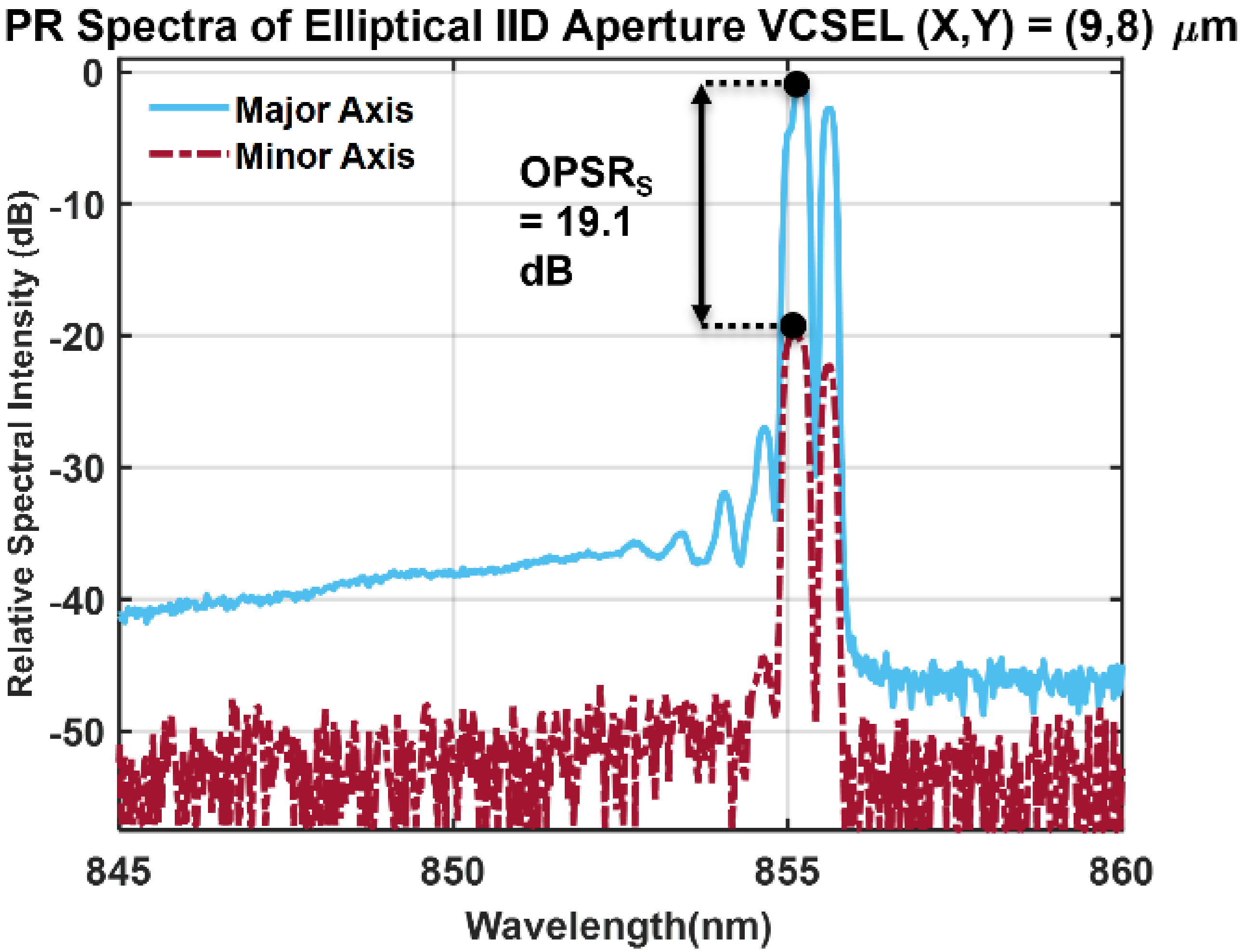

PR-LIV of Elliptically-Shaped 10 µm VCSELs

Elliptically-Shaped Disordered VCSELs

- PR-LIV of circular (9,9) µm IID VCSEL shows moderate polarizations switching
- PR-LIV of elliptical (9,8) µm IID VCSEL shows strong single-polarization emission
- PR-Spectra of elliptical (9,8) µm IID VCSEL confirms single-polarization emission with spectral OPSR >19 dB
- PR-LIV of elliptical (9,6) µm IID VCSEL shows single-polarization emission with less output power

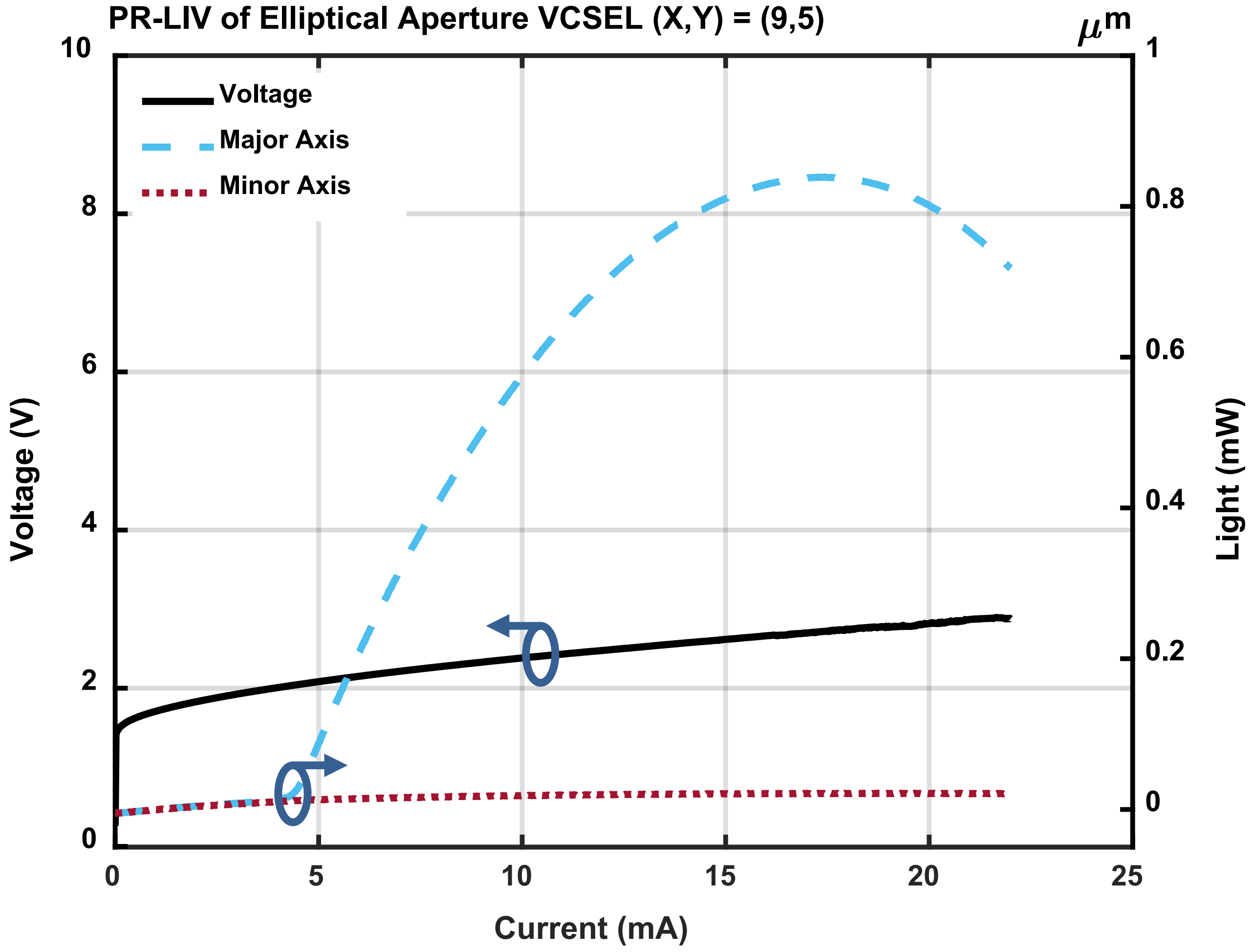

OPSR of Elliptically-Shaped 10 µm VCSELs

Elliptically-Shaped Disordered VCSELs

- Elliptical (9,8) µm IID VCSEL show strong (OPSR > 20 dB) single-polarization emission
- Shrinking minor axis only begins to degrade total output power and hence OPSR
- OPSR in these devices are limited by the amount of major axis output power

$$\text{OPSR} = 10\log_{10}\left(\frac{P_{maj.}}{P_{min.}}\right)$$

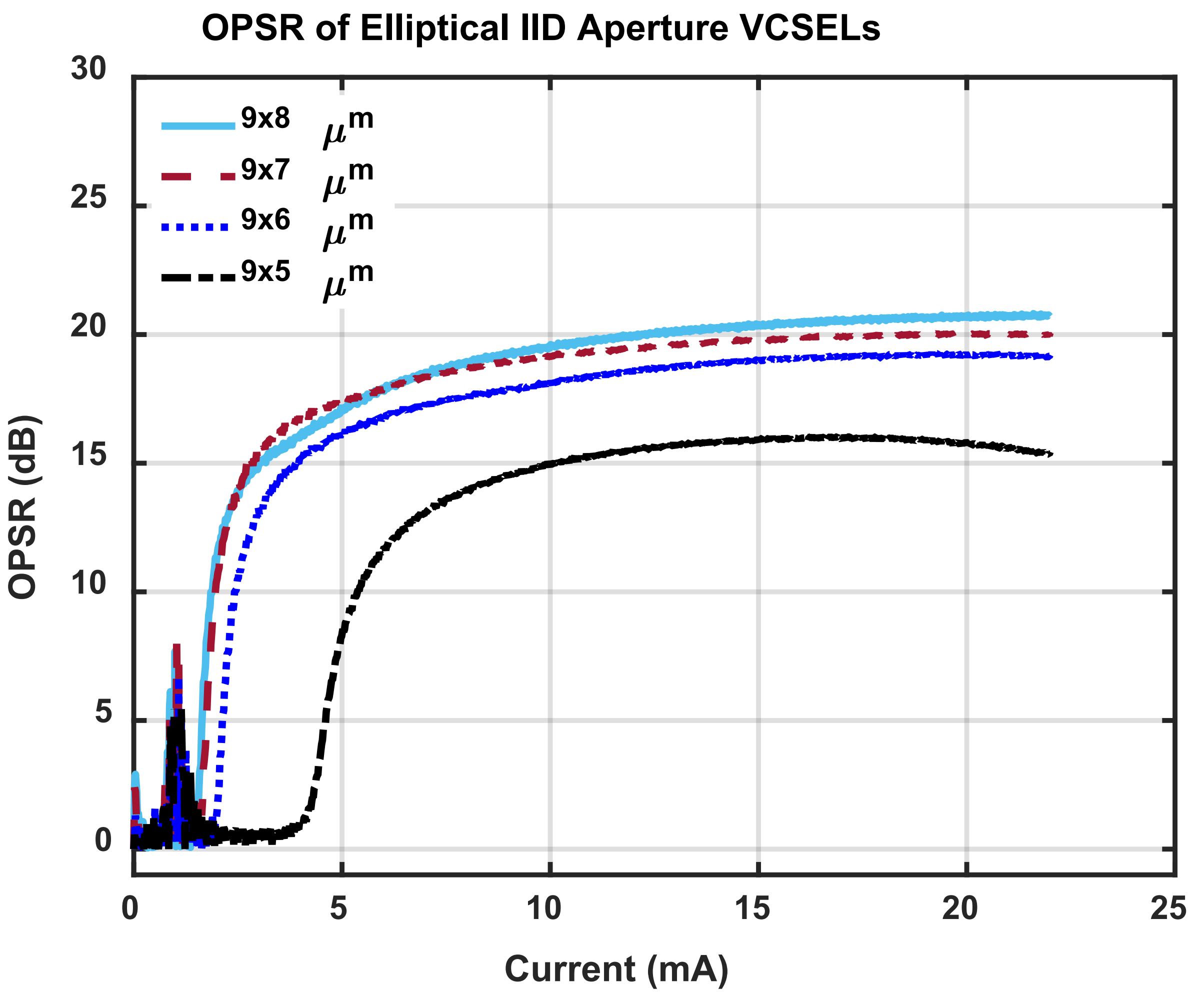

Summary of Polarization Control VCSEL

Single-Polarization IID VCSELs

- Demonstrated single-polarization (OPSR > 20 dB) disorder-defined VCSELs using elliptically-shaped apertures
- Polarization very sensitive and even a slightly asymmetric aperture can achieve high degree of polarization

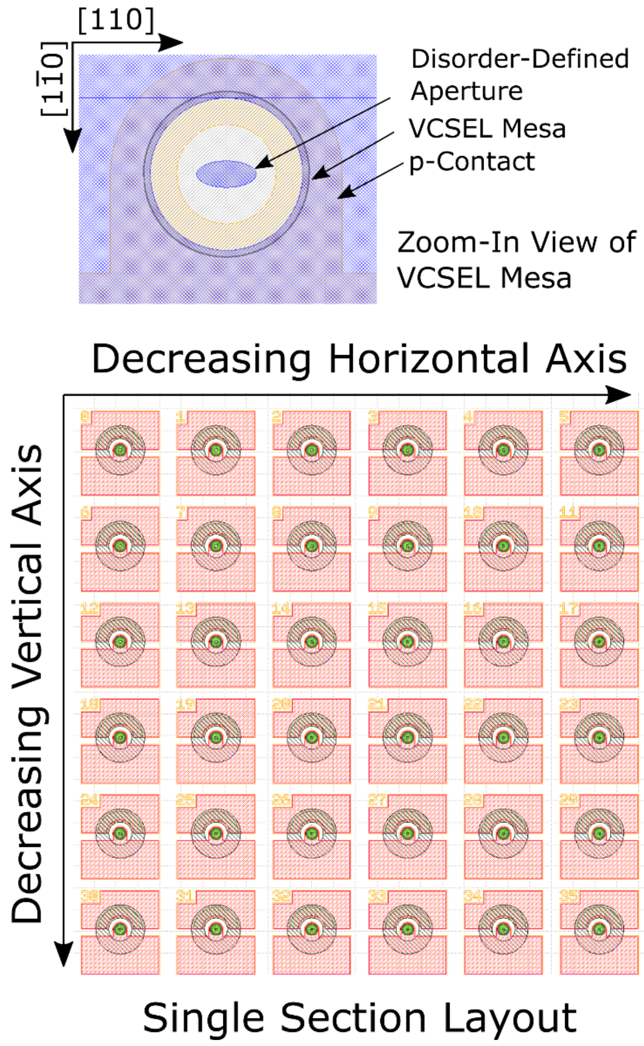

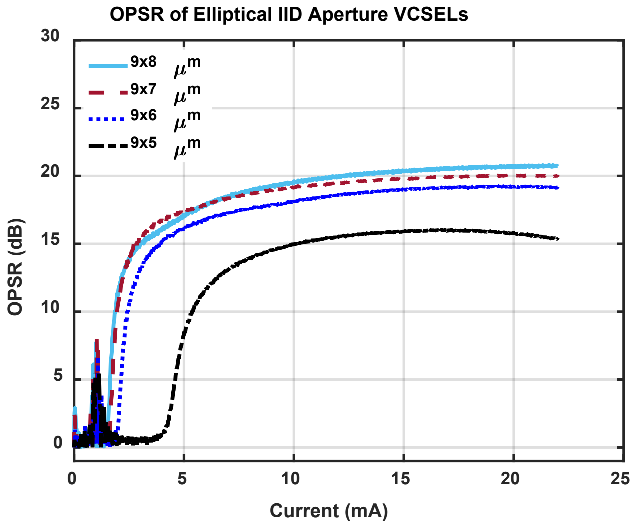

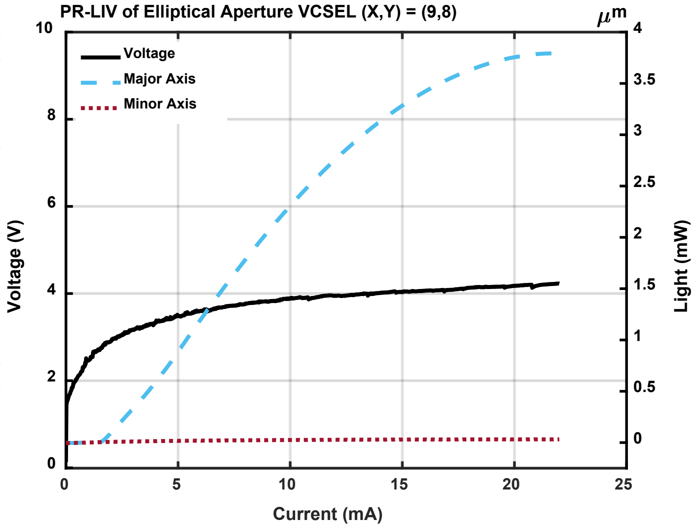

Presentation Outline

Single-Polarization VCSEL Motivation

- Optical Polarization Control for VCSELs

Polarization-Controlled IID VCSELs

- High-Power Single-Mode IID VCSELs
- Disorder-Defined Apertures for Single-Polarization
- Polarization-Resolved LIV and OPSR Analysis

Anti-Phase Coating VCSELs

- Anti-Phase Coating Theory and Simulation
- High-Power Single-Mode VCSEL Operation
- Single-Mode, Single-Polarization VCSELs

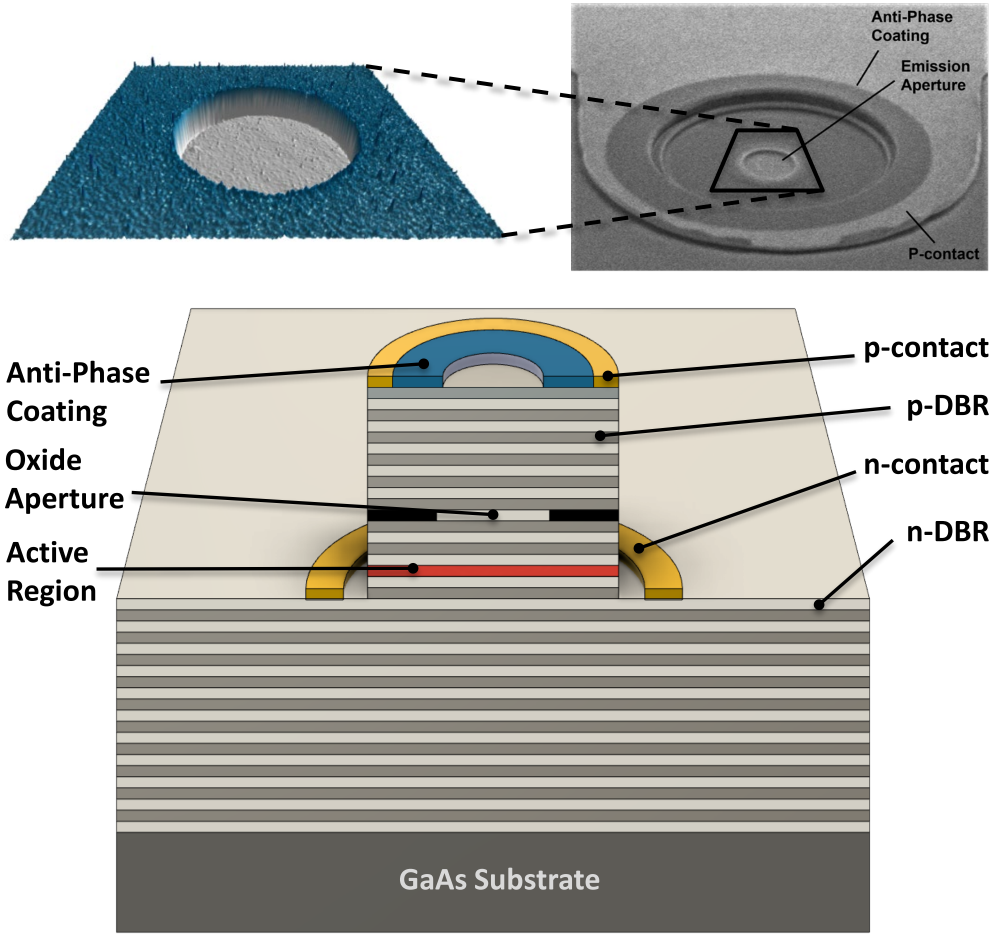

AFM (top, left) and SEM (top, right) Image of Anti-Phase Coating VCSEL with Cross-Sectional Schematic (bottom)

Anti-Phase Coating Motivation and Background

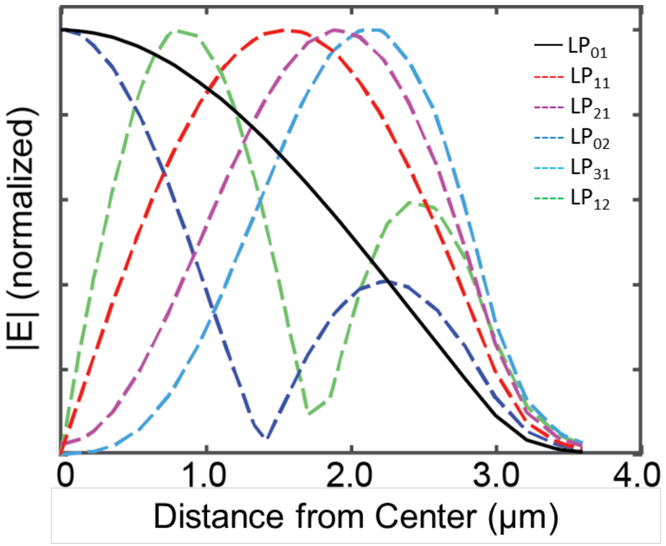

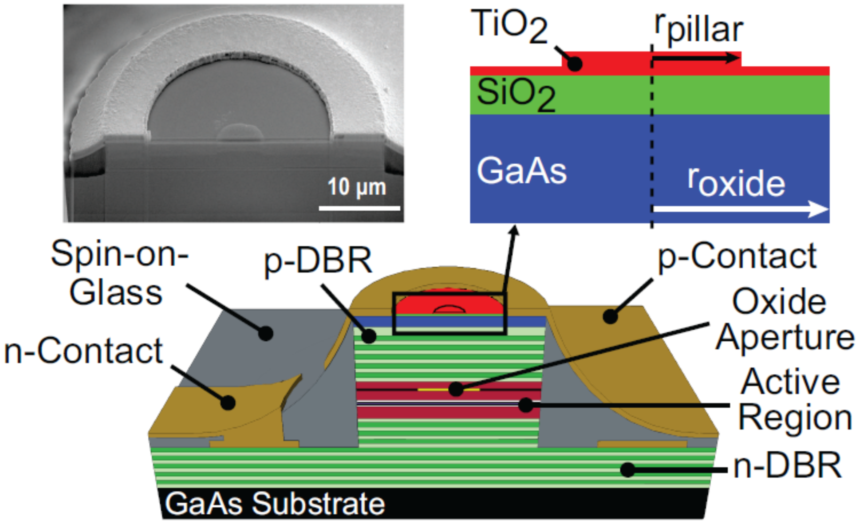

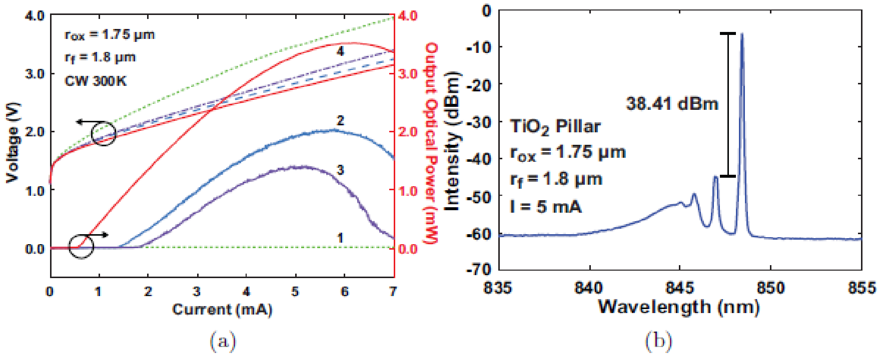

L-I-V and spectral characteristics of VCSEL after each filter layer is deposited: (a) (1) Bare VCSEL, (2) Blanket SiO_2 layer, (3) Blanket TiO_2 layer, and (4) TiO_2 pillar. (b) The optical spectrum indicates single-mode operation with a SMSR of 38.41 dBm and continues until thermal rollover.

- Anti-phase coating deposited atop device induces a spatially varying threshold modal gain higher in periphery of VCSEL, suppressing higher order modes and preferentially operating in a single-fundamental mode
- Previous work required complex, multilayer filter due to incomplete mirror in top p-type DBR
- Modest powers achieved of 3.51 mW with a side-mode suppression-ratio (SMSR) of 38.41 dBm (single mode > 30 dB, pseudo-single mode >25 dB)

O'Brien, T. Jr., "High-Power Single-Mode Vertical-Cavity Surface-Emitting Lasers via Impurity-Induced Disordering", Doctoral Dissertation, University of Illinois at Urbana-Champaign. (2017)

Kesler, Benjamin A. *Mode control in VCSELs using patterned dielectric anti-phase filters*. Diss. University of Illinois at Urbana-Champaign, 2017.

VCSEL Standing Wave Pattern

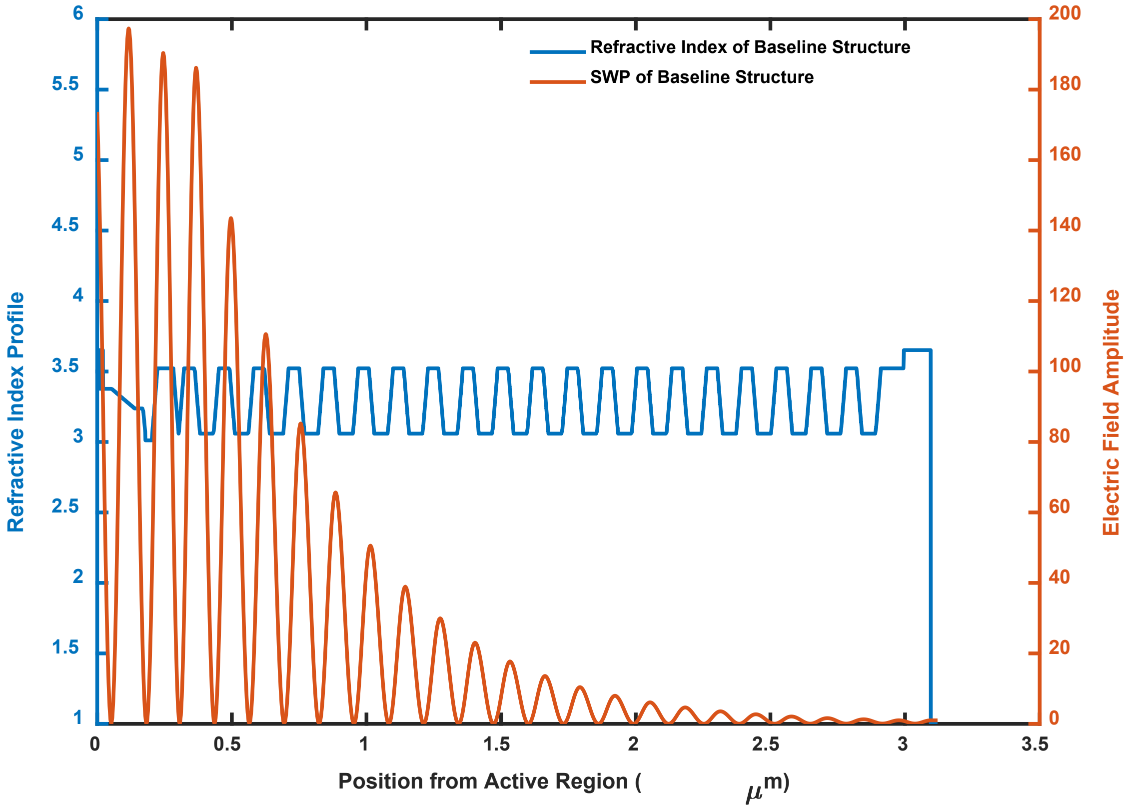

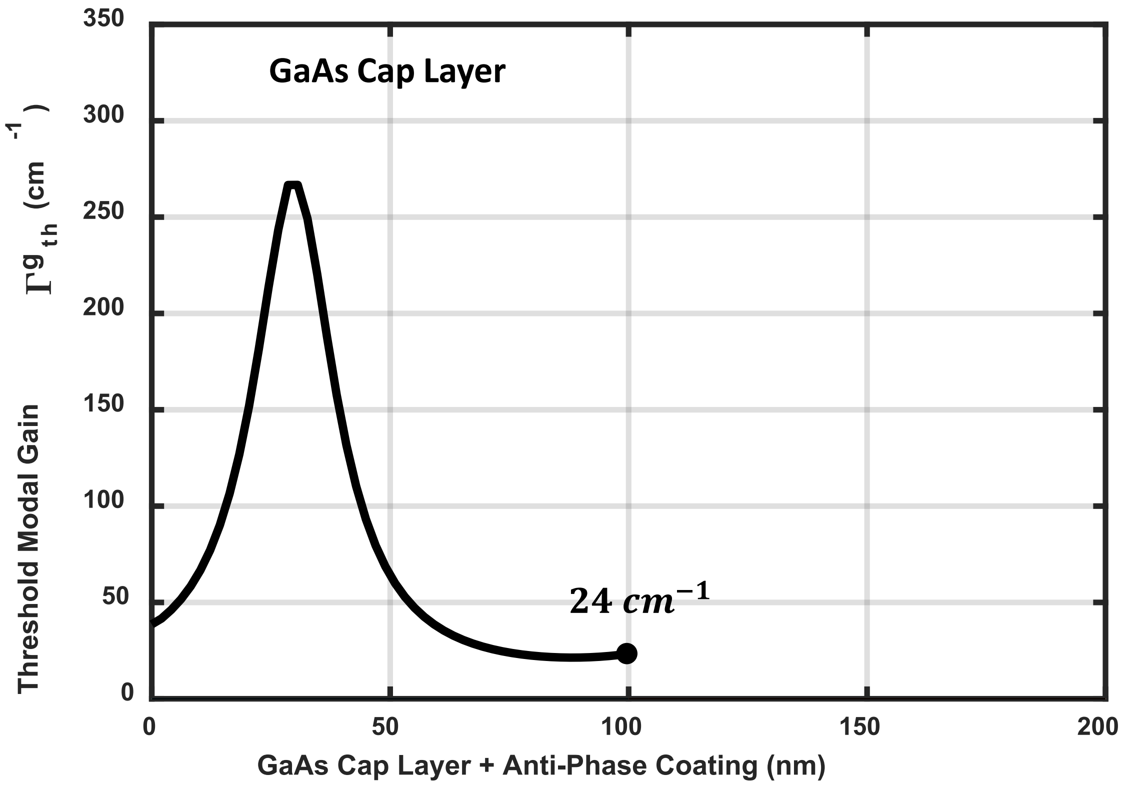

- Baseline structure designed with complete mirror for an in-phase electric field standing wave pattern with large amplitude peak overlapping the active region (0 μm)
- Threshold modal gain is minimized for fundamental mode and higher-order modes

VCSEL DBR Reflectivity

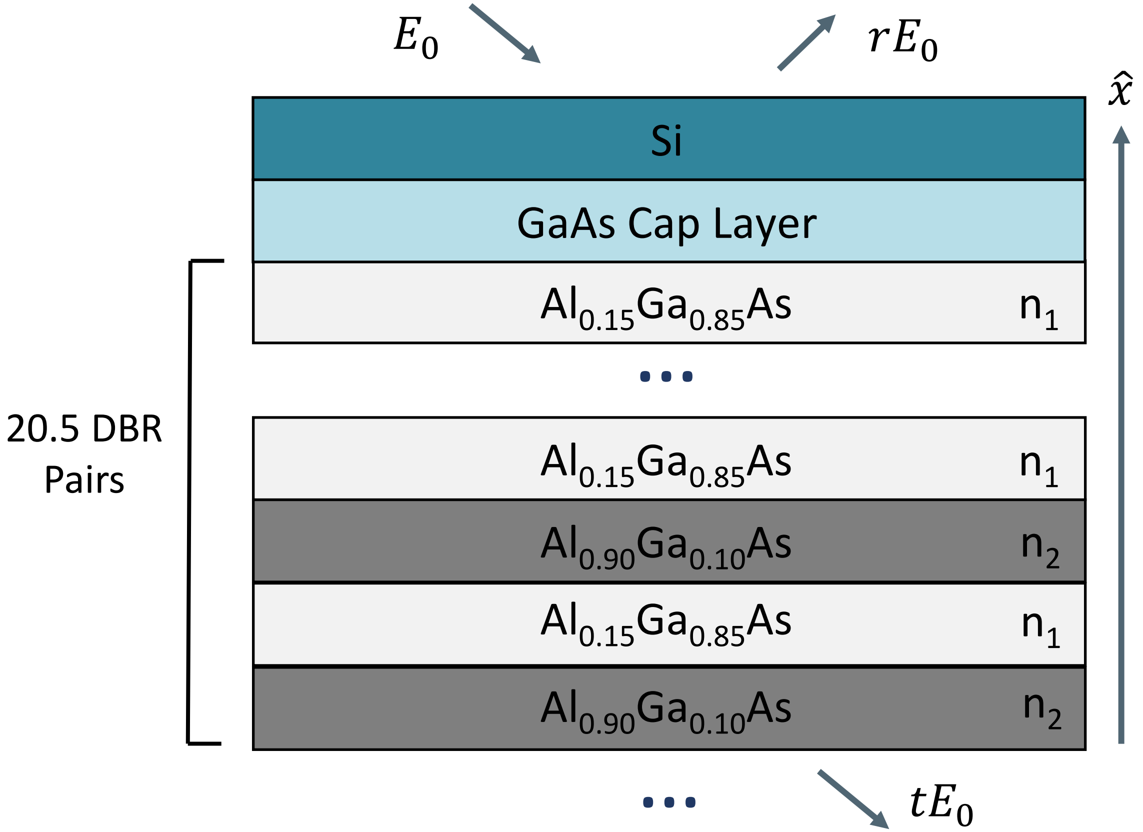

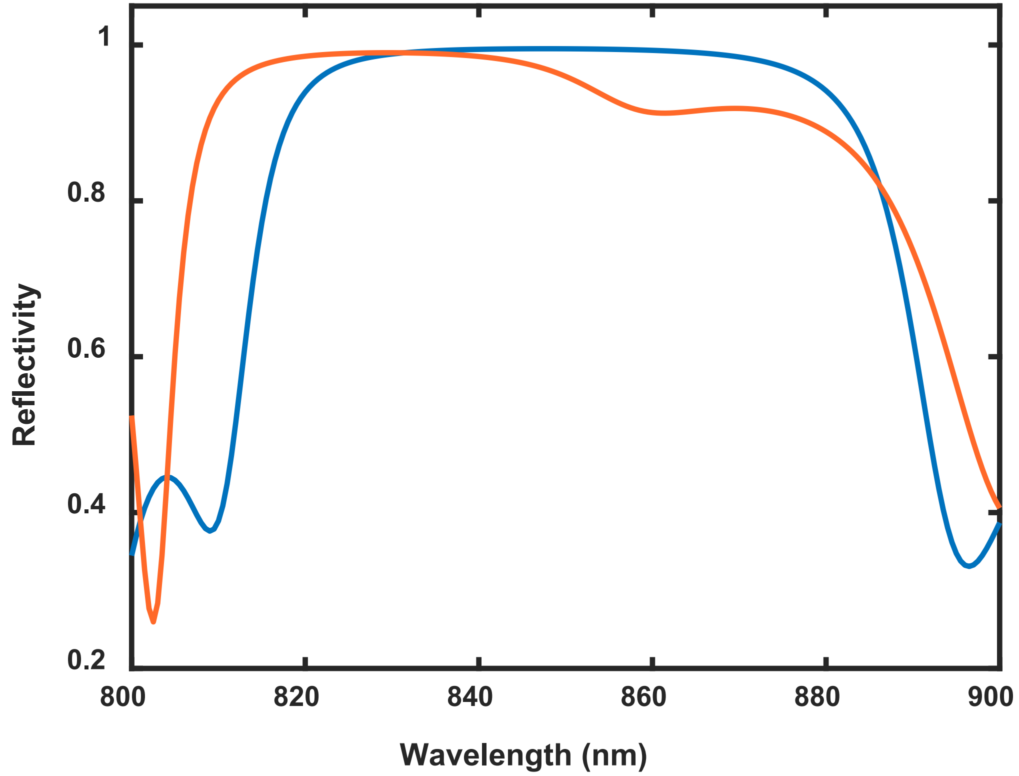

- Additional $\frac{\lambda}{4n}$ thick layer disrupts resonance condition, lowering top DBR reflectivity
- Deposit only in periphery of VCSEL to increase threshold modal gain for higher-order modes
- Degree of effect on reflectivity depends on refractive index of the coating

VCSEL Standing Wave Pattern

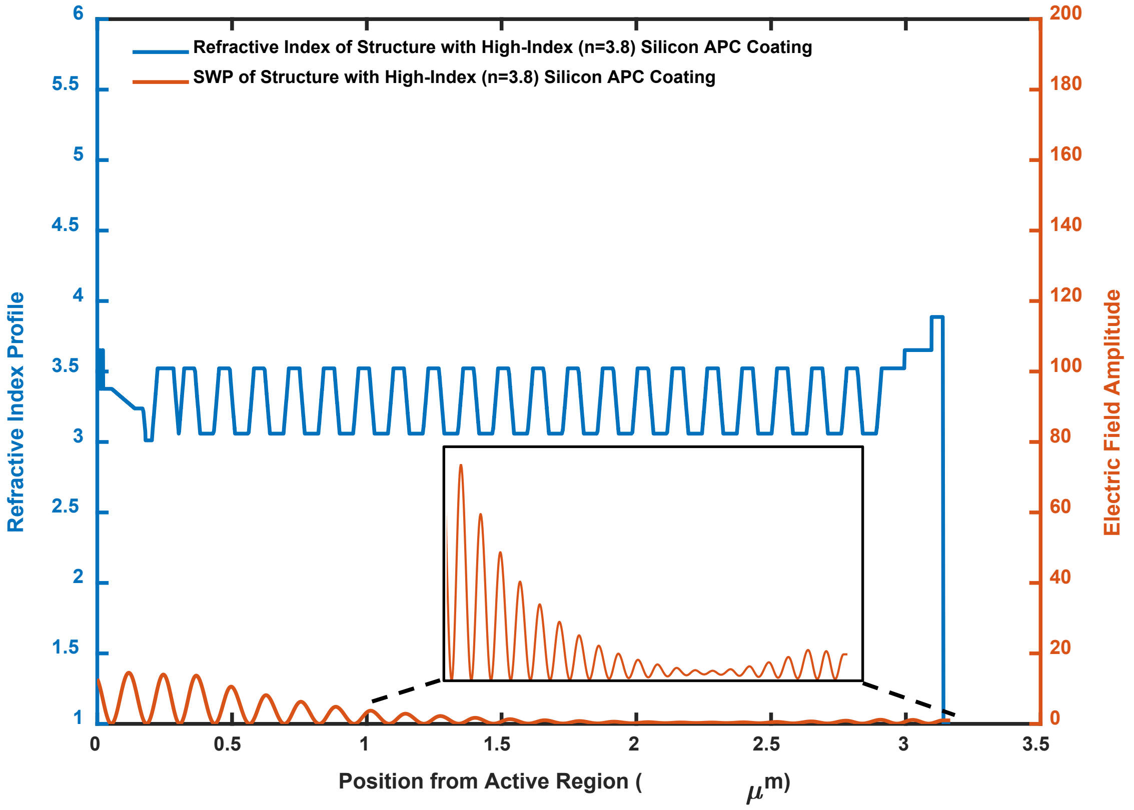

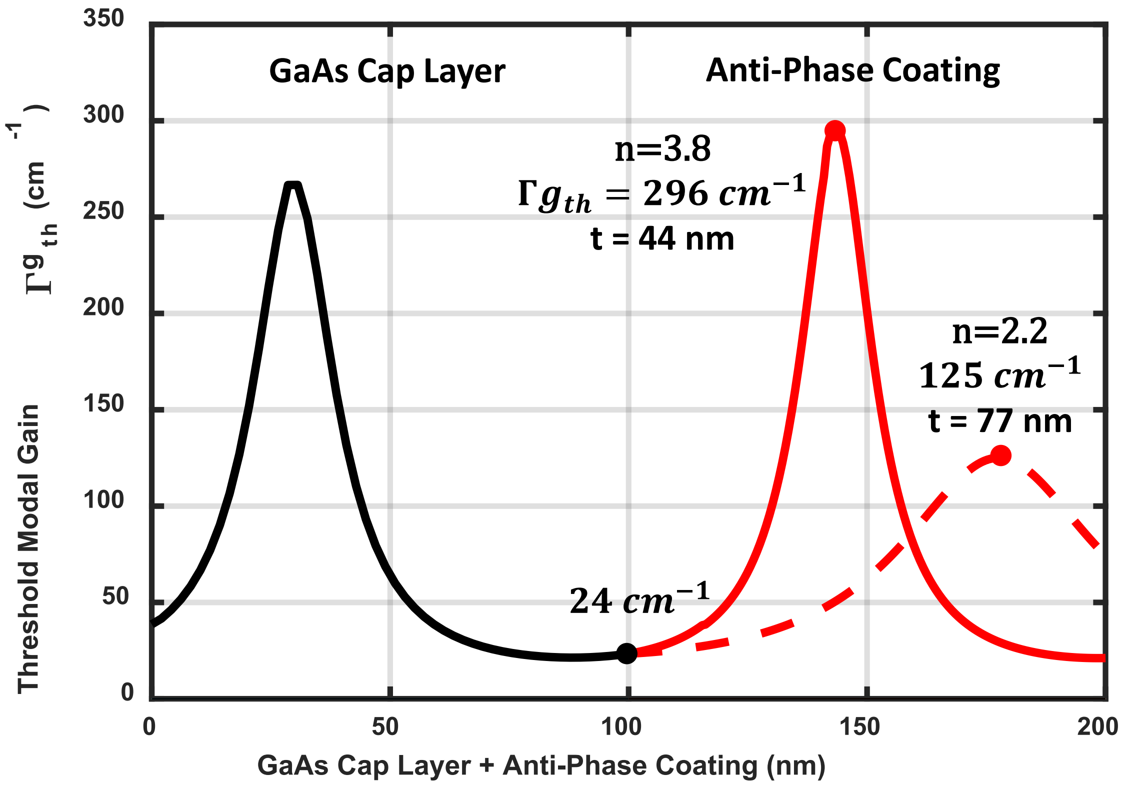

- Higher refractive index film further increases threshold modal gain 137% to 296 cm^{-1} at a thickness of 44 nm
- Visible ripples in standing wave pattern (inset) induced by larger anti-phase wave reflected from surface

Mode-Control VCSEL Fabrication

Epitaxial Layer Design

- VCSEL Epitaxial Design:
  - n-type GaAs Substrate
  - 32 n-type AlAs/AlGaAs DBR Pairs
  - 5 InGaAs quantum wells
  - 20 p-type AlGaAs DBR Pairs
  - 25 nm $Al_{0.98}GaAs$ layer for oxidation
- Multiple InGaAs quantum-wells provide high differential gain
- AlAs bottom DBR layers provide additional thermal conductance for heat dissipation

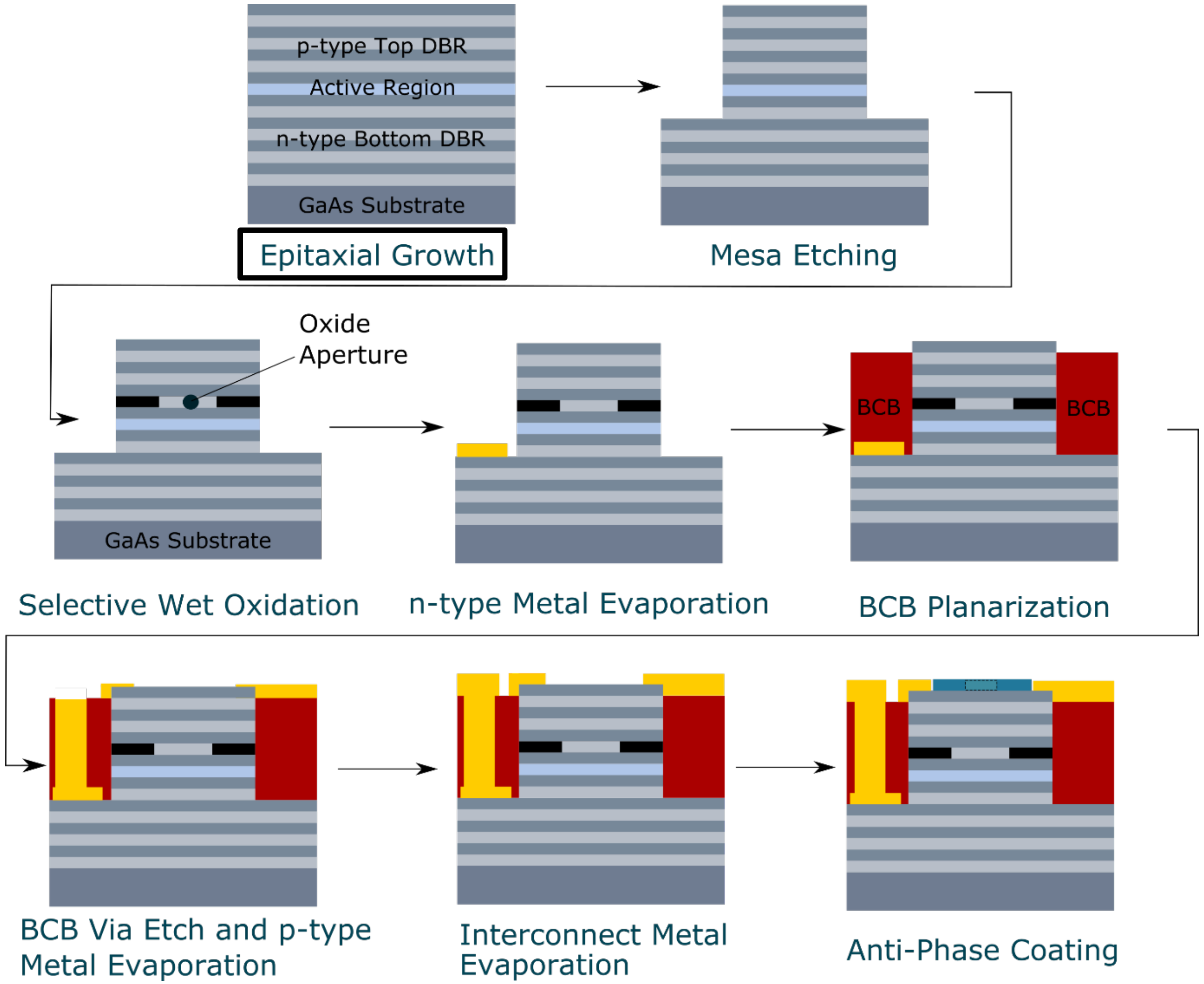

Authors are grateful to Quesnell Hartmann and Toby Garrod for growing VCSEL design at II-VI EpiWorks in Champaign, IL

Mode-Control VCSEL Fabrication

VCSEL Anti-Phase Coating

- Anti-phase coating is deposited using electron-beam evaporation and a photolithographic lift-off process
  - Magnitude of e-beam current determines magnitude refractive index of film
- Quartz witness sample loaded alongside VCSEL die for refractive index measurement
- Silicon film is characterized by stylus profiler and spectroscopic ellipsometry for thickness and index of refraction, respectively

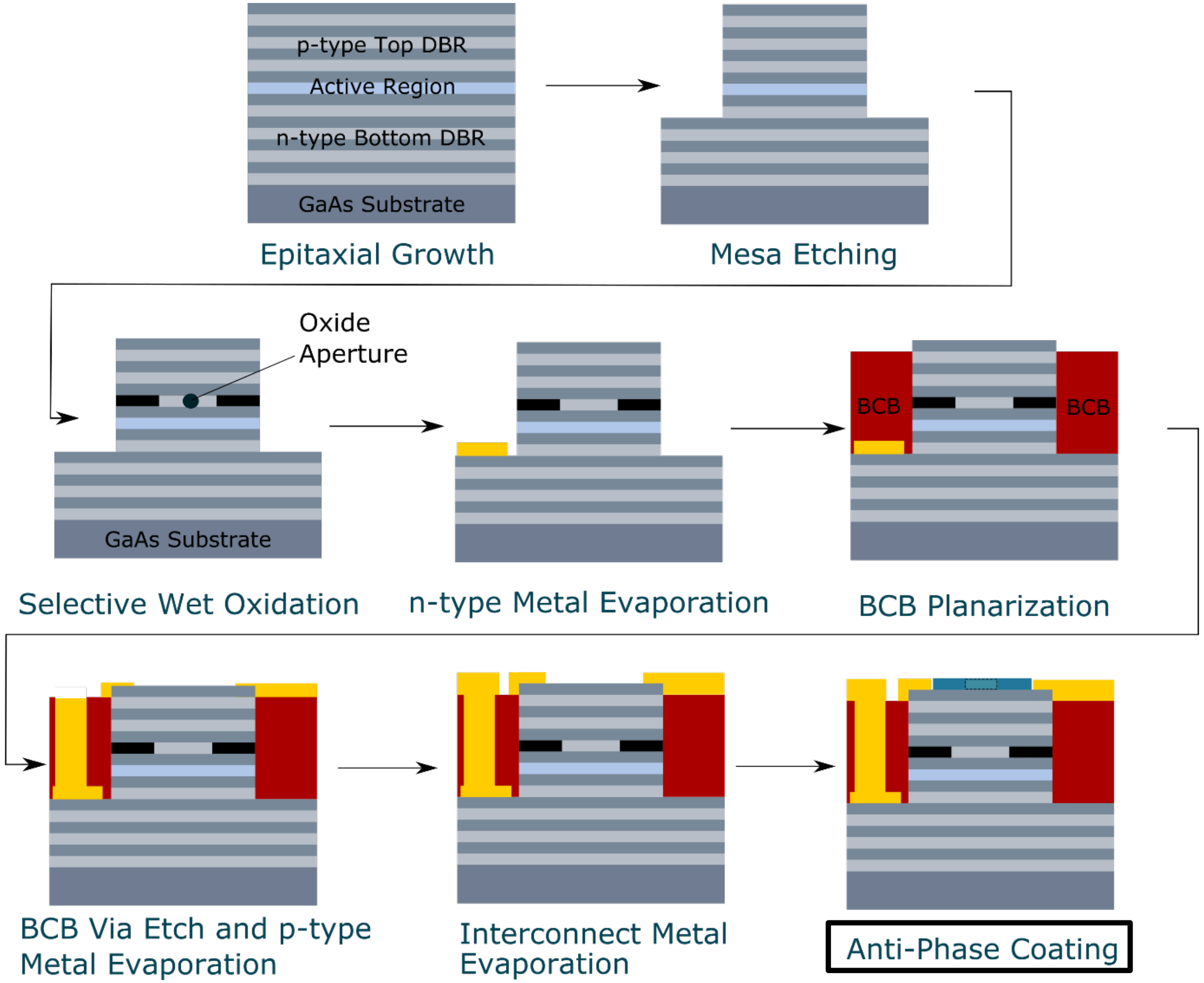

Silicon Film Optical Constants

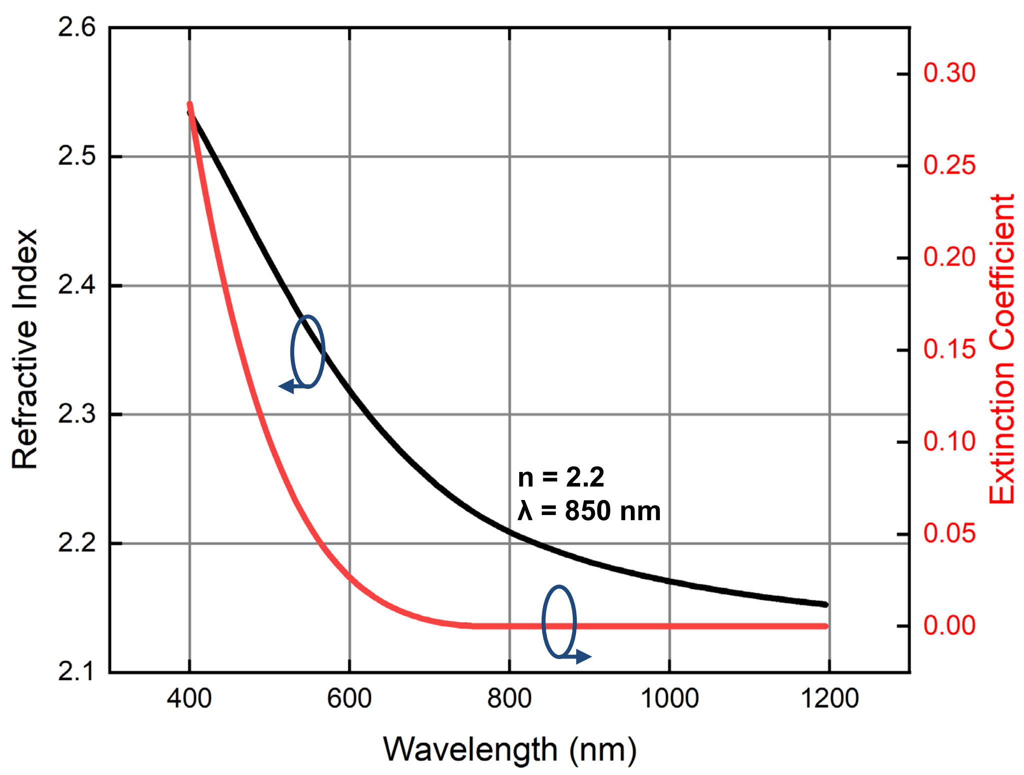

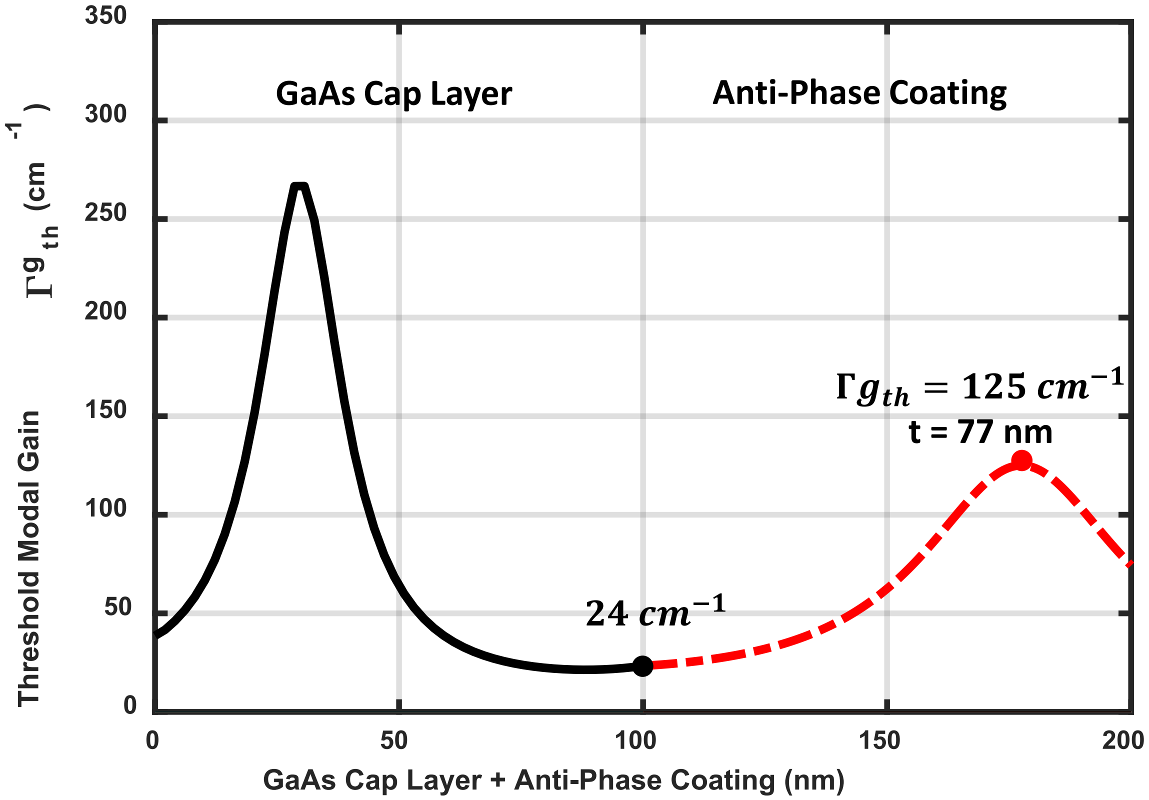

- Low refractive index value of 2.2 at operating wavelength (λ= 850 nm) compared to literature values ~3.8 [9] influences output of device
  - Mode suppression capabilities are lower compared to higher index film

High-Power VCSEL Performance

Baseline VCSEL Geometry

- Mesa Size: **25 µm**
- Oxide Aperture: **3 µm**
- Anti-Phase Coating Aperture: **N/A**

Baseline VCSEL Performance

- I_{th}= **0.40 mA**
- Peak Single-Mode Output Power: **4.9 mW**
- Thermal Rollover Current: **5.36 mA**

CW RT Operation

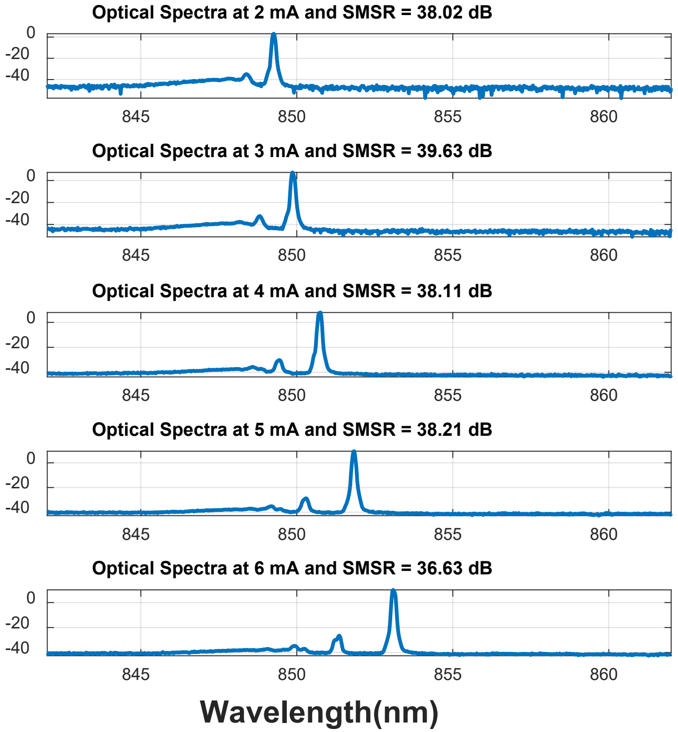

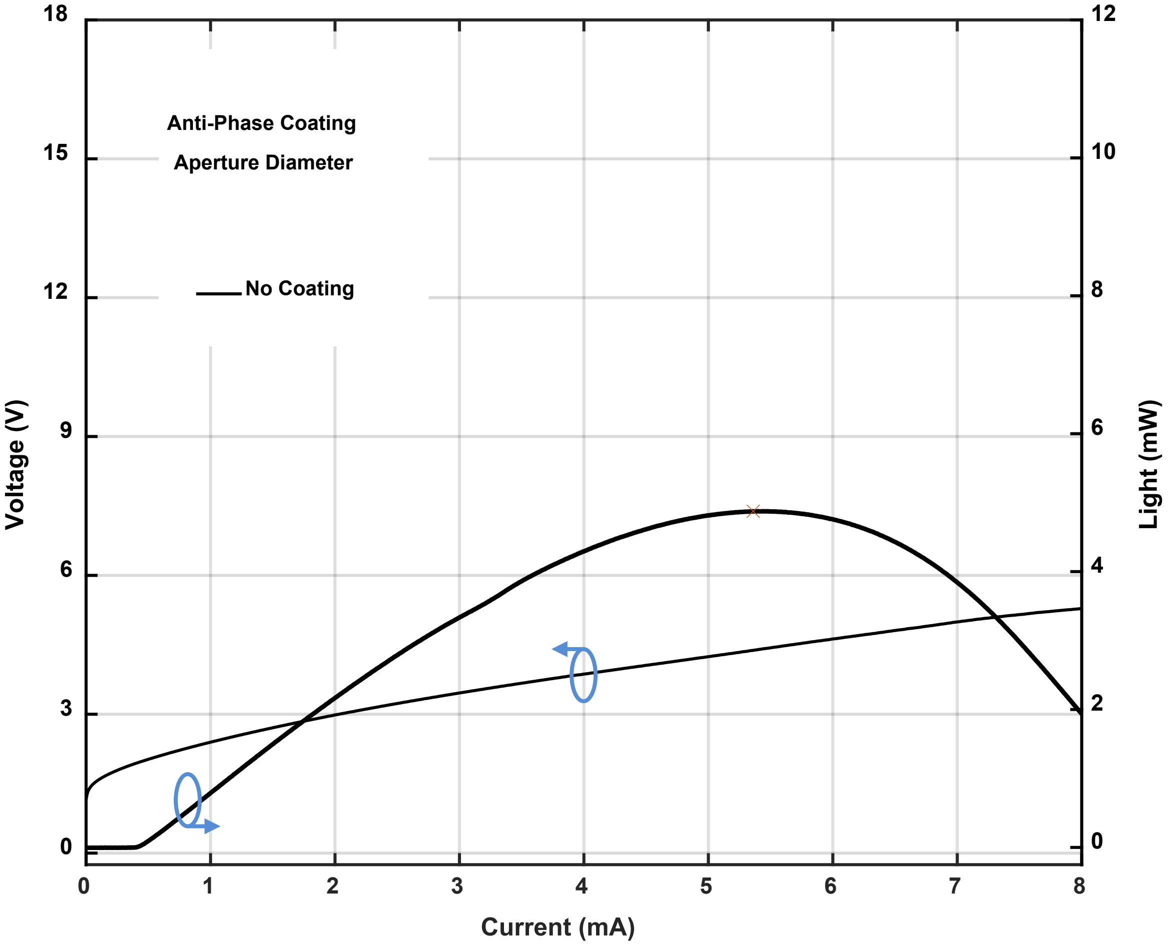

High-Power VCSEL Performance

Anti-Phase VCSEL Geometry

- Mesa Size: **25 µm**
- Oxide Aperture: **3 µm**
- Anti-Phase Coating Aperture: **0 µm**

Anti-Phase VCSEL Performance

- **I_{th}= 0.53 mA**
- Peak Single-Mode Output Power: **6.61 mW**
- Thermal Rollover Current: **6.5 mA**

CW RT Operation

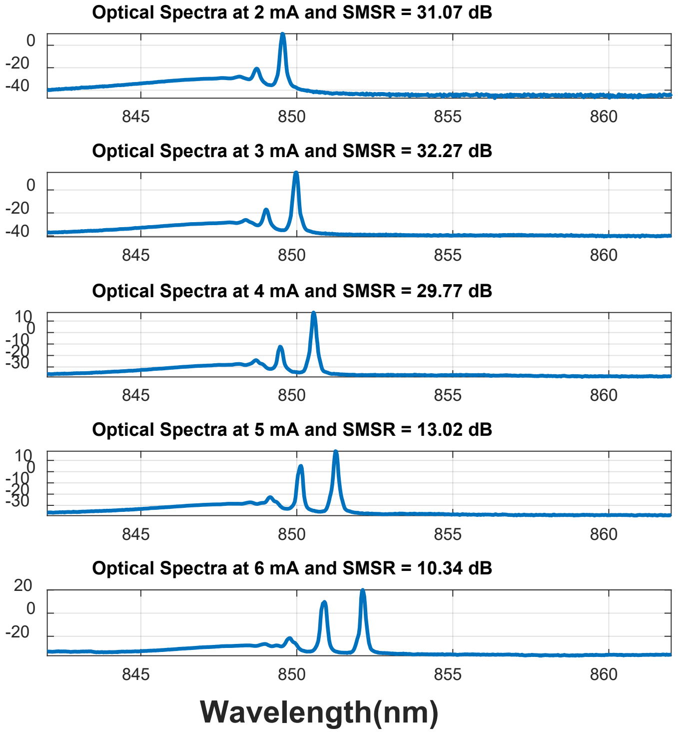

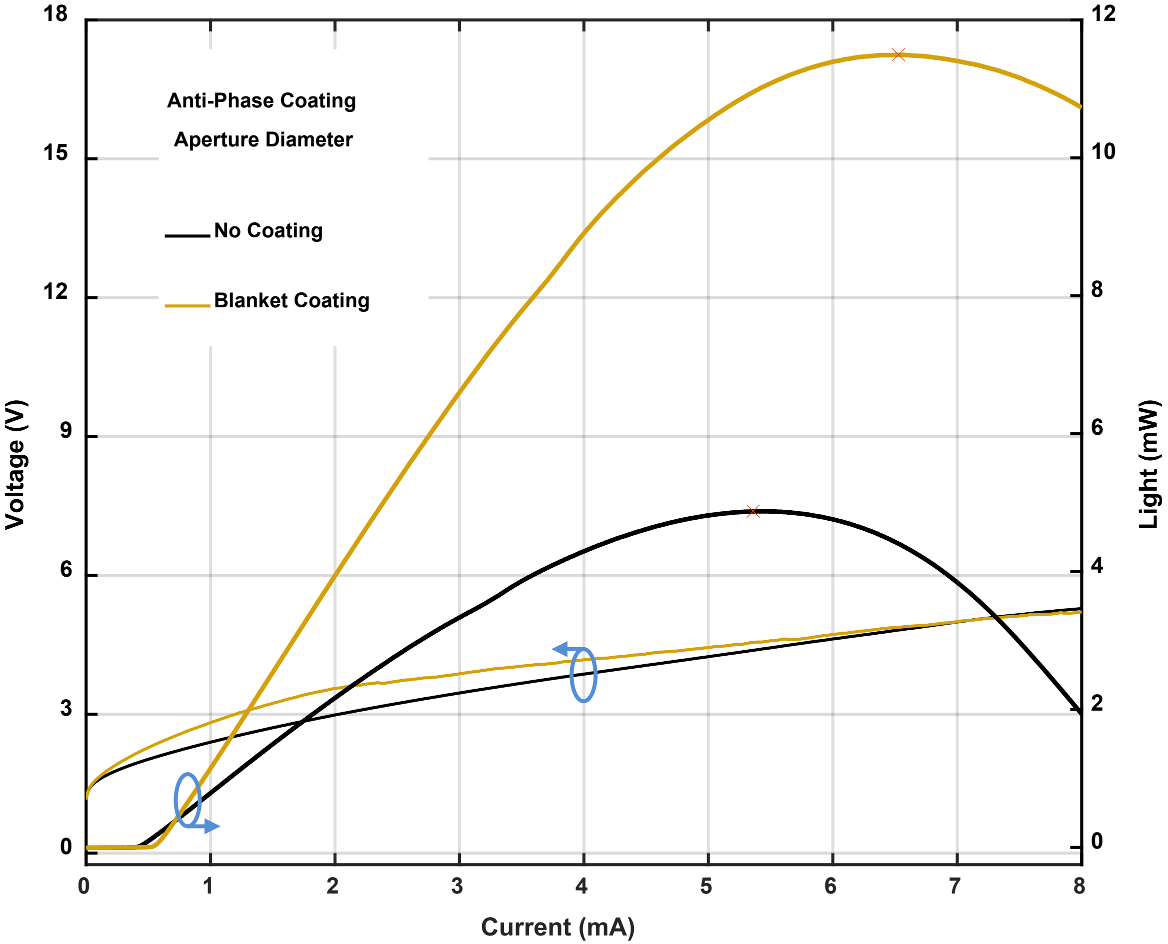

High-Performance VCSEL Performance

Anti-Phase VCSEL Geometry

- Mesa Size: **25 µm**
- Oxide Aperture: **3 µm**
- Anti-Phase Coating Aperture: **2 µm**

Anti-Phase VCSEL Performance

- I_{th} **= 0.48 mA**
- Peak Single-Mode Output Power: **10.2 mW**
- Thermal Rollover Current: **6.2 mA**

CW RT Operation

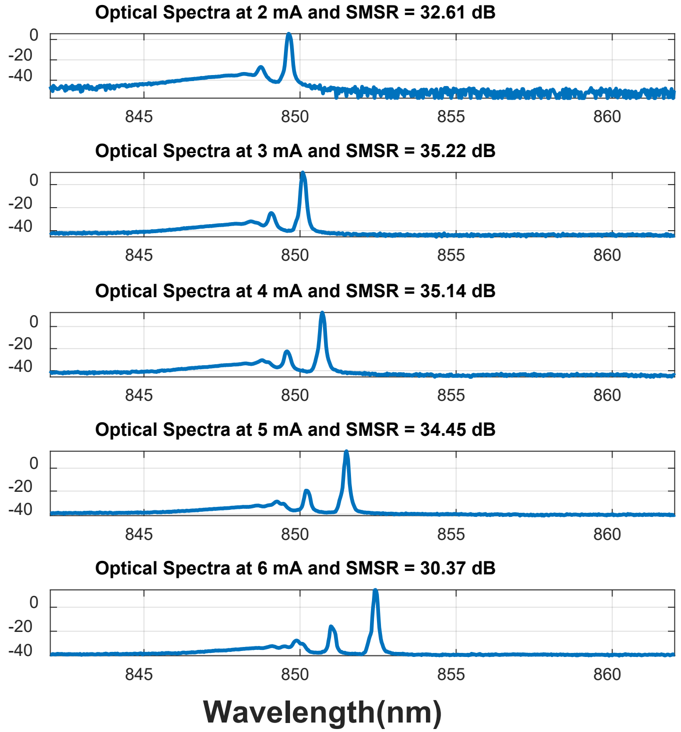

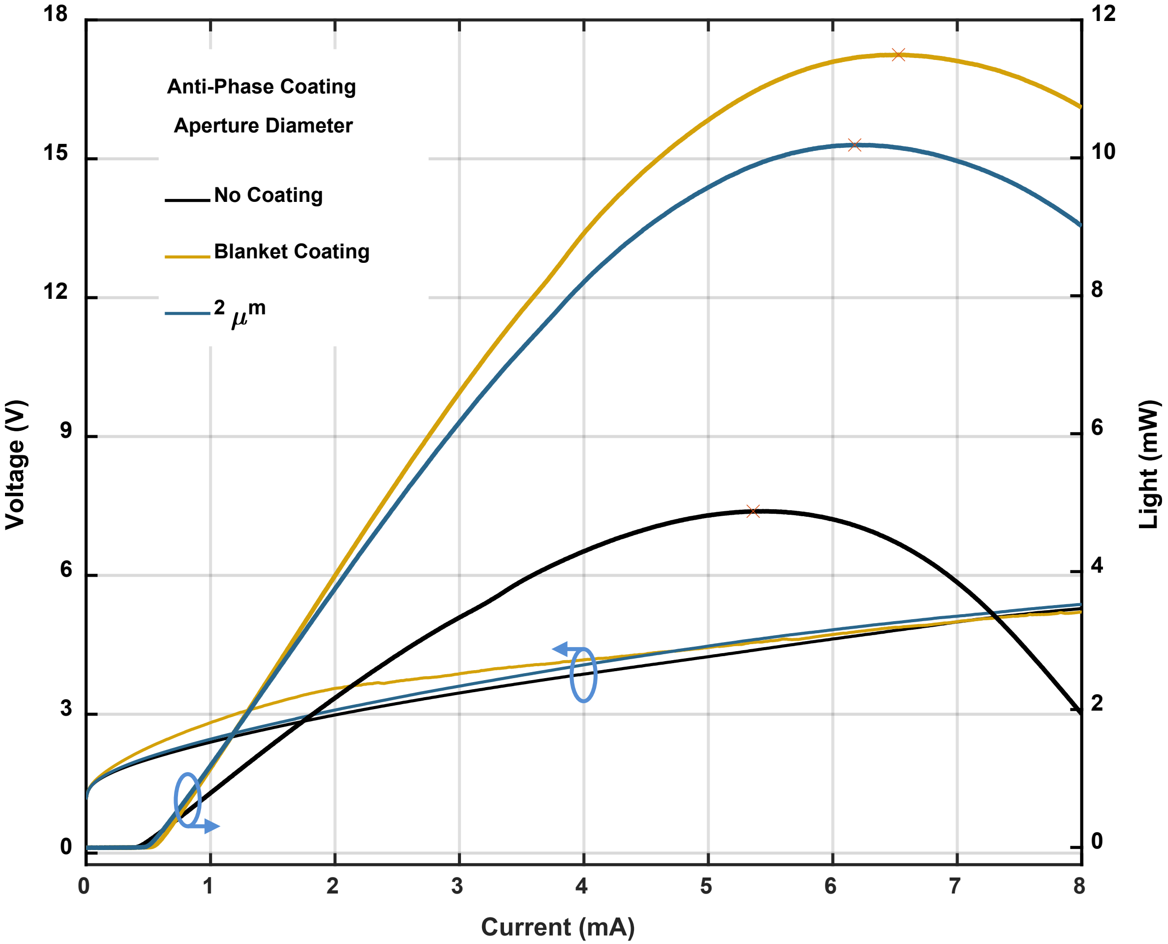

Wall-Plug and Slope Efficiency

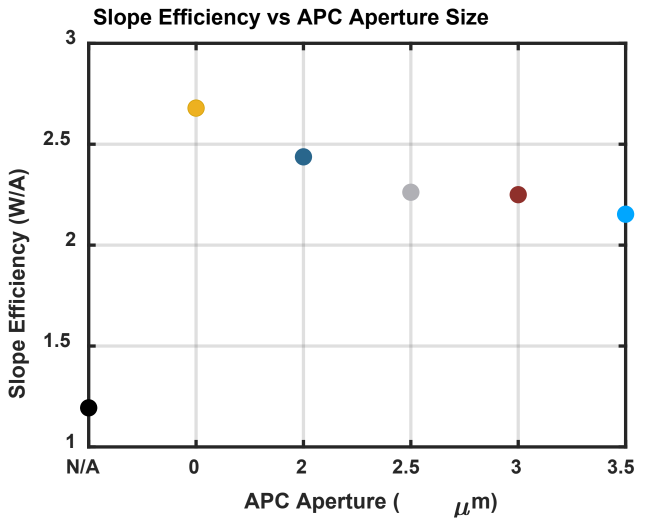

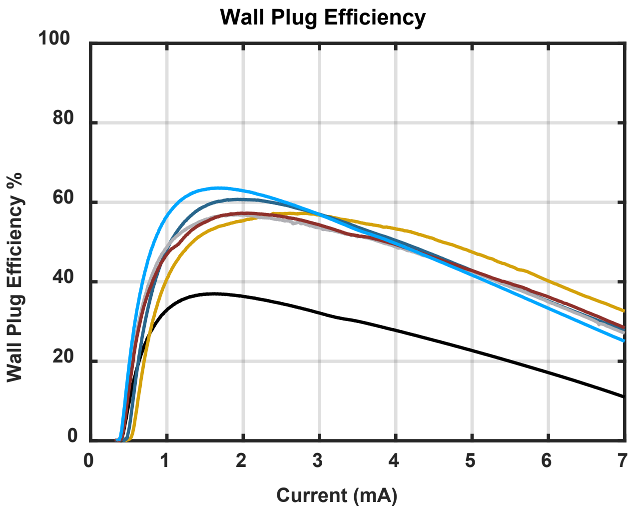

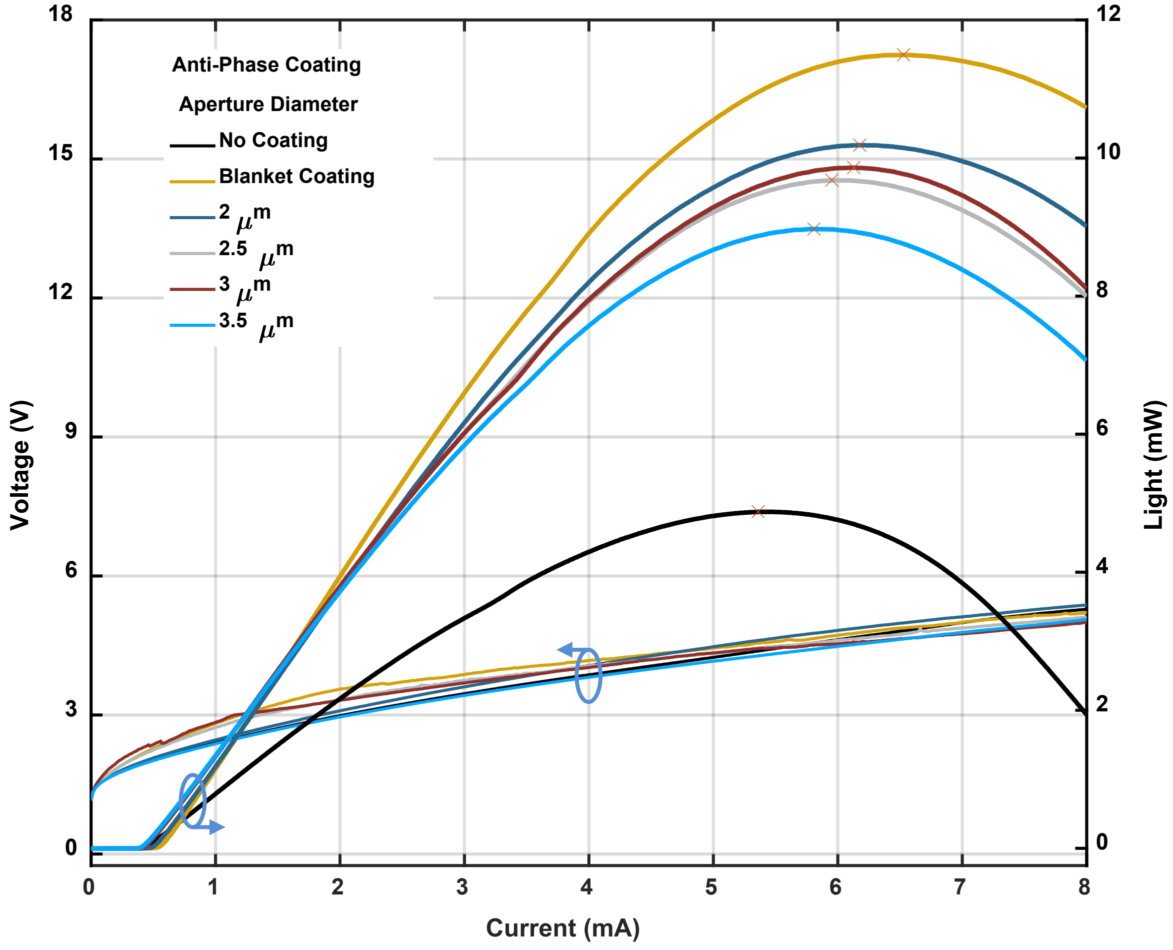

- Reduction of DBR reflectivity increases total cavity loss, increasing threshold current
  - Less internal absorption contributes leads to less heating and delay of thermal rollover
- Higher differential quantum efficiency and slope efficiency
  - S.E. = 2.6 W/A -> DQE = 171%

Enhanced Silicon Film Optical Constants

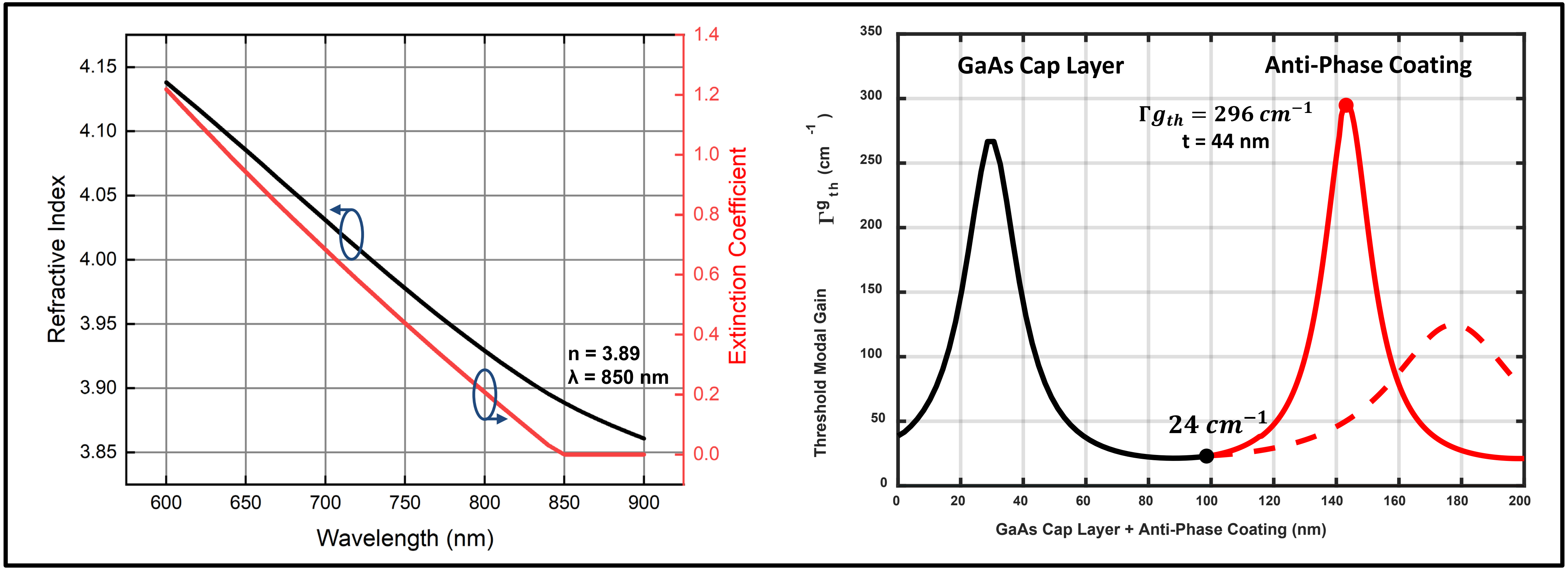

- Increasing the e-beam current (and therefore deposition rate) leads to a more robust film with a larger refractive index of 3.89 at 850 nm

- More enhanced film leads to increased capability of mode-control in inherently multimode VCSELs

Enhanced APC VCSEL Performance

Baseline VCSEL Geometry

- Mesa Size: **26 µm**
- Oxide Aperture: **4 µm**
- Anti-Phase Coating Aperture: **N/A**

Baseline VCSEL Performance

- **I_{th}= 0.41 mA**
- Peak Single-Mode Output Power: **N/A**
- Thermal Rollover Current: **8.28 mA**

CW RT Operation

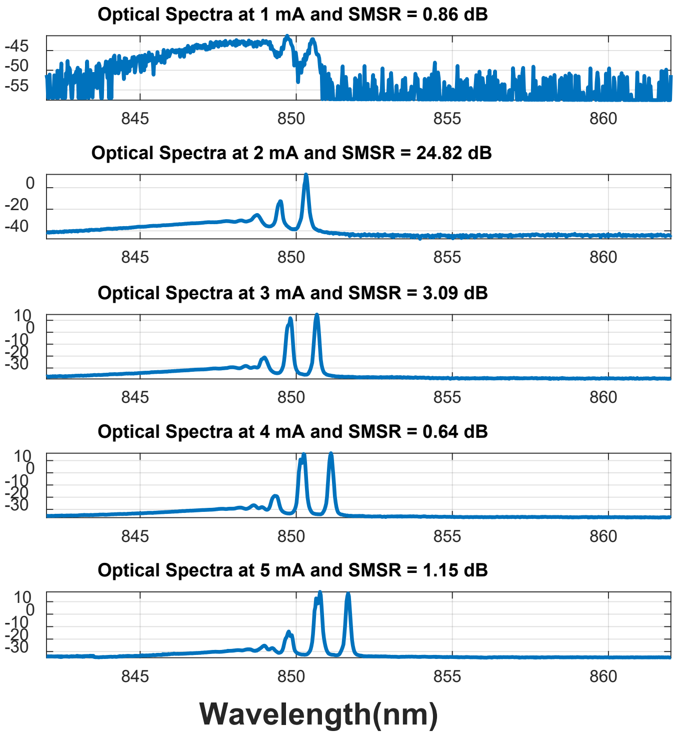

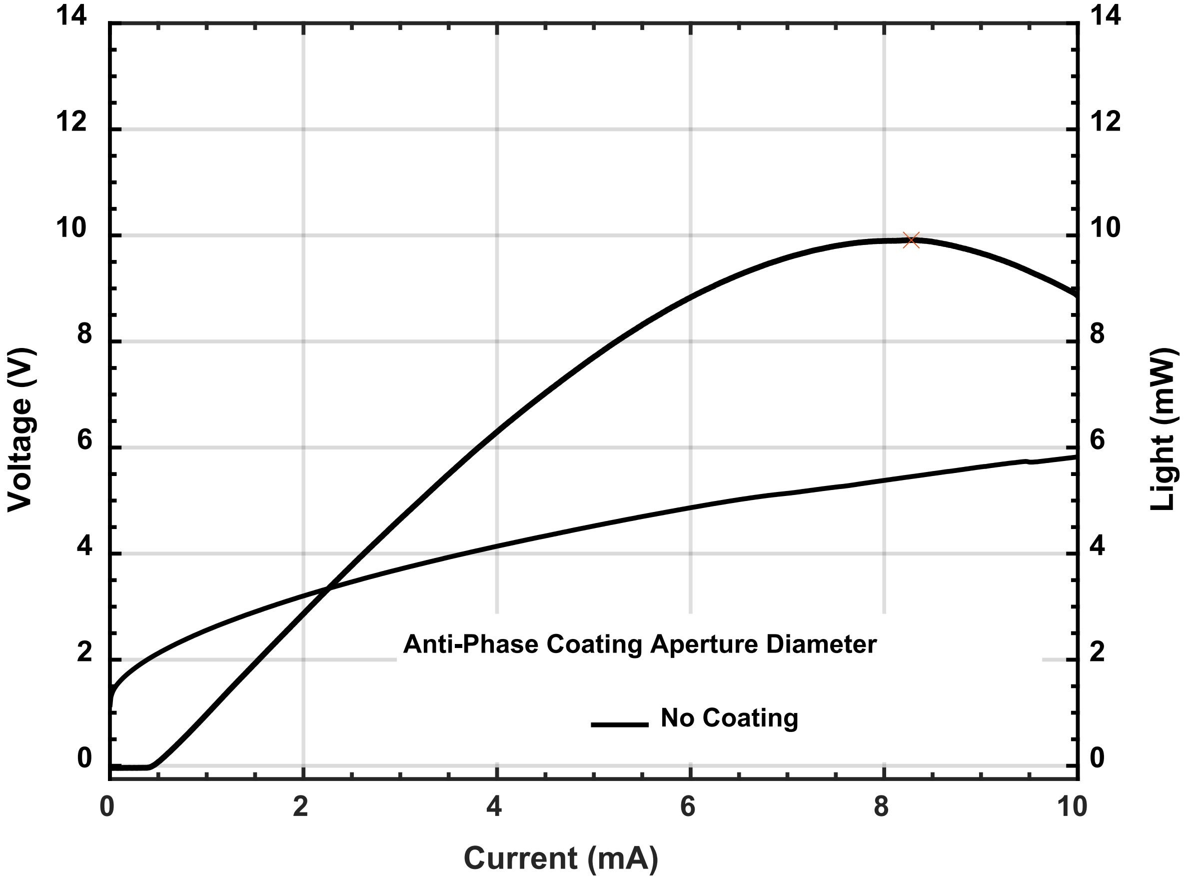

Enhanced APC VCSEL Performance

Anti-Phase VCSEL Geometry

- Mesa Size: **26 µm**
- Oxide Aperture: **4 µm**
- Anti-Phase Coating Aperture: **2 µm**

Anti-Phase VCSEL Performance

- **I_{th}= 1.06 mA**
- Peak Single-Mode Output Power: **N/A**
- Thermal Rollover Current: **9.26 mA**

CW RT Operation

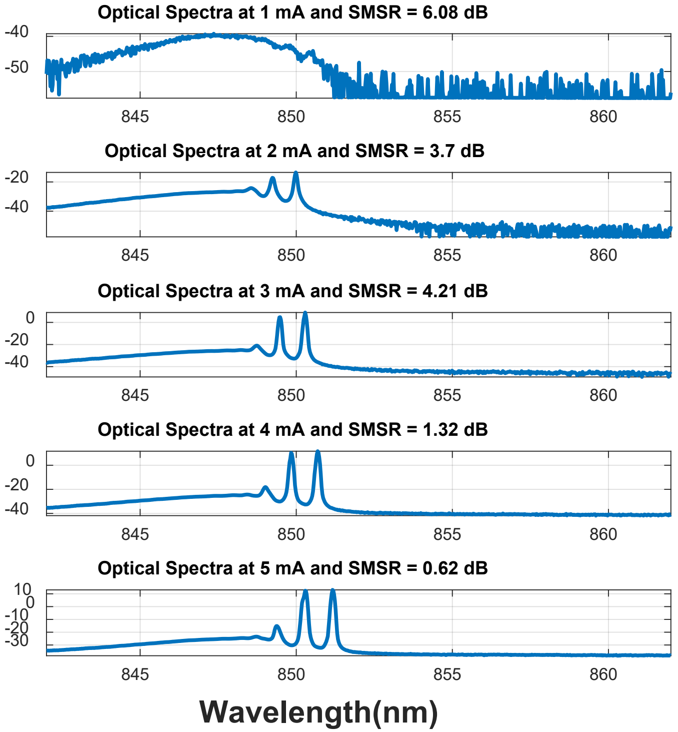

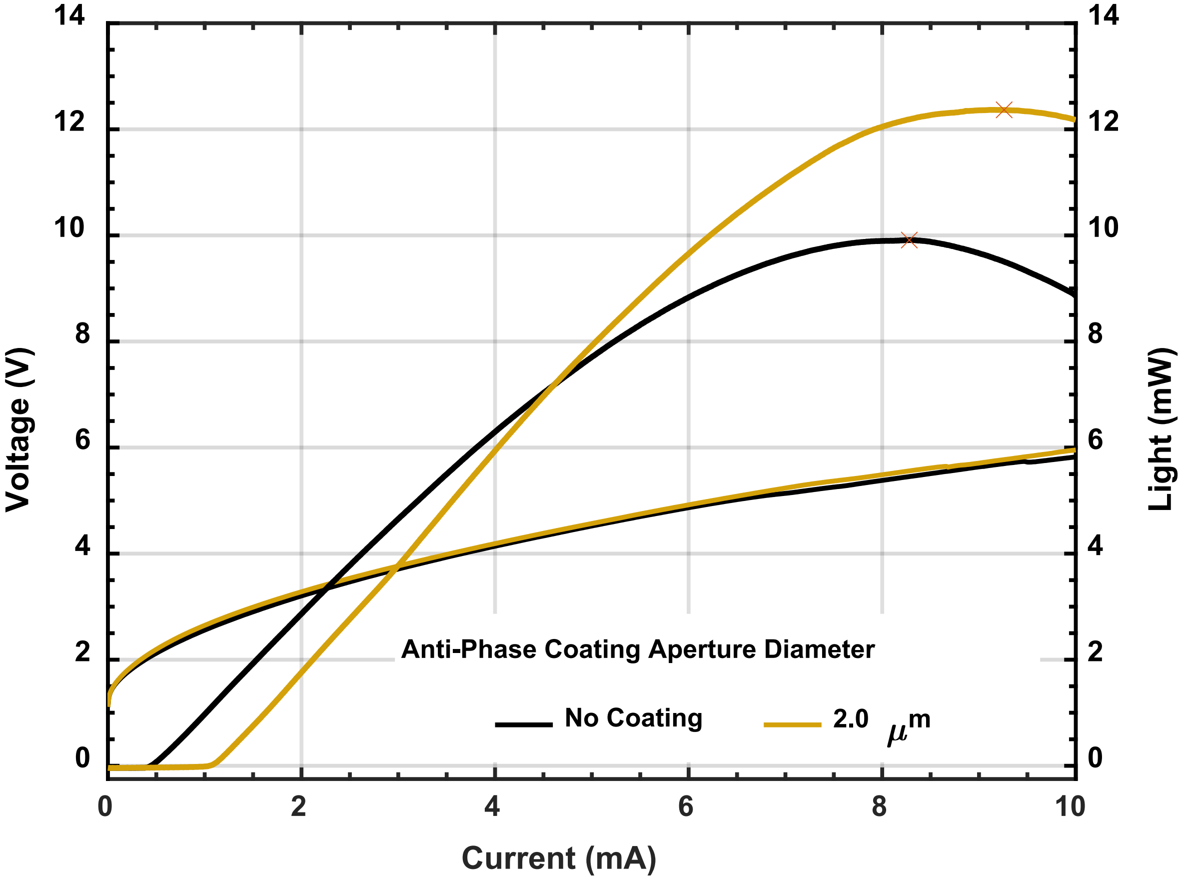

Enhanced APC VCSEL Performance

Anti-Phase VCSEL Geometry

- Mesa Size: **26 µm**
- Oxide Aperture: **4 µm**
- Anti-Phase Coating Aperture: **4 µm**

Anti-Phase VCSEL Performance

- **I_{th}= 0.62 mA**
- Peak Single-Mode Output Power: **7.78 mW**
- Thermal Rollover Current: **9.08 mA**

CW RT Operation

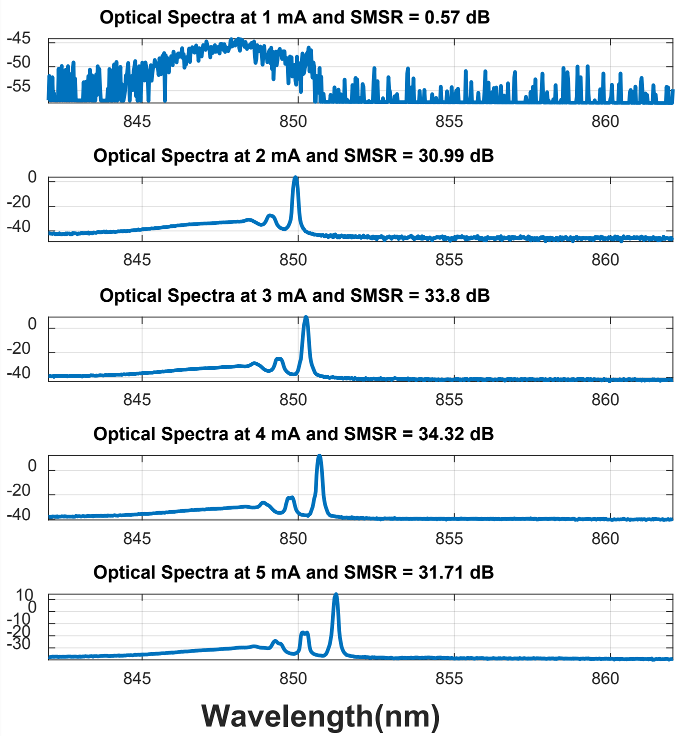

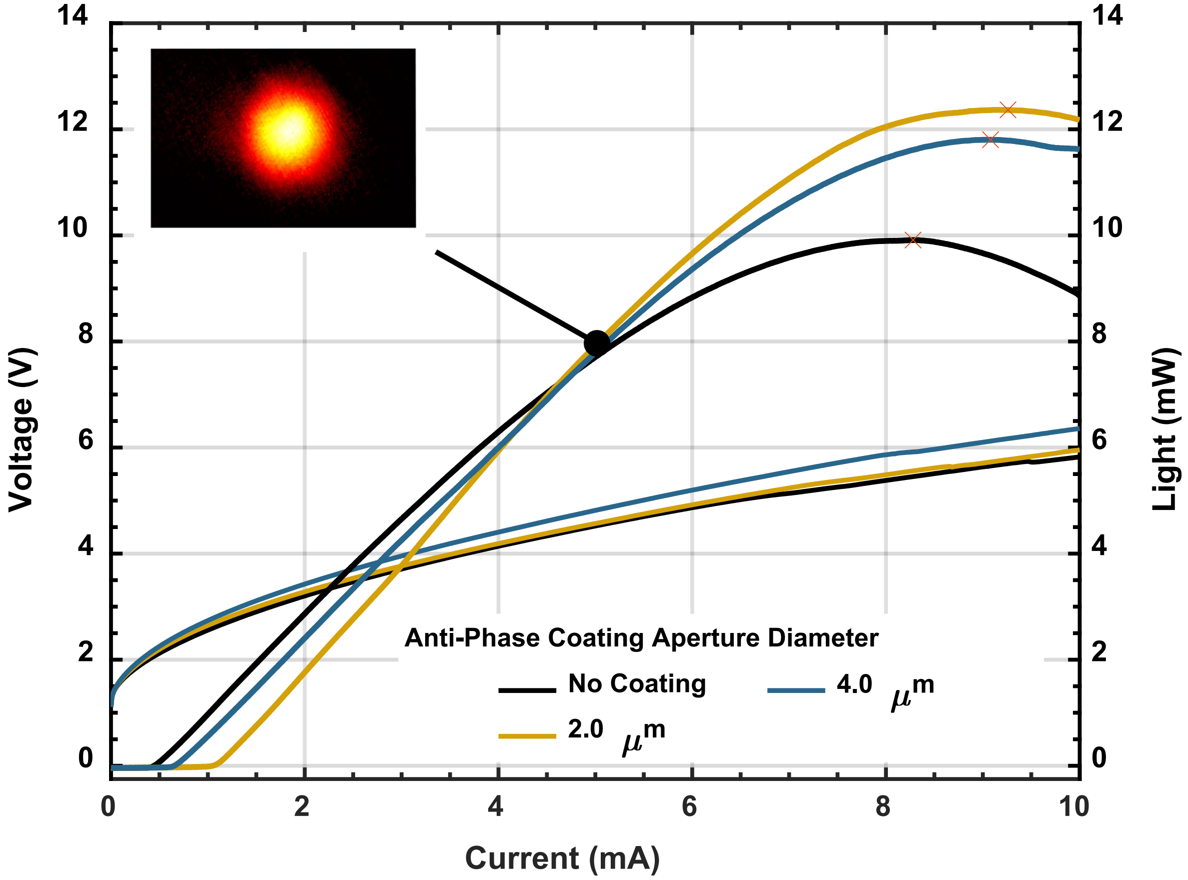

Polarization Control via Anti-Phase Coating

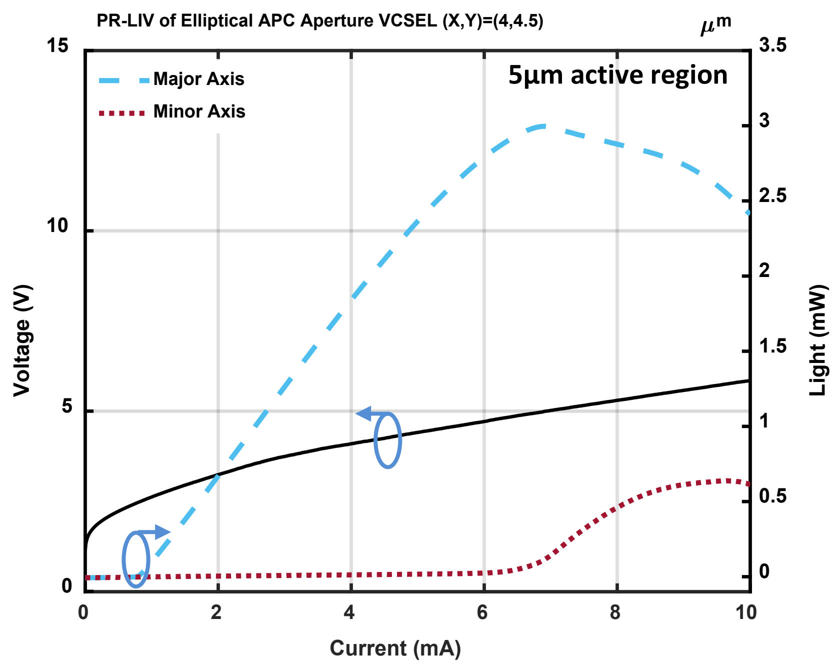

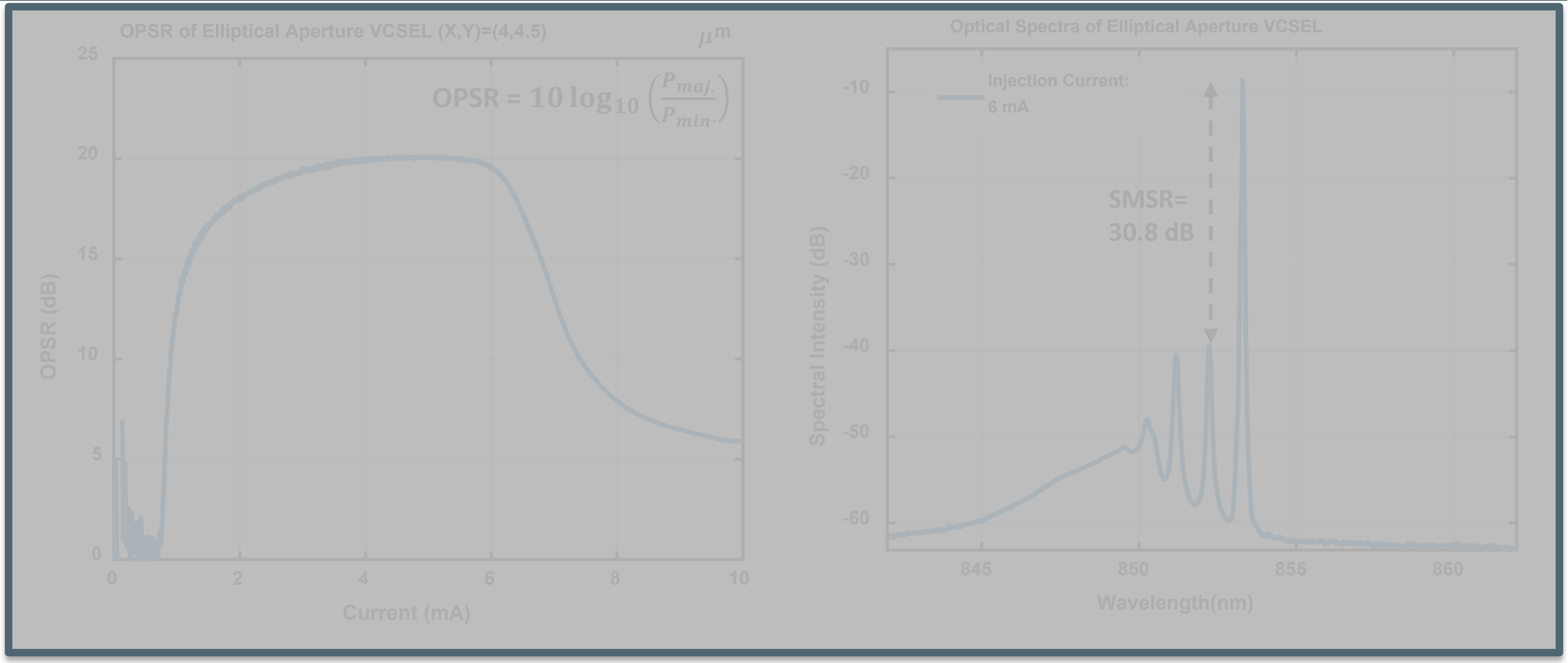

- With a slightly elliptical anti-phase coating aperture, undesired polarization state is suppressed without undesired encroachment onto fundamental transverse mode, resulting in 3 mW of output power
- Orthogonal-polarization suppression ratio (OPSR) of 20 dB measured at 6mA, achieving **single-polarization operation**
- SMSR of 30.8 dB measured, indicating simultaneous **single-mode operation**

Polarization Control via Anti-Phase Coating

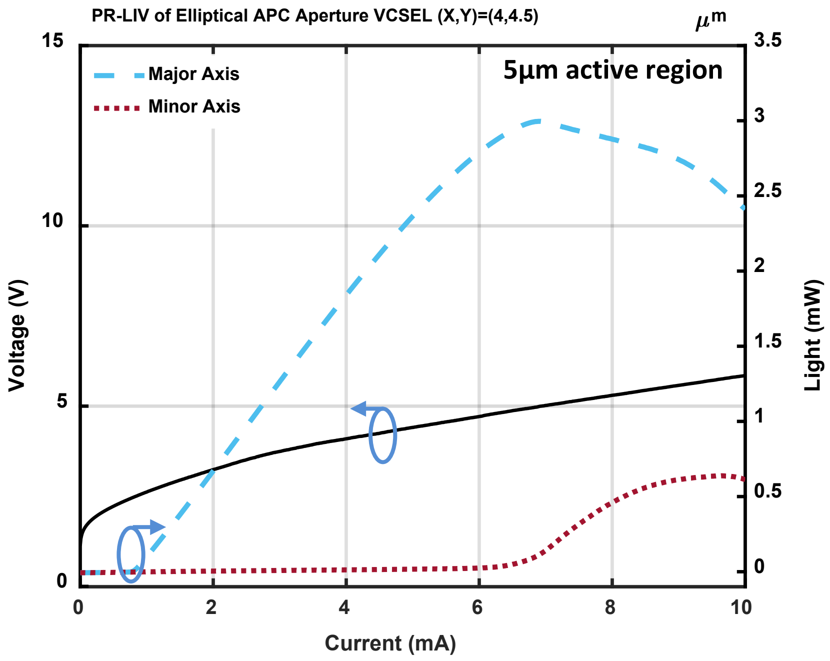

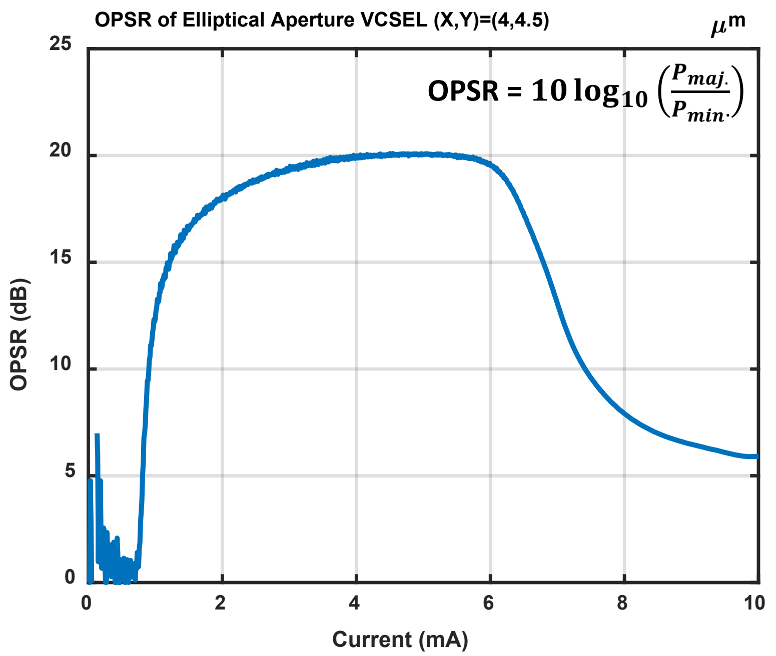

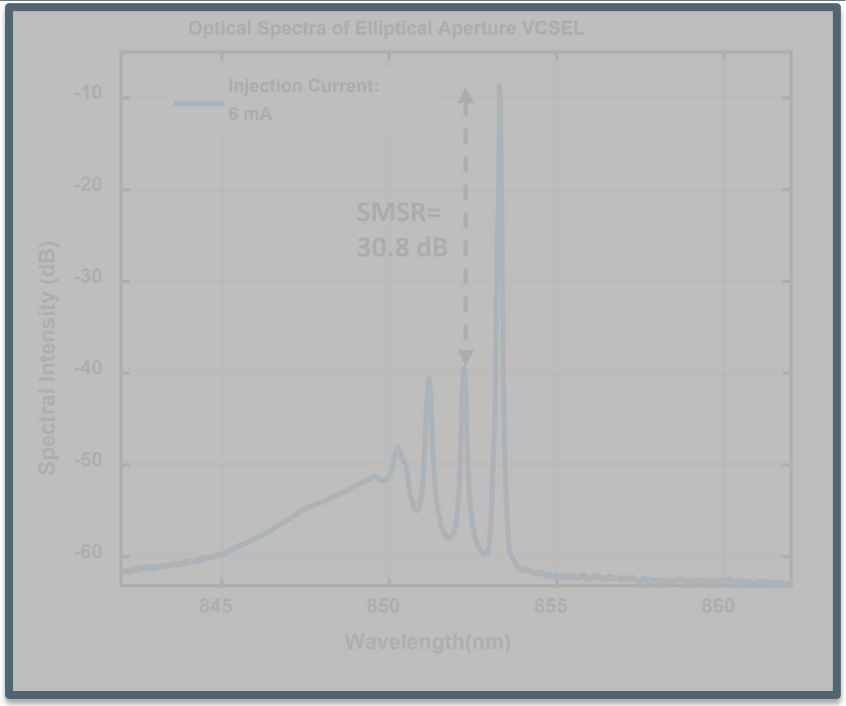

- With a slightly elliptical anti-phase coating aperture, undesired polarization state is suppressed without undesired encroachment onto fundamental transverse mode, resulting in 3 mW of output power
- Orthogonal-polarization suppression ratio (OPSR) of 20 dB measured at 6mA, achieving **single-polarization operation**
- SMSR of 30.8 dB measured, indicating simultaneous **single-mode operation**

Polarization Control via Anti-Phase Coating

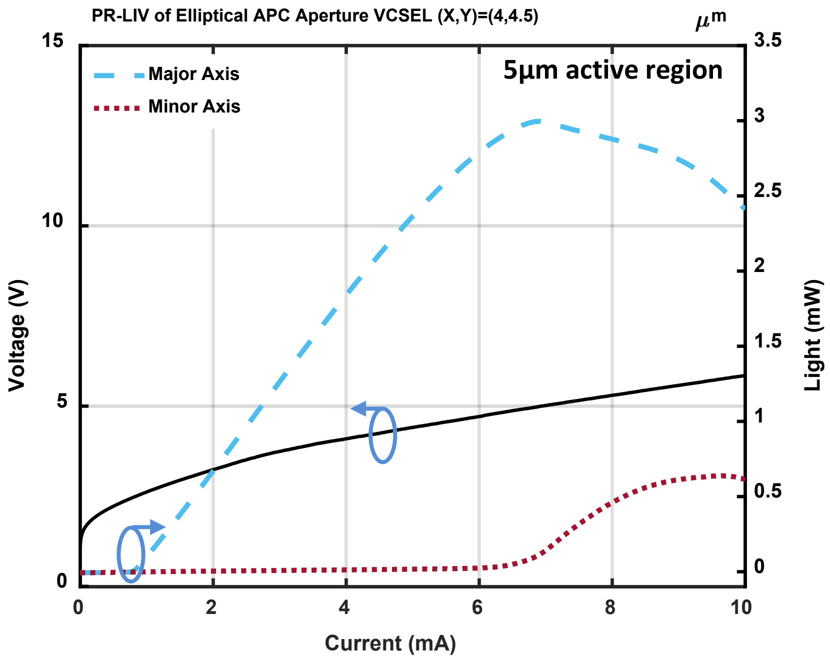

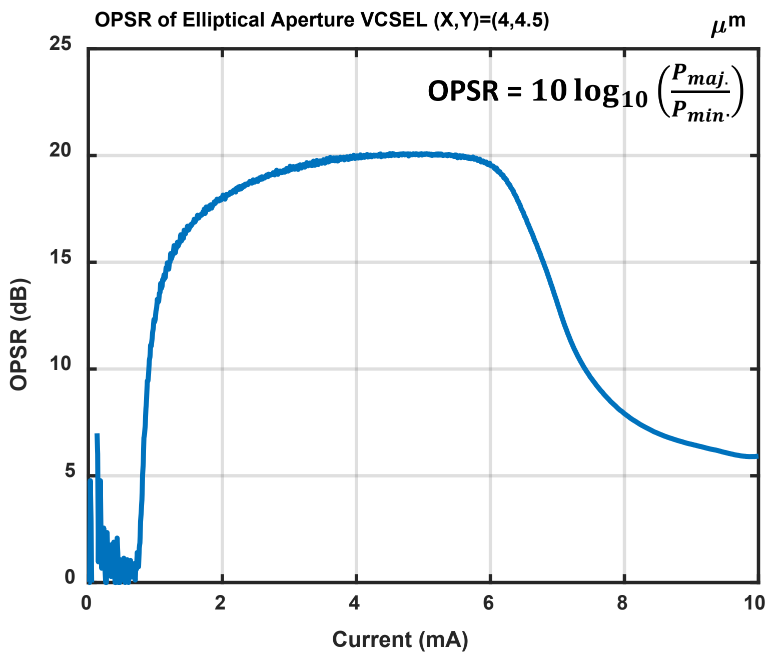

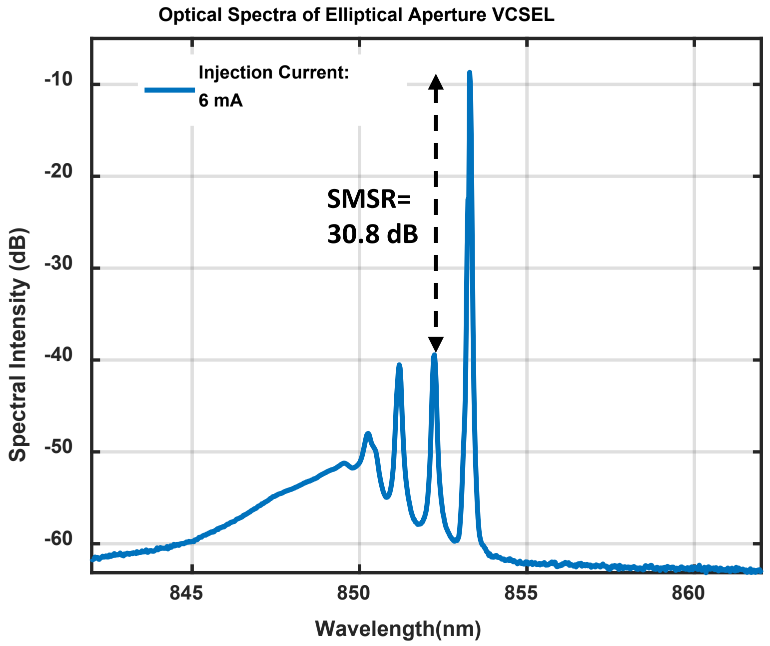

- With a slightly elliptical anti-phase coating aperture, undesired polarization state is suppressed without undesired encroachment onto fundamental transverse mode, resulting in 3 mW of output power
- Orthogonal-polarization suppression ratio (OPSR) of 20 dB measured at 6mA, achieving **single-polarization operation**
- SMSR of 30.8 dB measured, indicating simultaneous **single-mode operation**

Summary and Outlook

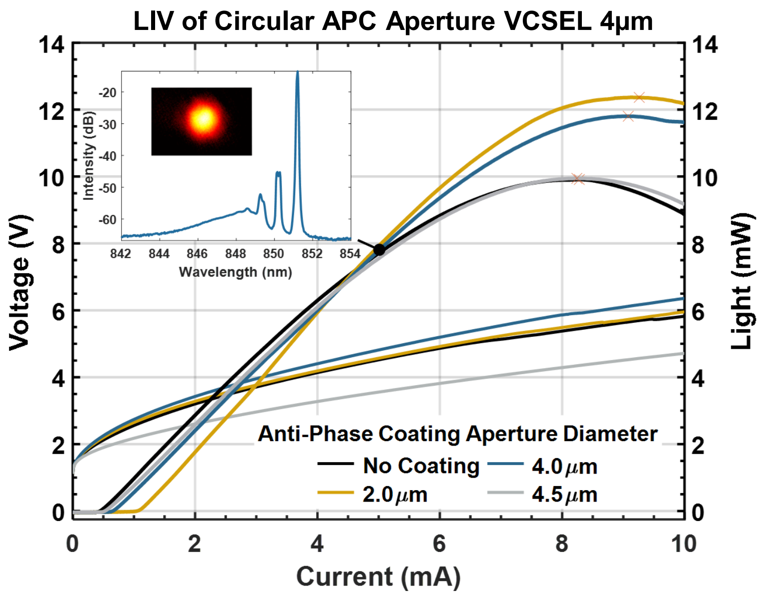

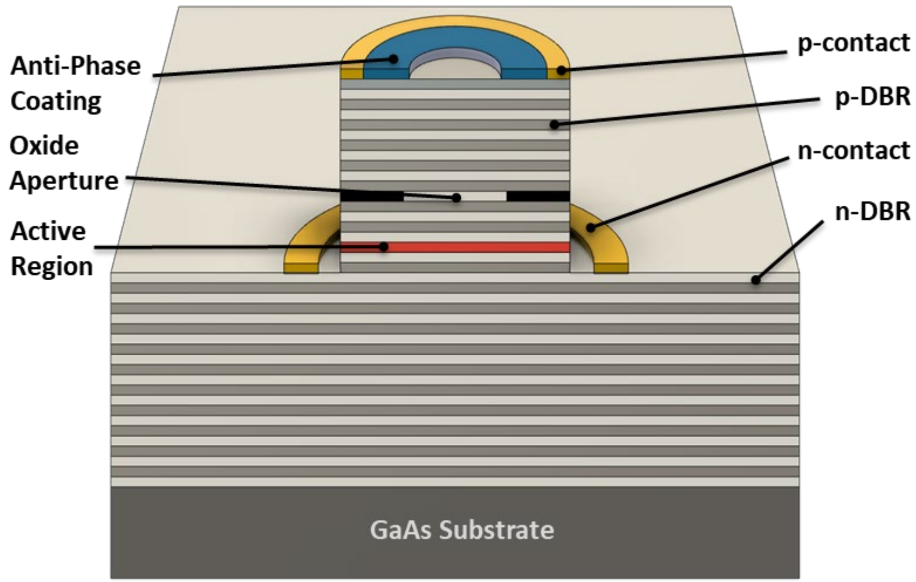

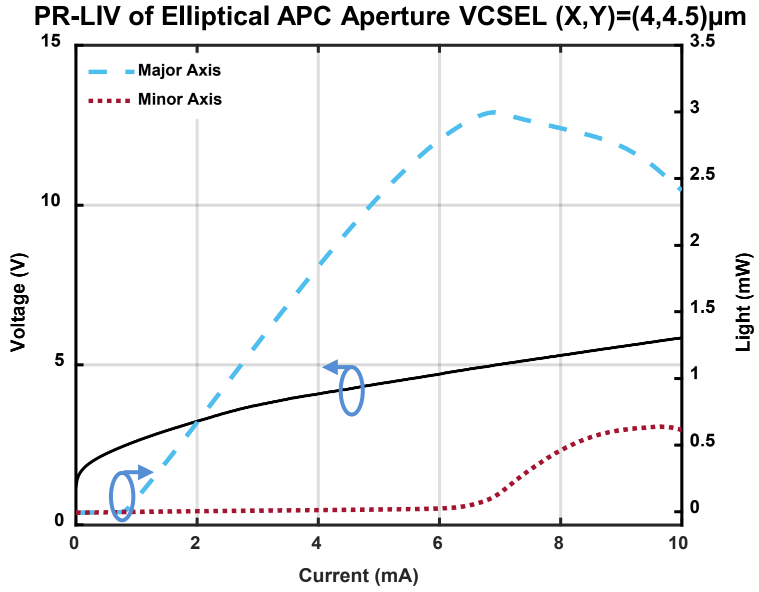

- Introduced the design and fabrication of VCSELs utilizing the additive high-refractive index anti-phase coating
- Achieved high-power single-mode operation in inherently single-mode and multi-mode 850 nm VCSELs
- Achieved single-mode, single-polarization VCSEL operation in accordance with the year 1 and year 2 tasks/milestones proposed in current block-gift grant
- Will apply knowledge learned to ongoing efforts to design and fabricate 2D-VCSEL arrays operating in a single-mode, single-polarization state

Near- and Far-Field Imaging

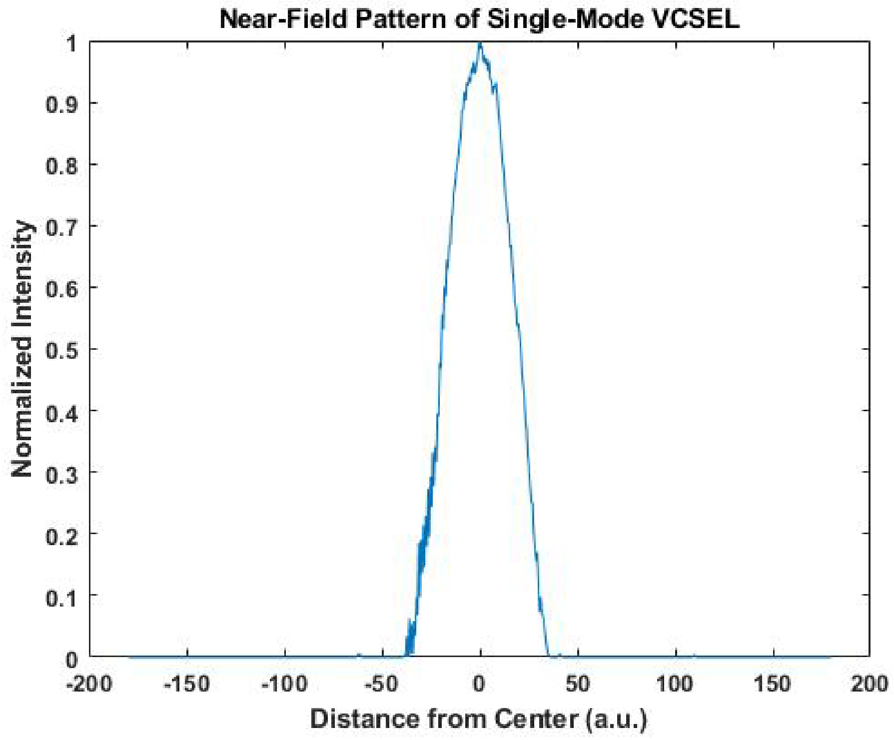

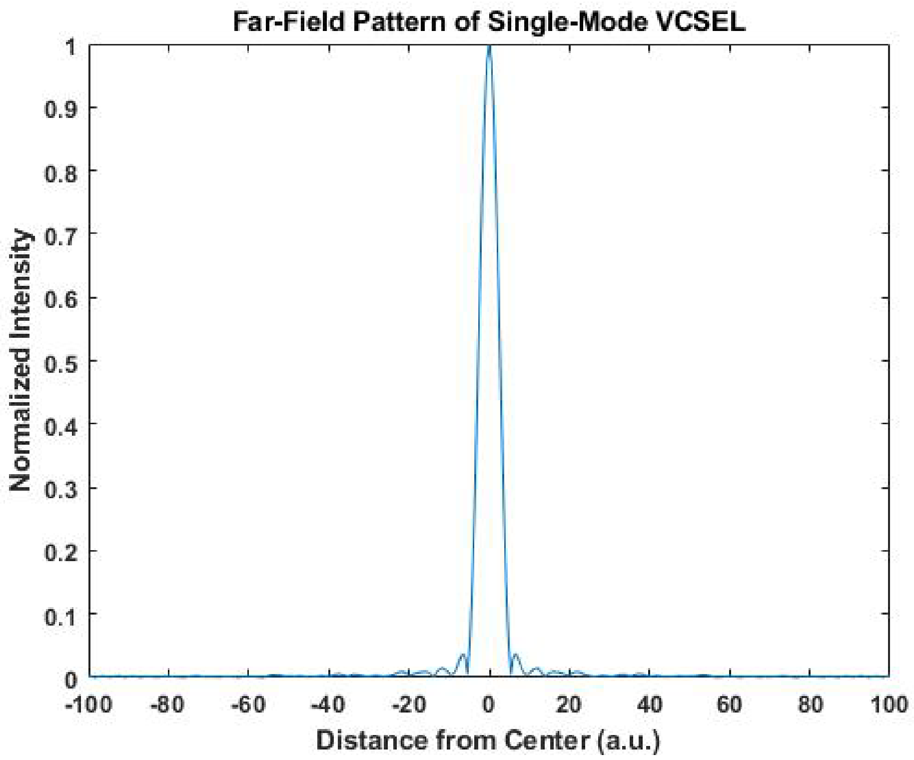

- Near-field pattern of single-mode VCSEL imaged via CMOS imaging camera with OD9 attenuator
- Via a Fourier transform of the near-field pattern, the far-field pattern of the device can be theoretically calculated

2D-VCSEL Arrays

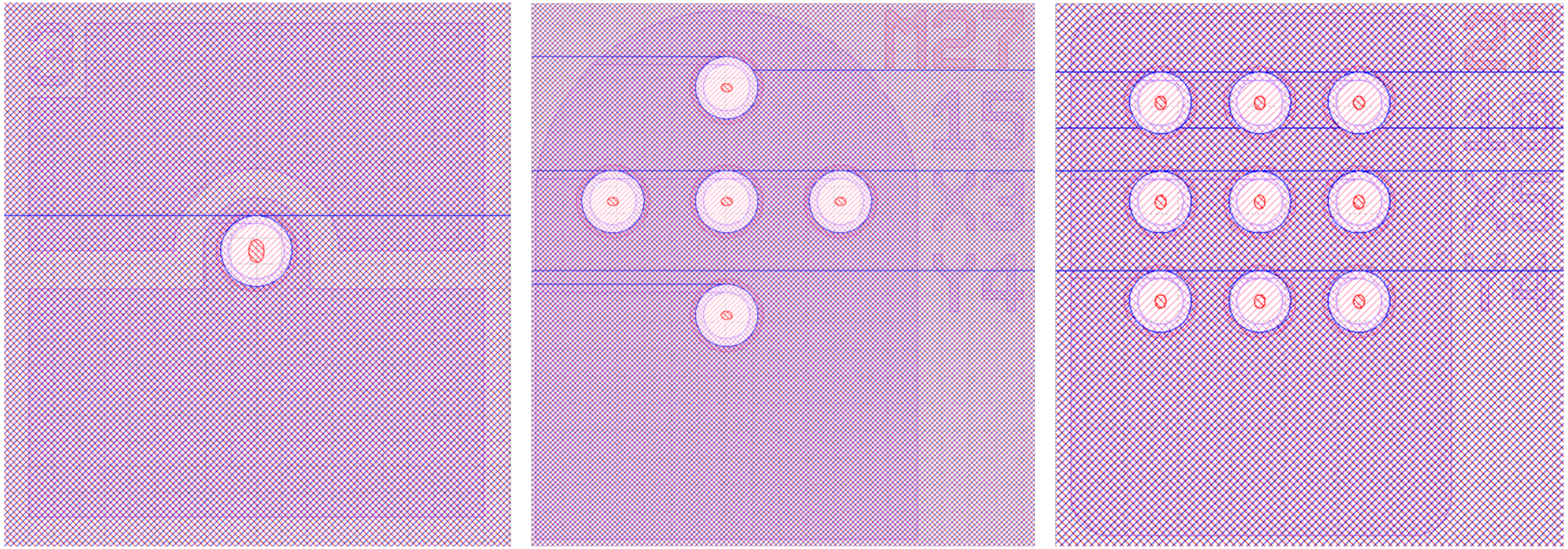

- Single-discrete, 5- and 9-VCSEL arrays are designed for processing, with mask designs seen above
- Similar process flow to standard discrete VCSEL fabrication, main difference includes coverage and size of top p-metal contact
- Current efforts have resulted in spontaneous emission only due to large oxide apertures and pinched off disorder-defined apertures

Next Steps for Block-Gift Grant

- **IID VCSELs for single-polarization single-mode operation**
  - Tailor oxidation/disordering rate to encroach further onto higher-order modes, suppressing their ability to lase

- **2-D single-mode single-polarization VCSEL arrays utilizing both polarization-state suppression techniques**
  - Fine-tune IID fabrication steps to achieve lasing in 2D-arrays
  - Begin array fabrication utilizing anti-phase coating

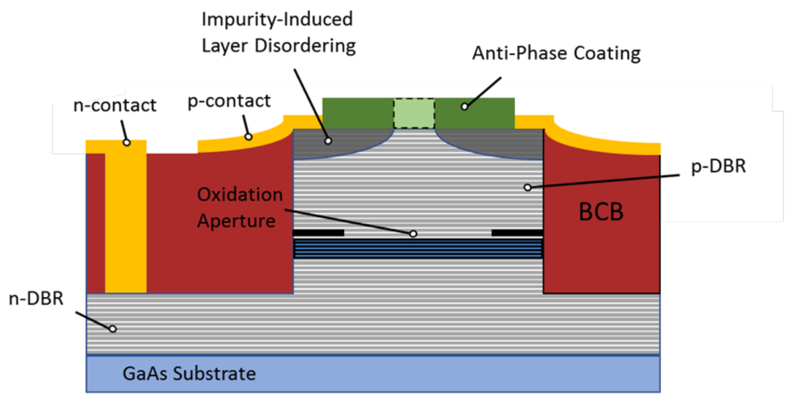

Polarization-Controlled VCSEL Cross-Sectional Schematic

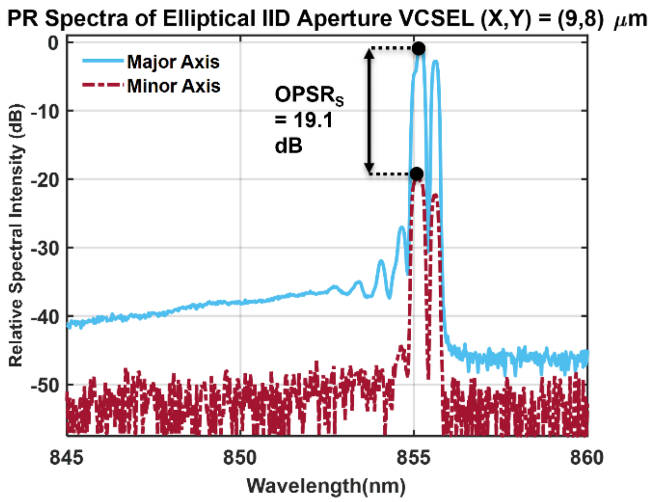

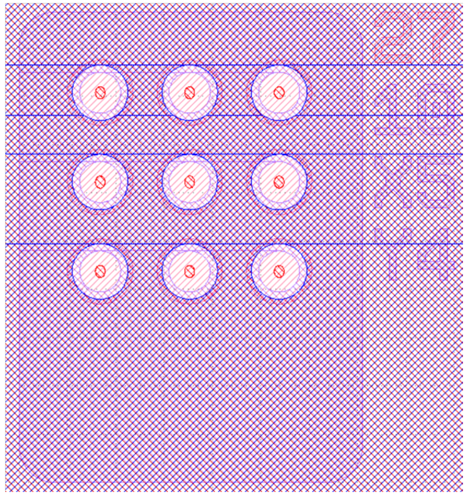

Acknowledgements

The authors are grateful for the support from the Coherent/II-VI Foundation and VCSEL epitaxial material from II-VI Epiworks in Champaign, IL.

Research Group

Contact:
Kevin Pikul: kpikul2@illinois.edu
Leah Espenhahn: leahe2@illinois.edu
Dr. John Dallesasse: jdallesa@illinois.edu

Publications and Conference Proceedings

1. O’Brien, Thomas, et al. "Mode behavior of VCSELs with impurity-induced disordering." *IEEE Photonics Technology Letters* 29.14 (2017): 1179-1182.
2. O'Brien Jr, Thomas R. *High-power single-mode vertical-cavity surface-emitting lasers via impurity induced disordering*. Diss. University of Illinois at Urbana-Champaign, 2017.
3. O'Brien, Thomas R., Benjamin Kesler, and John M. Dallesasse. "Transverse mode selection in vertical-cavity surface-emitting lasers via deep impurity-induced disordering." *Vertical-Cavity Surface-Emitting Lasers XXI*. Vol. 10122. International Society for Optics and Photonics, 2017.
4. Su, Patrick, et al. "Wafer-Scale Method of Controlling Impurity-Induced Disordering for Optical Mode Engineering in High-Performance VCSELs." *IEEE Transactions on Semiconductor Manufacturing* 31.4 (2018): 447-453.
5. Su, Patrick, et al. "Controlling impurity-induced disordering via mask strain for high-performance vertical-cavity surface-emitting lasers." *2018 International Conference on Compound Semiconductor Manufacturing Technology, CS MANTECH 2018*. 2018. Best Student Paper
6. Su, Patrick, et al. "Strain-controlled impurity-induced disordered apertures for high-power single-mode VCSELs." *Vertical-Cavity Surface-Emitting Lasers XXIV*. Vol. 11300. International Society for Optics and Photonics, 2020.
7. Kesler, Benjamin, et al. "Facilitating single-transverse-mode lasing in VCSELs via patterned dielectric anti-phase filters." *IEEE Photonics Technology Letters* 28.14 (2016): 1497-1500.
8. Kesler, Benjamin, Thomas O'brien, and John M. Dallesasse. "Transverse mode control in proton-implanted and oxide-confined VCSELs via patterned dielectric anti-phase filters." *Vertical-Cavity Surface-Emitting Lasers XXI*. Vol. 10122. International Society for Optics and Photonics, 2017.
9. Kesler, Benjamin A. *Mode control in VCSELs using patterned dielectric anti-phase filters*. Diss. University of Illinois at Urbana-Champaign, 2017.
10. Pikul, Kevin P., et al. "Standing Wave Engineering for Mode Control in Single-Mode Oxide-Confined Vertical-Cavity Surface-Emitting Lasers." *2021 International Conference on Compound Semiconductor Manufacturing Technology, CS MANTECH 2021*. 2021. Best Student Paper/Presentation
11. P. Su, K. Pikul, L. Espenhahn, M. Kraman, J. M. Dallesasse, “(Invited) Achieving High-Power Single-Mode Operation in Vertical-Cavity Surface-Emitting Lasers via Scalable, Higher-order Mode Suppression Techniques”, ECS Transactions (2022).
12. P. Su, K.Pikul, M. Kraman, J. M. Dallesasse, “ High-power single-mode vertical-cavity surface-emitting lasers using strain-controlled disorder-defined apertures.”, Applied Physics Letters (2021). DOI: 10.1063/5.0068713. Editor’s Pick.
13. M. Kraman, P.Su, K. Pikul, J. M. Dallesasse, “Impact of Diffusion Profile on the Modulation Response of Single-Mode Disorder-Defined VCSELs”, IEEE Photonics Technology Letters, (2022). Manuscript in review.

References (1 of 2)

[1] Hallereau, Sylvain. “VCSEL in Smartphone Comparison 2019 - System Plus Consulting.” VCSEL in Smartphone Comparison, System Plus Consulting, Mar. 2019, https://www.systemplus.fr/wp-content/uploads/2019/04/SP19426-VCSEL-in-Smartphone-Comparison-2019_SAMPLE.pdf.

[2] Mayo, Benjamin, “Face ID deemed too costly to copy, Android makers target in-display fingerprint sensors instead”, Retrieved July 25, 2022, from https://9to5mac.com/2018/03/23/face-id-premium-android-fingerprint-sensors/.

[3] Yole Développement, “VCSELs- Market and Technology Trends 2019 Report”. www.yole.fr. Accessed Jan, 4, 2022.

[4] Dedezade, Esat, “Oculus Quest Pro preview: what we know about Meta’s mystery headset”, Retrieved July 25, 2022 from https://www.stuff.tv/news/oculus-quest-pro-preview-what-we-know-about-metas-mystery-headset/.

[5] Subramaniam, Vaidyanathan, “Apple AR/VR headset to feature dual 8K displays, changeable prescription lenses, and M1 Pro SoC with fan, could be priced on lines of entry-level Macbook Pro 14”, Retrieved July 25, 2022 from https://www.notebookcheck.net/Apple-AR-VR-headset-to-feature-dual-8K-displays-changeable-prescription-lenses-and-M1-Pro-SoC-with-fan-could-be-priced-on-the-lines-of-entry-level-MacBook-Pro-14.593361.0.html.

[6] Fiber Optic Share, “Hot 100G Fiber Optic Transceiver for Data Center”, Retrieved July 25, 2022 from https://www.fiberopticshare.com/hot-100g-fiber-optic-transceivers-for-data-center.html.

[7] AMS, “ams as leading VCSEL Supplier”, Retrieved July 25, 2022 from https://ams.com/lidar.

[8] Analog Devices, “Analog Devices Launches Industry’s First High-Resolution Module fro 3D Depth Sensing and Vision Systems”

[9] Emmanuel Ocbazghi, S. K. (2017, November 17). We used an infrared camera to show how the iphone X's FaceID actually works. Business Insider. Retrieved January 31, 2022, from https://www.businessinsider.com/how-face-id-iphone-x-works-infrared-dots-scan-technology-2017-11

[10] Finisar, “Using VCSELs in 3D Sensing Applications”, SEMICON China, Shanghai, March 21, 2019.

[11] Daqri, “Depth Cameras For Mobile AR: From iPhones to Wearables and Beyond”, April 25, 2018. (Web: https://medium.com/@DAQRI/depth-cameras-for-mobile-ar-from-iphones-to-wearables-and-beyond-ea29758ec280).

[12] Pierce, Daniel T., and Wo E. Spicer. "Electronic structure of amorphous Si from photoemission and optical studies." *Physical Review B* 5.8 (1972): 3017.

References (2 of 2)

[13] Su, Patrick et al. "High-power single-mode vertical-cavity surface-emitting lasers using strain-controlled disorder-defined apertures." Applied Physics Letters 119.24 (2021): 241101. Editor’s Pick.

[14] Su, Patrick, et al. “Impact of Diffusion Mask Strain on Impurity-Induced Disordered VCSELs Designed for Single-Fundamental-Mode Operation." 2022 International Conference on Compound Semiconductor Manufacturing Technology, CS MANTECH 2022.

[15] Su, Patrick, et al. “(Invited) Achieving High-Power Single-Mode Operation in Vertical-Cavity Surface-Emitting Lasers via Scalable, Higher-Order Mode Suppression Techniques”, ECS Transactions, 2022. (Manuscript submitted).

[16] M. Kraman, P.Su, K. Pikul, J. M. Dallesasse, “Impact of Diffusion Profile on the Modulation Response of Single-Mode Disorder-Defined VCSELs”, IEEE Photonics Technology Letters, (2022). Manuscript Accepted.

Thank You

Research Group

Contact:
kpikul2@illinois.edu
leahe2@illinois.edu
jdallesa@illinois.edu